

Schlußbericht

zum Fördervorhaben

„Methoden und Algorithmen zur Ozean-Fernerkundung mit MOS“

Laufzeit: 01.01.1992 – 31.12.1998

Autoren: A. Neumann, Projektleiter
B. Gerasch
M. Hetscher
H. Krawczyk
C. Tschentscher
T. Walzel

Ausführende Stelle: DLR-Standort Berlin-Adlershof
Institut für Weltraumsensorik und Planetenerkundung
12484 Berlin
Rudower Chaussee 5

Das Vorhaben wurde gefördert durch

- die Deutsche Agentur für Raumfahrtangelegenheiten (DARA) GmbH
unter dem Förderkennzeichen 50EE9203
- das Bundesministerium für Bildung, Wissenschaft und Technologie (BMBF), vertreten
durch den Projektträger Biologie, Energie, Umwelt (BEO)
unter dem Förderkennzeichen 03EE9203

Berlin, März 1999



Der Schlußbericht besteht aus zwei Teilen. Dem eigentlichen Berichtsteil (28 Seiten) und den Anlagen, die Detailinformationen zu technischen und wissenschaftlichen Fragen enthalten.

Anlagen:

1. MOS User Guide (Titelblatt und Inhaltsverzeichnis)
2. Algorithm Theoretical Basis Document: MOS-IRS Level 1-B Products (ATBD Level 1B)
3. Algorithm Theoretical Basis Document: MOS-IRS Ocean Colour Level 2 Algorithm (ATBD Level 2)
4. Kurzdokumentation der Softwaretools

0. Vorbemerkung

Das Fördervorhaben „Ozean-Fernerkundung mit MOS-PRIRODA“ (FKZ 50EE9203) war Bestandteil des Verbundvorhabens „Fernerkundungsexperiment MOS-PRIRODA“ und ursprünglich für den Zeitraum 1992-1995 angelegt. Bedingt durch die Startverzögerungen des PRIRODA-Moduls und der später auftretenden Probleme mit der Datenverfügbarkeit wegen technischer Schwierigkeiten an Bord der MIR-Station wurde das Vorhaben um zwei weitere Jahre bis zum 1. Quartal 1998 aufgestockt und später kostenneutral bis Ende 1998 verlängert. Anfang 1997 wurde auf Grund der Beschädigung von MOS-PRIRODA mit der DARA als Zuwendungsgeber vereinbart, die Daten des Schwestergerätes MOS-IRS unter Beibehaltung der Projektzielstellungen zu nutzen.

Das Projektteam war somit in die Vorstartarbeiten und in die Datenanalyse für zwei Fernerkundungsmissionen einbezogen. Die Arbeiten umfaßten dabei Softwareentwicklungen und Datenanalysen während der Laboruntersuchungen und Startvorbereitungen ebenso wie die Entwicklung der Primärprozessoren bis Level-1B und die Entwicklung und Testung von qualitativ neuen Interpretationsverfahren, speziell für Küstengewässer (case-2). Der präoperationelle Charakter der Mission IRS-P3 erforderte dabei einen erhöhten Arbeitsumfang zur Absicherung der Datenprozessierung und Nutzerbetreuung, ermöglichte aber andererseits durch den regulären, täglichen Datenfluß auch Untersuchungen, wie sie mit MOS-PRIRODA kaum möglich gewesen wären (z.B. zur zeitlichen Variation in Küstenzonen).

Die Darstellung der Arbeiten im Schlußbericht erfolgt thematisch gegliedert und damit in inhaltlich zusammenhängender Reihenfolge, was nicht immer dem chronologischen Ablauf entspricht.

1. Projektressourcen, Kooperationen

Das Vorhaben wurde mit gemischter Finanzierung aus DLR-Programmatik und DARA-Förderung realisiert. Auf der Personalseite standen 2 Personaljahre p.a. für die gesamte Laufzeit aus den Drittmitteln und 4 Personaljahre p.a. aus der Grundfinanzierung (Teilprogramm „Küstenzonen und Gewässer“) zur Verfügung, d.h. ein Verhältnis von 1:2. Bei den Sachmitteln erfolgte eine nur geringfügige Förderung, der Großteil (ca. 80 %) wurde aus der Programmatik abgesichert. Ein umgekehrtes Verhältnis lag bei den Reisekosten vor, wo der überwiegende Teil aus den Fördermitteln bestritten wurde. Im Bereich von Investitionen/Anlagekosten standen nur im ersten Projektjahr geringe Mittel zur Verfügung. Somit wurde fast die gesamte technische Ausrüstung (Workstations, PCs, Drucker und weitere Peripherie) aus der DLR-Grundfinanzierung abgedeckt.

Der Finanzierungsplan des Vorhabens wurde insgesamt eingehalten, mußte jedoch auf Grund der Verschiebungen im PRIRODA-Projekt auf russischer Seite mehrmals präzisiert werden. Da die geplanten internationalen Arbeitsgruppen zu PRIRODA nie richtig installiert wurden, fanden viele der geplanten Arbeitsberatungen nicht statt. Daher wurde die im Fördervorhaben geplanten Reisekosten nicht voll ausgeschöpft.

Bei der Arbeit an einem solch umfangreichen Satellitenprojekt ist die Kooperation mit anderen Forschungseinrichtungen im nationalen und internationalen Rahmen unabdingbar. Neben der Zusammenarbeit im eigentlichen PRIRODA-Projekt entwickelten sich auf Grund des großen Interesses an Ozeandaten Kooperationen und Abstimmungen mit weiteren Institutionen und Projekten (z.B. dem SeaWiFS-Programm der NASA). Die folgende Tabelle gibt einen Gesamtüberblick über die Einrichtungen/Projekte, mit denen im Verlauf des Fördervorhabens Kooperationen entstanden sind. Der Großteil wird auch in der Gegenwart im Rahmen der Mission MOS-IRS auf grundfinanzierter Basis und in neuen Projekten weitergeführt.

Tabelle 1: Kooperationen im Rahmen des Fördervorhabens

Einrichtung	Gegenstand der Zusammenarbeit
Deutsches Fernerkundungsdatenzentrum des DLR, Neustrelitz und Oberpfaffenhofen	MOS-Datenempfang Primärprozessierung Datenarchivierung und –verteilung Nutzerbetreuung Datenprodukte
German Space Operations Centre des DLR, Oberpfaffenhofen	MOS-Kommandierung Dienstsystem – Überwachung
Institut für Ostseeforschung, Warnemünde	Biooptisches Ostsee-Modell Meßkampagnen Validierung
Institut für Gewässerphysik, GKSS, Hamburg	Algorithmenentwicklung Validierung
Institut für Radioelektronik der russischen AdW, Moskau	PRIRODA Datenkonzept und Wissenschaftsprogramm PRIRODA Datenzentrum
RKK Energia, Moskau	PRIRODA Datenzentrum Prozessorentwicklung
Institut für Kosmosforschung der russischen AdW, Moskau	MOS-Entwicklung und –testung Prüfsoftware Datenkompression
Institut für Kybernetik der estnischen AdW, Tallinn	Datenkompression
Marines Hydrophysikalisches Institut der Ukrainischen AdW, Sewastopol	Algorithmenentwicklung Meßkampagnen Validierung
Instituto Canario de Ciencias Marinas, Grand Canaria	Anwendungsbeispiele Meßkampagnen Validierung
Centro de Investigacion y Cultivo de Especies Marinas, Huelva	Anwendungsbeispiele Meßkampagnen Validierung
Space Application Institute, JRC Ispra	Algorithmenentwicklung European Ocean Colour Kalibration
ESA ESTEC, Noordwijk	MERIS Precursor-Programm
ESA ESRIN, Frascati	MOS-Empfang Maspalomas Primärprozessierung Datenarchiv
INTA, Spanien	MOS-Empfang Maspalomas Primärprozessierung Datenarchiv
Goddard Space Flight Centre, NASA, Greenbelt	MOS-Empfang Wallops Primärprozessierung Datenarchiv SeaWiFS-Interkalibration SIMBIOS-Programm Kalibration
ISRO SAC, ISAC, ISTRAC Bangalore und Ahmedabad	Missionsplanung und –durchführung Algorithmenentwicklung Wissenschaftleraustausch
National Remote Sensing Agency, Hyderabad	MOS-Empfang Empfangsstationen in Drittländern Primärprozessierung Datenarchiv

2. Softwareentwicklung – Vorstart

2.1 Prüfsoftware

Im Rahmen des Vorhabens „Fernerkundungsexperiment MOS-PRIRODA“ (FKZ 50EE9201) wurde das abbildende Spektrometer MOS entwickelt, gebaut und getestet. Dafür wurden für Labormessungen und die Vorstarttests entsprechende spezielle Meß- und Prüftechnik realisiert. Entsprechend den Anforderungen der Bordgeräteentwicklung wurden im hier abgerechneten Vorhaben Softwaresysteme für die Prüftechnik entwickelt. Diese umfaßten:

- Software für die Werks-KIA (KIA = russische Abkürzung für komplexe Prüfeinrichtung), die im Rahmen der Labortests und Qualifizierungen eingesetzt wurde. Sie ermöglichte eine Steuerung der Optikblöcke des Monochromators und der Schrittmotoren im Laboraufbau, die Dateneinlesung in einen Rechner und die Aufbereitung der Daten mit systematischen Korrekturen sowie die Bestimmung von Fokussierung, Apparatefunktion und Modulations-Transferfunktion mit grafischer und numerischer Ergebnisausgabe.
- Software zur Datenauswertung mit der System-KIA während der Vorstarttests in Rußland. Hier war der Funktionsnachweis der verschiedenen Betriebsmodi von MOS und wesentlicher Qualitätsparameter des Instrumentes im autonomen Betrieb und während der Integration am PRIRODA-Modul gefordert. Sie wurde auch von der russischen Seite während der verschiedenen Phasen der Startvorbereitung zur Bewertung der Funktion von MOS eingesetzt.

Für beide Softwaresysteme liegen interne Dokumentationen bei dem DLR vor.

2.2 Bildverarbeitungssystem Pro-Image

Da zum Zeitpunkt des Beginns der Arbeiten am Fördervorhaben keine geeigneten kommerziellen Bildverarbeitungsprogramme auf PC-Plattform verfügbar waren, diese aber im Projekt zur operativen und mobilen Arbeit benötigt wurden, wurde ein Bildverarbeitungssystem für PC unter MS-DOS realisiert. Es erlaubt neben der flexiblen Behandlung verschiedener Rohdatenformate wesentliche mathematische Standardoperationen und Bildmanipulationen in mehreren unabhängigen Bildspeichern. Es wurde zur Datenanalyse und –darstellung während der Tests am technologischen Muster MOS genutzt.

Mit der späteren Verfügbarkeit des PC-UNIX-Systems LINUX stand dann eine leistungsfähigere Softwarebasis zur Verfügung, so daß Pro-Image nicht weiterentwickelt wurde. Die Programmdokumentation kann als internes Dokument beim DLR abgefordert werden.

2.3 Quick-Look-Software für Bodenspektrometer HiRES

Für ground-truth-Validierungsmessungen wurden im Vorhaben „Fernerkundungsexperiment MOS-PRIRODA“ (FKZ 50EE9201) die Bodenspektrometer HiRES zur Messung optischer Parameter über Wasser und der Atmosphäre realisiert. Für den Einsatz dieser Geräte auf Meßkampagnen wurde im Rahmen des hier abgerechneten Vorhabens eine Quick-Look-Software entwickelt und implementiert, die systematische Korrekturen der Meßdaten, grafische und numerische Ausgabe der gemessenen Spektren und einfache Auswertalgorithmen enthält. Sie kam während der ersten Meßkampagnen zum Einsatz. Die Beschreibung des Programms liegt als interne Dokumentation beim DLR vor. Die Abbildung 2.1 zeigt die Programmstruktur, Abbildung 2.2 ein Beispiel der Benutzeroberfläche.

Hauptmenü

File Menü	Datei- und Directory- bezogene Operationen	
	Open File	Meßdatei(en) öffnen
	File Info	Inhalt des Dateiheaders anzeigen
	Select DKL	nicht benutzt
	Select CAL	Kalibrierdatei auswählen
	Select PRNU	nicht benutzt
	Select DSNU	Dunkelwert-Korrekturdatei auswählen
	Data Directory	Datendirectory ändern
	Cal. Directory	Kalibrierdirectory ändern
	Exit	Programm beenden

Options Menü	Einstellung von Parametern für die Programmabarbeitung, Hilfsfunktionen	
	Select Channels	Wellenlängenbereich und Bandbreite wählen
	Averaging	zeitliche Mittelung von Spektren
	Corrections	Auswahl der angewandten systematischen Korrekturen
	Output Mode	Ausgabemodus (Grafik/Numerik)
	Radiance/Reflectance	Auswahl Radianz/Reflektanz
	Multiple Files	Auswahl mehrerer Spektren, Zeitverlauf
	Calibration	interne Funktion zur Erzeugung von Kalibrierdaten
	Correct Header	Headerinhalt korrigieren/ändern

Interpretation Menü	Quick-Look- und Interpretationsalgorithmen	
	Almu	Auswertung einer Almukantarar-Meßfolge
	Sun	Auswertung von Sonnenmessungen (Transmission)
	Nadir	Auswertung von Nadirmessungen
	Global	Auswertung von Globalmessungen
	Raw Data	Anzeige unkorrigierter Rohdaten

DOS-Shell	Kommandoausführung in einer DOS-Shell, eingestellte Programmoptionen bleiben unverändert	
-----------	--	--

Abb. 1.1: Programmstruktur des HiRES Quick-Look und Auswerteprogramms

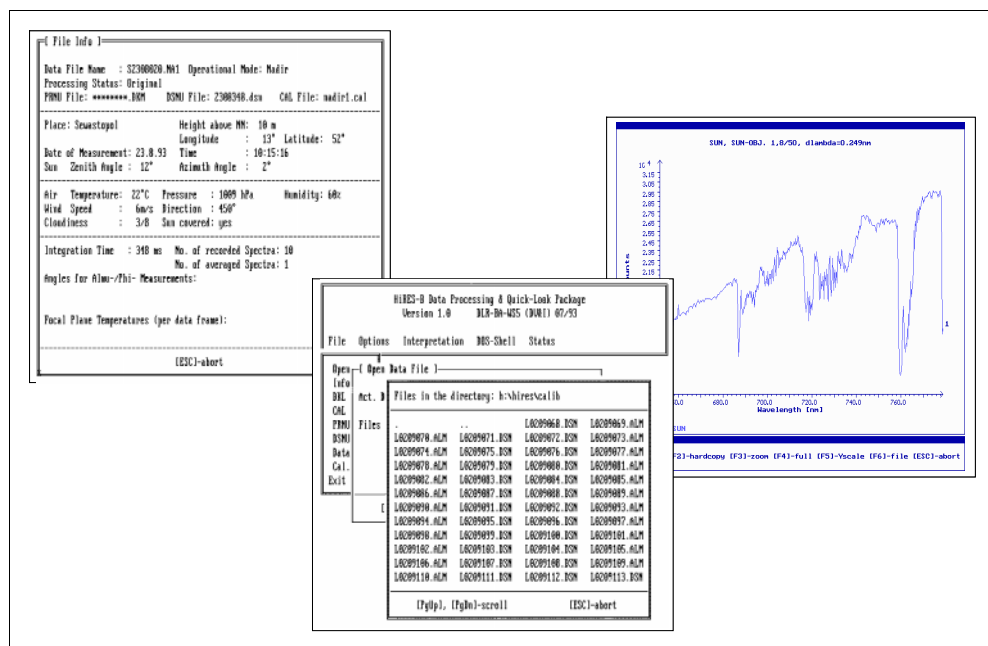


Abb. 2.2: Benutzeroberfläche des HiRES-Programms

3. MOS-PRIRODA Datenkonzept

Während der Vorarbeiten zu MOS-PRIRODA, noch am Institut für Kosmosforschung, wurde die erste Version der Datenkonzeption erarbeitet. Mit Beginn des Fördervorhabens wurde auf dieser Basis das Gesamtkonzept für die Primärverarbeitung, Archivierung und Verteilung von MOS- und anderen PRIRODA-Daten ausgearbeitet. Das Konzept wurde gemeinsam mit dem Deutschen Fernerkundungsdatenzentrum DFD in Neustrelitz und den Partnern in Rußland (Institut für Radioelektronik IRE als wissenschaftlicher Koordinator von PRIRODA und RKK Energia als technischer Leiter) entwickelt.

3.1. Konzept zur Primärverarbeitung MOS-PRIRODA

Für das deutsche PRIRODA-Programm wurden die Teilaspekte Datenempfang, Routineprozessierung, Datenarchivierung und Verteilung im Fördervorhaben „PRIRODA-Bodensegment“ (FKZ 50EE9204) vom DFD realisiert. Abbildung 3.1 zeigt die schematische Struktur. Das Konzept ging von technisch weitgehend identischen Datenzentren in Moskau und beim DLR aus. Die Primärverarbeitung für MOS-PRIRODA (systematische Datenkorrekturen, Kalibration, Formatierung der Daten und Schnittstellen zum Archivsystem) mußte sich in dieses Gesamtsystem einordnen. Dazu wurde als Basis für die Softwareentwicklung das detaillierte Konzept entwickelt und im Dokument „MOS-PRIRODA Data Processing, Software und Data Products“ fixiert. Abbildung 3.2 zeigt die Struktur des MOS-Datenhandlings mit den Schnittstellen zum Bodensegment. Für MOS-IRS, das im weiteren Vorhabensverlauf an Stelle von MOS-PRIRODA genutzt wurde, ergab sich ein modifiziertes Szenario, das schematisch in Abb. 3.3 dargestellt ist.

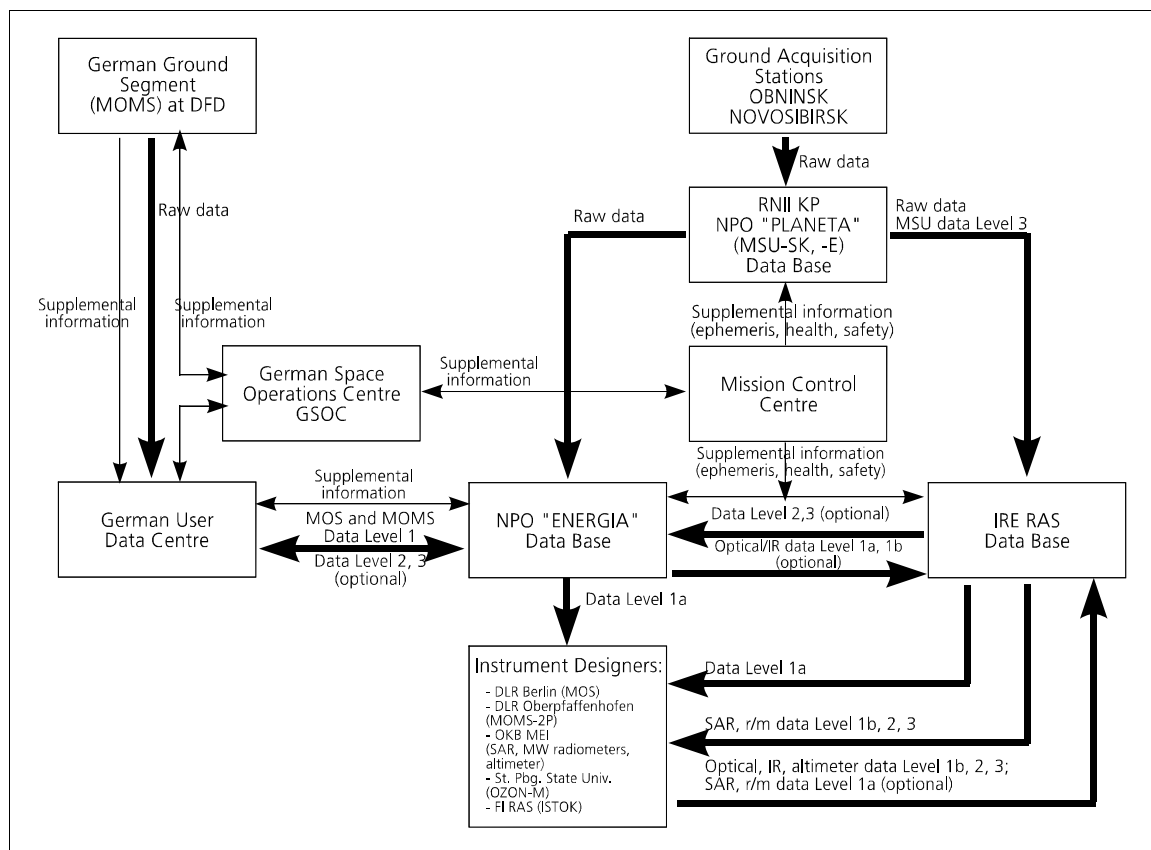


Abb. 3.1: Struktur Datenempfang, -austausch, -prozessierung, -archivierung und -verteilung im internationalen PRIRODA-Projekt

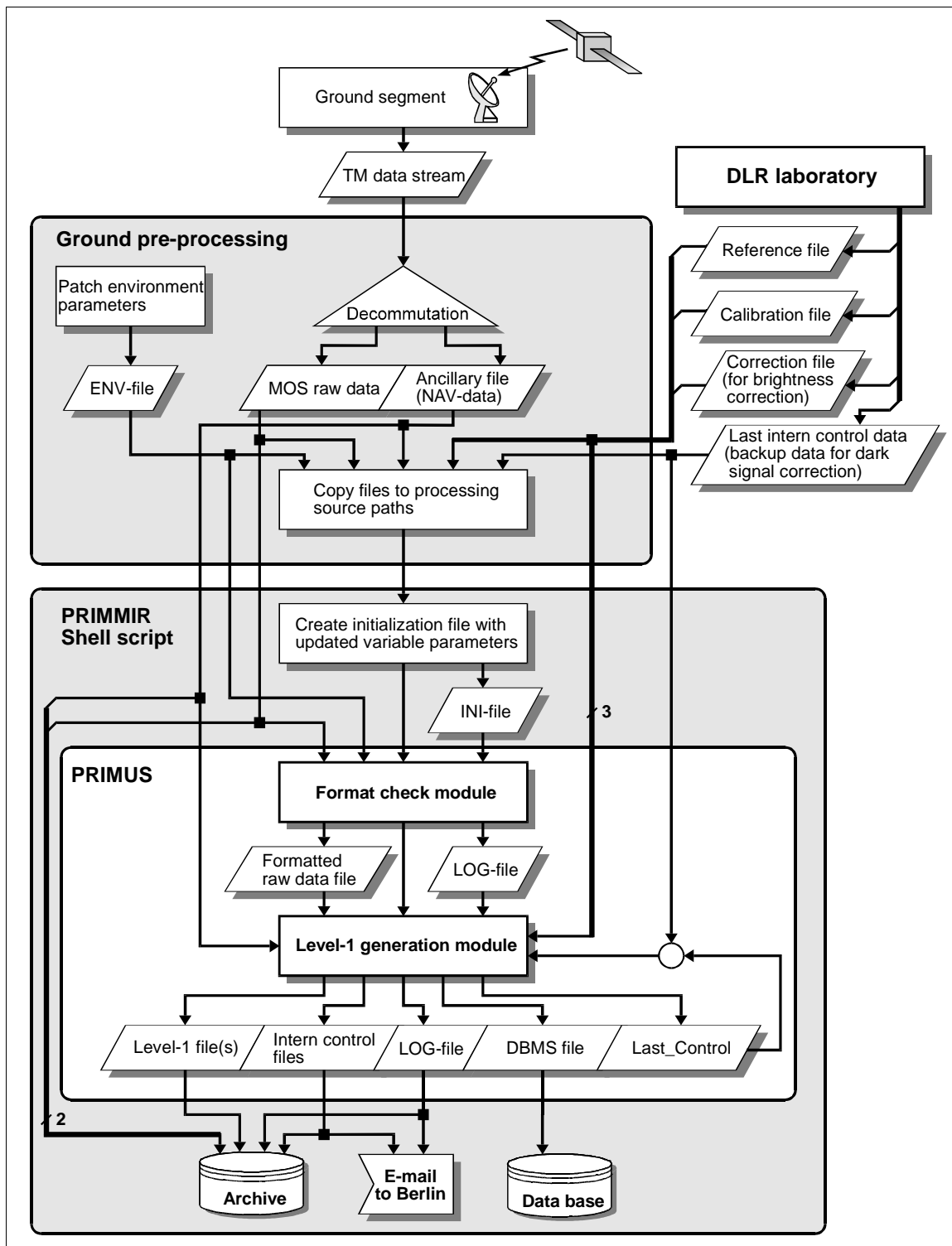


Abb. 3.2: Struktur des Datenhandlings für die Level-1B – Prozessierung von MOS-PRIRODA

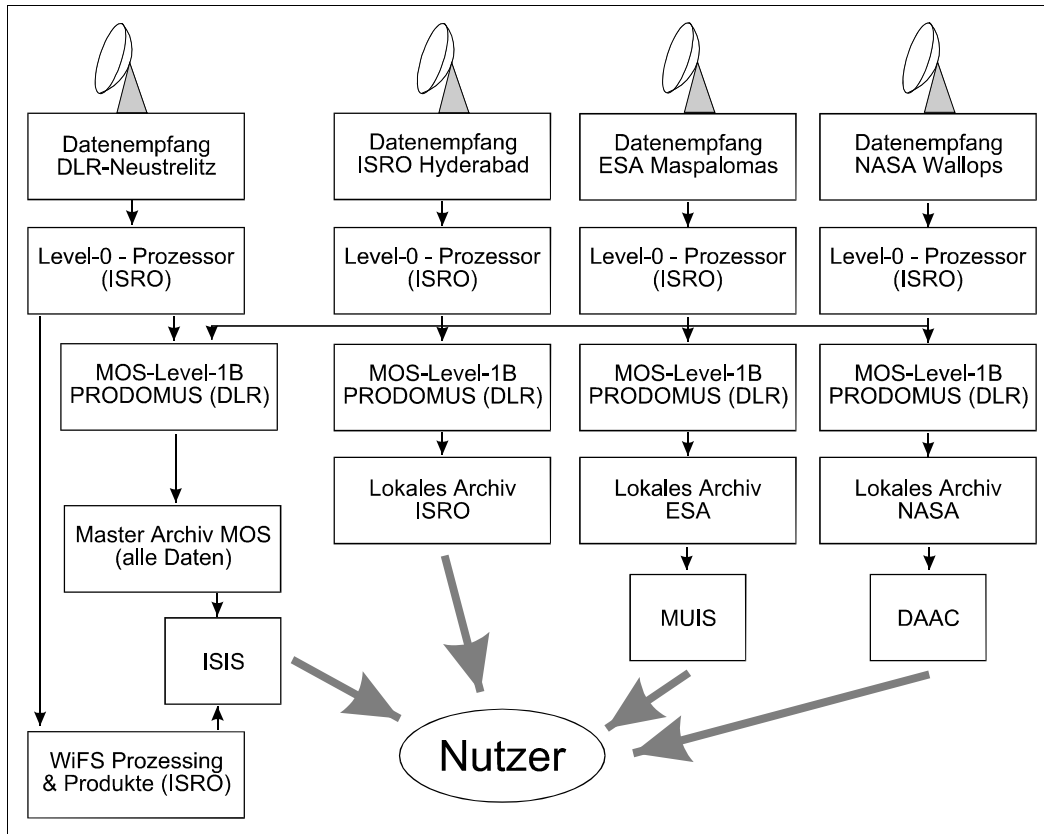


Abb. 3.3: Dateneingang, Prozessierung und Datenaustausch MOS-IRS

3.2. MOS User Guide

In Vorbereitung auf die Betriebs- und Nutzungsphase von PRIRODA, die nach mehreren Startverschiebungen ab 1995 geplant war, wurde der „MOS-PRIRODA User Guide“ erarbeitet, mit dem der Nutzergemeinschaft eine umfassende Dokumentation zur Verfügung gestellt wurde. Der Guide umfaßte die Themen:

- PRIRODA-Mission (Instrumentierung, wissenschaftliches Programm, Orbit und Missionsplanung)
- Organisation des internationalen PRIRODA-Programms
- Abbildendes Spektrometer MOS (technische Beschreibung, Kenndaten, Pre-Launch und in-Orbit-Kalibrierung)
- MOS-Prozessierung, Software und Datenprodukte
- Datenzugriff über das PRIRODA-Nutzungszentrum.

In dem User Guide sind im wesentlichen die Ergebnisse der Arbeiten zum Instrument und zur Softwareentwicklung bis zum Start von PRIRODA im April 1996 zusammengefaßt. Auf Grund der technischen Probleme an Bord der MIR-Station und später der Beschädigung von MOS-PRIRODA konnte das Konzept jedoch nicht vollständig umgesetzt werden. Allerdings war damit ein Basiskonzept entstanden, das mit einigen Modifikationen bei dem später begonnenen Projekt MOS-IRS weitgehend umgesetzt wurde und bis heute erfolgreich bei der Mission genutzt wird.

Das ursprüngliche Fördervorhaben endete 1995. Da der Start von PRIRODA auf 1996 verschoben worden war, wurde für das Verbundvorhaben „PRIRODA“ eine Verlängerung und Aufstockung bis 1998 beantragt. Im Ergebnis der Statuspräsentation vom November 1995 und auf Empfehlung der Gutachter wurde der MOS-PRIRODA User Guide nicht weitergeführt, sondern als verkürzte Version „Experiment MOS-PRIRODA: Executive Summary“ abgeschlossen.

3.3 Internationale Koordinierung

Wie bereits dargestellt, ordnet sich das Experiment MOS in den Gesamtkomplex des internationalen PRIRODA-Projektes ein. Im Rahmen des Fördervorhabens wurden entsprechend der PRIRODA-Koordinierungsstruktur (Science Council und dem untergeordnete Facharbeitsgruppen) die Verantwortungen in den Arbeitsgruppen „Express-Datenanalyse“, „Optische Sensoren“ und „Ozean“ wahrgenommen. Bis auf eine Ausnahme fanden allerdings keine Beratungen dieser PRIRODA-Arbeitsgruppen statt. Ursache waren finanzielle und technische Probleme beim Aufbau des PRIRODA-Bodensegments durch IRE und RKK Energia. Dadurch kam es ebenfalls zu Verzögerungen bei der Realisierung und Testung von Teilen der MOS-Software, da notwendige Angaben zu Schnittstellen von der russischen Seite erst nach dem Start von PRIRODA zur Verfügung gestellt wurden. Dies, die starken Störungen des PRIRODA-Telemetriesystems und die spätere Beschädigung von MOS-PRIRODA führten dazu, daß der Primärprozessor (s. Kapitel 3) nicht voll mit realen Daten getestet werden konnte und daher auch nicht an die russische Seite übergeben wurde.

Die nicht stattfindenden Beratungen der internationalen Arbeitsgruppen waren auch der Grund für den verbleibenden Mittelbestand im Reisekostenbudget des Vorhabens.

4. Primärprozessierung MOS

Ein wesentlicher Bestandteil des Fördervorhabens war die Entwicklung des MOS-Primärprozessors bis zum Datenlevel 1B (kalibrierte, systematisch korrigierte und georeferenzierte Radianzwerte am Oberrand der Atmosphäre). Erste Versionen des Prozessors wurden bis 1995 realisiert.

4.1. Algorithm Theoretical Basis Document MOS-Level 1 B

Im Zusammenhang mit der Vorhabensaufstockung wurde vom Gutachtergremium die Auflage erteilt, alle Algorithmen zur Generierung von MOS-Datenprodukten in Form von Algorithm Theoretical Basis Documents (ATBD) nach ESA-Standard zu dokumentieren. Für den Level-1B von MOS-PRIRODA wurde dieses ATBD zur Statuspräsentation im März 1996 vorgelegt. Eine Überarbeitung u.a. mit der Einarbeitung von Modifikationen und Erfahrungen aus der Einsatzphase erfolgte nicht, da im Verlauf des Vorhabens keine regulären Daten von MOS-PRIRODA empfangen wurden (vgl. Schlußbericht „Fernerkundungsexperiment MOS-PRIRODA“, FKZ 50EE9201).

Andererseits wurden nach dem erfolgreichen Start von IRS-P3 und der Inbetriebnahme von MOS-IRS dessen Daten zur Bearbeitung der Aufgaben des Fördervorhabens genutzt. Daher ist in der Anlage das ATBD-Level 1 für MOS-IRS beigefügt. Es stellt ausführlich alle Schritte während der MOS-Primärprozessierung dar.

4.2. MOS-PRIRODA Level-1B Prozessor PRIMUS

Wie bereits dargestellt, war die Erarbeitung des Primärprozessors für MOS-PRIRODA die Basisentwicklung für alle MOS-Prozessoren. Entsprechend der Abstimmung mit den russischen Partnern wurden zwei Versionen entwickelt, die sich bei identischen Eingabe- und Ausgabedaten durch die Art der Steuerung unterschieden:

- a) interaktive Version mit X-11-Benutzeroberfläche zum Einsatz im russischen Datenzentrum PRIRODA
- b) Batch-fähige Version für automatischen Betrieb am DFD des DLR.

Die Abarbeitungsschritte sind detailliert im ATBD „MOS-PRIRODA Level-1B Products“ vom März 1996 dargestellt, Abbildung 4.1 zeigt die Programmstruktur des Prozessors.

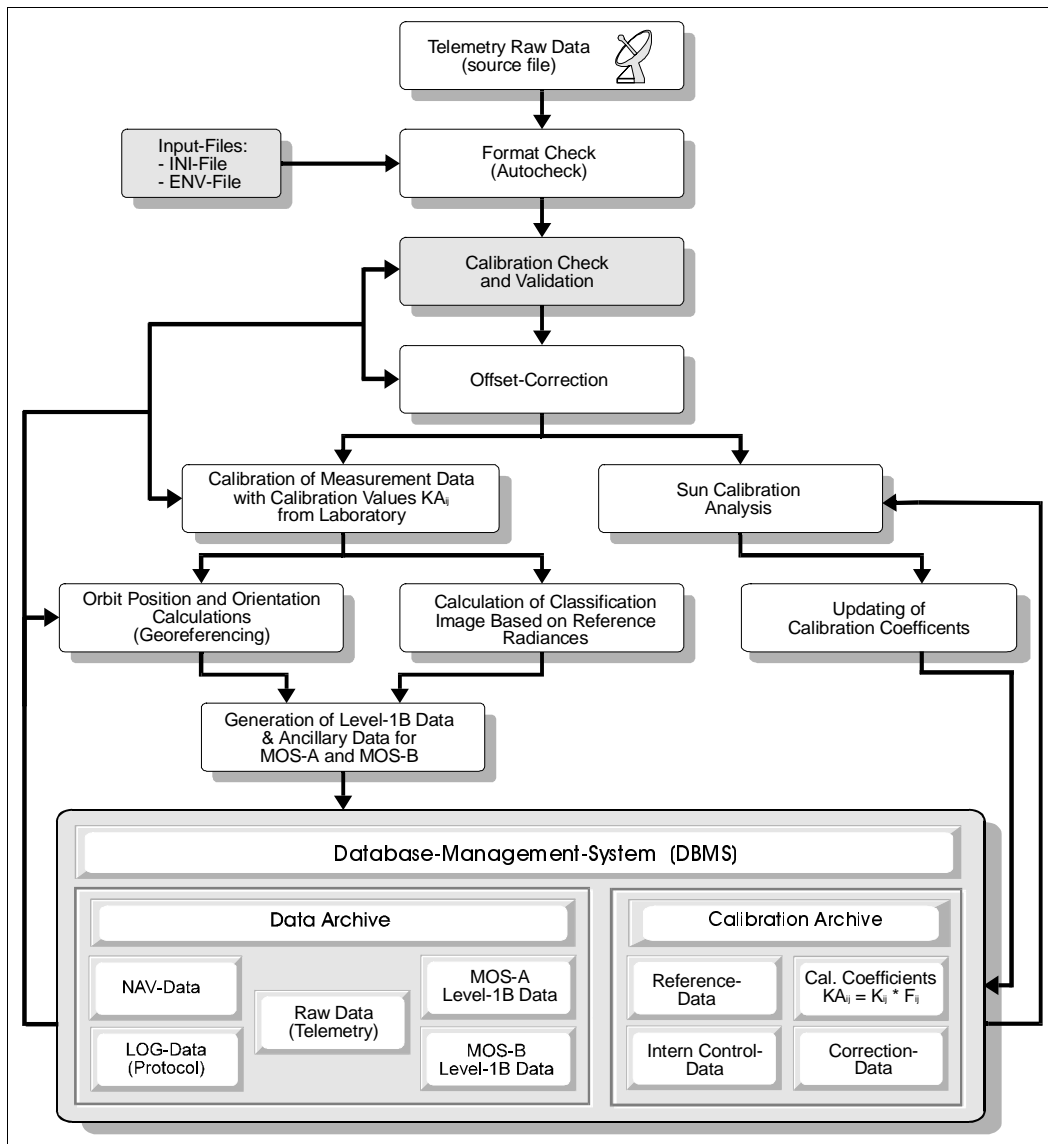


Abb. 4.1: Programmstruktur des Primärprozessors MOS-PRIRODA (PRIMUS)

Die interaktive X-11-Version von PRIMUS (Abb. 4.2) enthält neben der Prozessorfunktion auch die Möglichkeit, das in den Level-1B-Daten enthaltene Quick-Look-Bild und das Klassifikationsbild darzustellen. Auf Grund der Verzögerungen bei der endgültigen Fixierung des Datensystems auf russischer Seite und der fehlenden MOS-PRIRODA-Daten wurde die interaktive PRIMUS-Version nicht bis zu Ende geführt und getestet. Während der Untersuchungen an den wenigen, aber stark gestörten MOS-PRIRODA-Daten wurde die Kommandozeilenversion an Hand realer Daten getestet und vervollkommen, konnte aber nie wirklich operationell genutzt werden. Insgesamt wurden 14 Datentakes von MOS-PRIRODA übertragen. Die Daten waren auf Grund von Telemetriefehlern bzw. der Beschädigung von MOS nicht mit Standardroutinen auswertbar, sondern mußten von Hand korrigiert und lesbar gemacht werden (Bitverschiebungen, doppelte Datenblöcke u.ä.). Abbildung 4.3 zeigt ein Beispiel für die ersten MOS-Daten (interne Kalibrierung) und verdeutlicht die schlechte Telemetriequalität (s.a. Abschlußbericht „Fernerkundungsexperiment MOS-PRIRODA“, FKZ 50EE9201). Für den realisierten Stand der MOS-PRIRODA-Prozessoren liegen die Programmdokumentationen beim DLR vor.

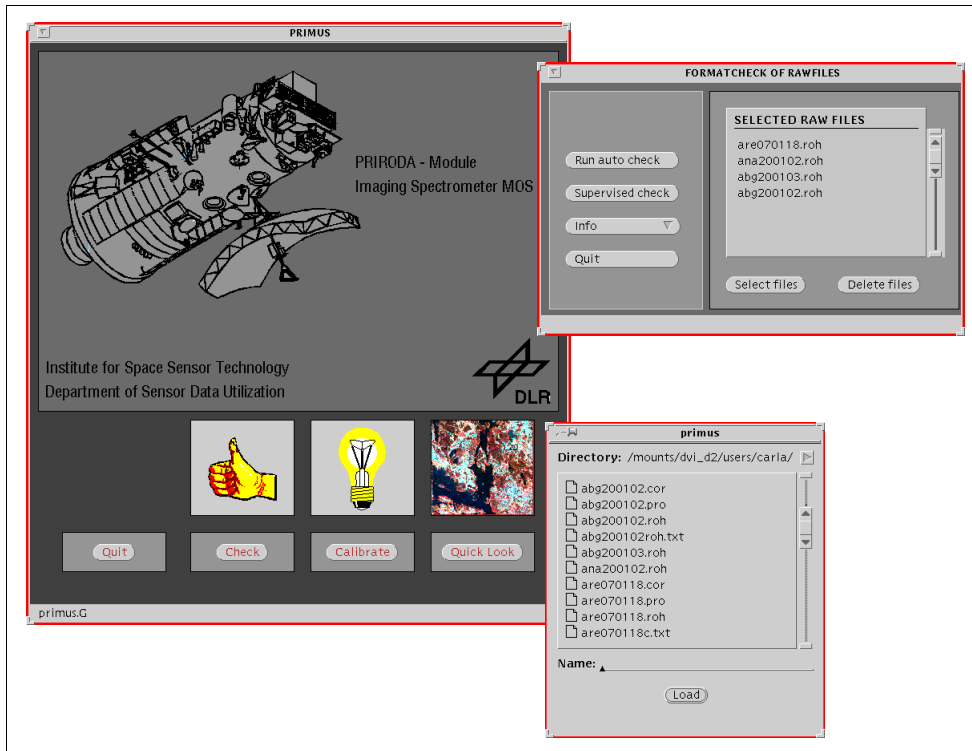


Abb. 4.2: Grafisches Benutzerinterface für PRIMUS

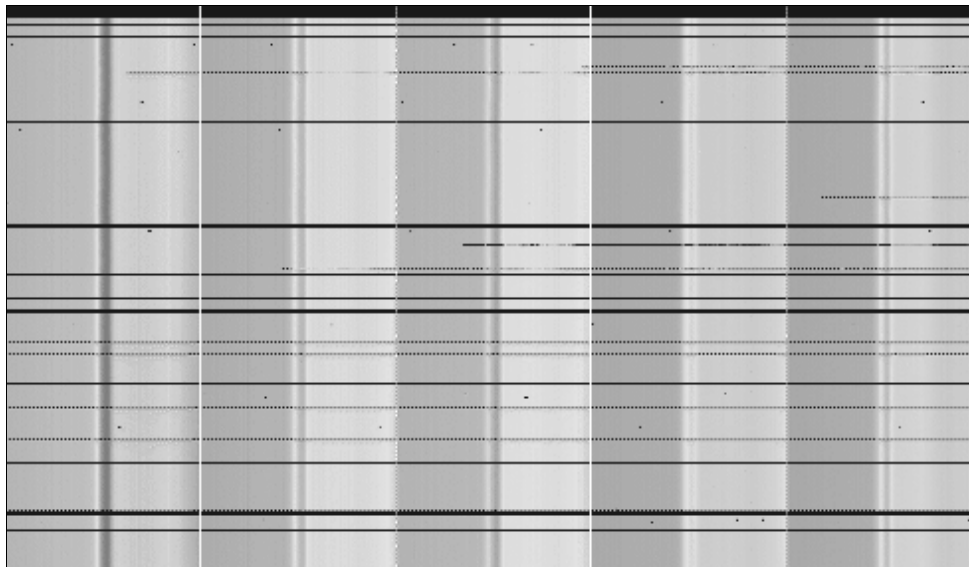


Abb. 4.3: Illustration der Telemetriestörungen bei MOS-PRIRODA: das Bild zeigt einen Datenauszug nach der Synchronisation von Hand. Schwarz sind durch das Telemetriesystem verursachte Datenausfälle.

4.3. MOS-IRS Level-1B Prozessor PRODOMUS

Parallel zum Projekt MOS-PRIRODA wurde auf grundfinanzierter Basis und mit Unterstützung des BMBF das DLR-Projekt MOS-IRS für den gemeinsamen deutsch-indischen Fernerkundungssatelliten IRS-P3 realisiert. Das auf diesem Satelliten eingesetzte abbildende Spektrometer ist eine Weiterentwicklung von MOS-PRIRODA mit verbesserter Bodenauflösung und erweitertem Spektralbereich (SWIR-Kanal MOS-C). Im Gegensatz zum MOS-PRIRODA, wo Daten in zeitlich größerem Abstand und bezogen auf Meßkampagnen erwartet wurden, arbeitet MOS-IRS mit einem präoperationellen Szenario, wobei täglich

Daten von vier Bodenstationen empfangen werden (DLR Neustrelitz, ISRO Hyderabad, ESA Maspalomas, NASA Wallops Island). Für die Prozessierung, Archivierung und Verteilung der Daten wurde daher ein operationell arbeitendes Datensystem implementiert, das auch den Datenaustausch mit verschiedenen Empfangsstationen im Netzwerk ermöglicht. Das Bodensegment des DLR in Neustrelitz übernimmt dabei die Rolle des Master-Archivs, in dem alle verfügbaren MOS-Daten der verschiedenen Empfangsbereiche gesammelt werden.

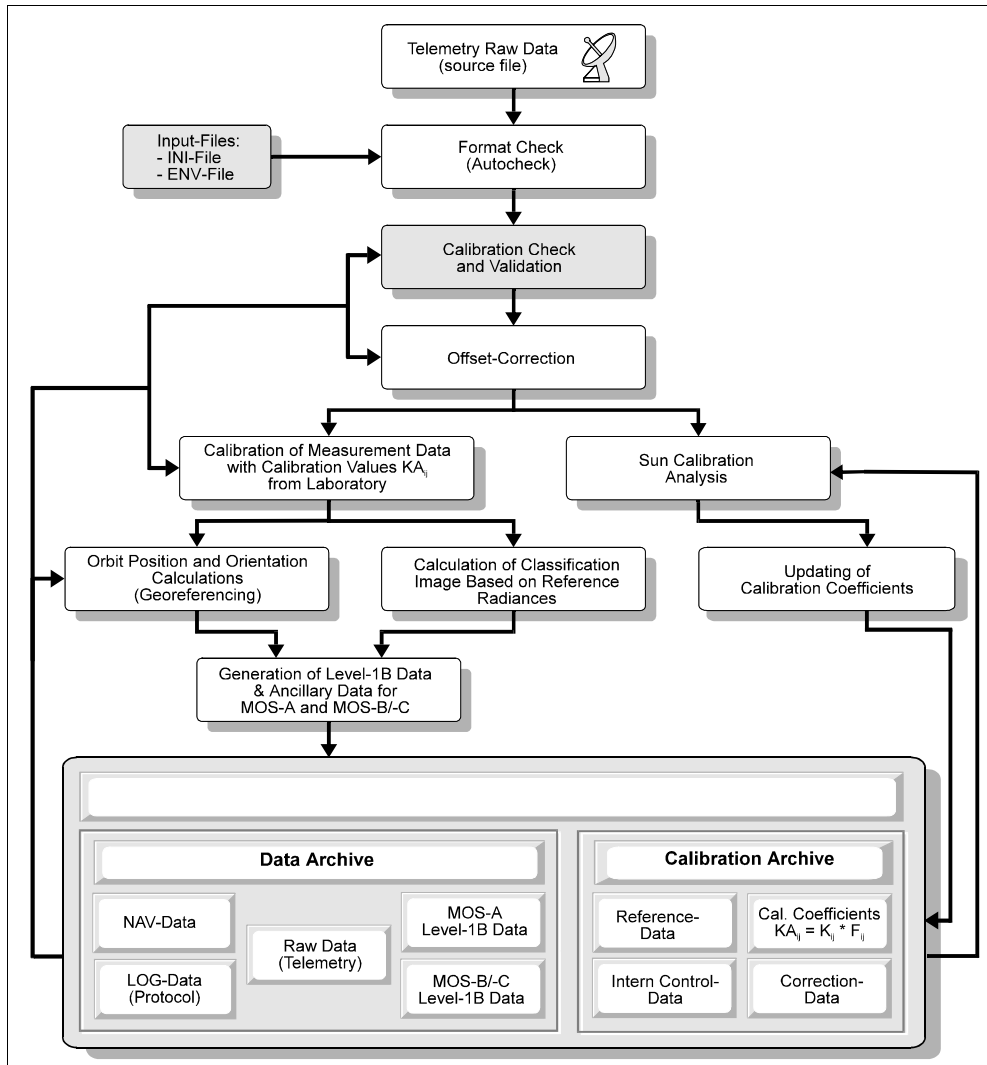


Abb. 4.4: Programmstruktur des Primärprozessors für MOS-IRS (PRODOMUS)

Der MOS-PRIRODA-Primärprozessor diente als Ausgangsbasis für die Entwicklung des MOS-IRS Prozessors PRODOMUS. Dazu wurden entsprechend den modifizierten Datenformaten und Geräteparametern sowie den operationellen Anforderungen Anpassungen vorgenommen. Die Grundstruktur des Prozessors blieb dabei unverändert (Abbildung 4.4). Eine interaktive Version mit grafischem Interface wurde für MOS-IRS nicht realisiert, da der Prozessor im automatisierten Batch-Modus eingesetzt werden sollte. Die Visualisierung der Quick-Looks erfolgt durch das GISIS-Datenbankinterface, die Bilddaten und Headerinformationen aus den Level-1B-Dateien können mittels HDF-Tools und Standard-Bildverarbeitungssoftware dargestellt werden. Eine detaillierte Beschreibung der Datenverarbeitung und Datenformate liegt im ATBD „MOS-IRS Level 1B Data Processing and Products“ vor. Der Prozessor PRODOMUS, der aktuell von vier Bodenstationen im Routinebetrieb genutzt wird, wurde laufend verbessert und mit aktualisierten Kalibrationsdaten versehen. Das Gesamtschema ist dabei so flexibel gestaltet worden, daß auch eine automatische Reprozessierung älterer Datenbestände möglich ist.

4.4. Softwaretools

Zusätzlich zum Standard-Level-1B Prozessor und den Auswertealgorithmen (vgl. Kap. 5) wurden eine Reihe weiterer Werkzeuge implementiert. Diese sind u.a. notwendig für die Inbetriebnahme und Überprüfung der Empfangsstationen und die schnelle Datenanalyse während Meßkampagnen. Weitere Tools dienen der Erleichterung des Umgangs mit den MOS-Daten und der Verbesserung der Datenqualität. Sie stehen den registrierten MOS-Nutzern für ihre Arbeit zur Verfügung und werden entsprechend neuer Erkenntnisse laufend aktualisiert. Die Kurzdokumentationen können dem Anhang entnommen werden. Im einzelnen handelt es sich um folgende Werkzeuge:

- Simulation von MOS-Level-0-Daten zur Testung von Prozessoren und Inbetriebnahme von Bodenstationen
- Anzeige und Analyse von MOS-Housekeeping-Daten zur Testung des Datenempfangs und der Präprozessoren
- Extraktion von Bilddaten aus MOS-Level-0-Daten für Prüf- und Testzwecke
- Extraktion einzelner oder mehrerer Spektralkanäle aus den Level-1B-HDF-Daten in verschiedenen Datenformaten (16-bit integer, Radianzwerte, Reflektanzwerte, Klassifikationsbild, single band, multi band)
- Automatisches Zusammenfügen von Einzelszenen zu längeren Datentakes
- Resampling auf pixelkongruente MOS-A-, -B und -C-Daten
- Konvertierung des MOS-Level-1B-Datenformates (HDF) in das Tera-Scan-Format TDF (SeaSpace Corp., USA) zur Weiterverarbeitung in diesem Programmsystem (Mapping, Mosaicing)
- Korrektur der Georeferenzierung auf TDF-Basis und Aktualisierung der HDF-Header-Information. Dieses Tool ermöglicht auch die nachträgliche Referenzierung von Daten ohne Orbitanbindung (z.B. von mobiler Empfangsstation)
- Streifen- und Reflexionskorrektur der MOS-Daten

Abb. 4.5 gibt eine Übersicht über den Gesamtsoftwarekomplex

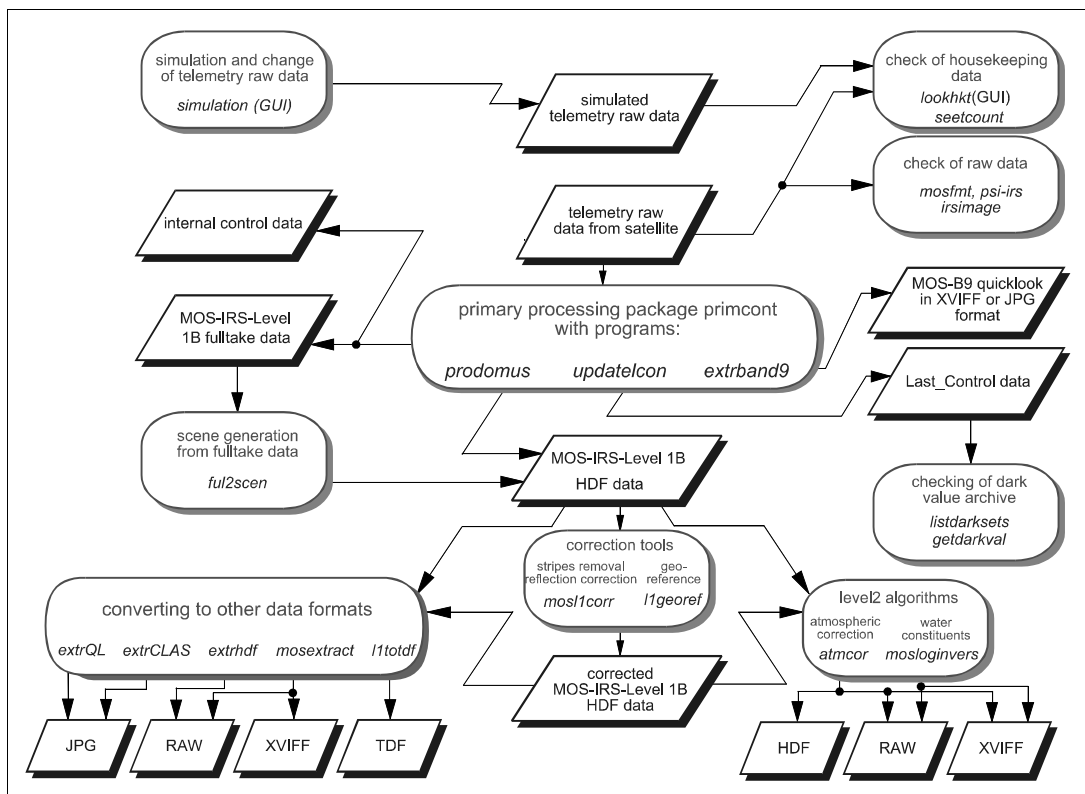


Abb. 4.5: Übersicht über die erstellten Softwarepakete und Utilities für das MOS-Datenhandling

4.4.1. Streifen- und Reflexionskorrektur

Auf das letztgenannte Tool soll hier kurz näher eingegangen werden, da damit eine deutliche Verbesserung der Datenqualität erreicht werden konnte.

Nach dem Start von MOS wurde an Hand der Bilddaten festgestellt, daß durch schwache Mehrfachreflexion zwischen Spaltträger und Eingangsobjektiv sehr lichtschwache Spiegelbilder auftreten. Auch wenn dieses Signal unter 1 % liegt, erzeugt es für die Auswertung von Daten über Wasser bei gemischten Land/Wasser-Szenen ein deutliches Störsignal. Basierend auf der Analyse einer großen Anzahl von MOS-Szenen konnte ein mathematisches Modell zur Korrektur dieser Reflexionen entwickelt werden (Ab. 4.6).

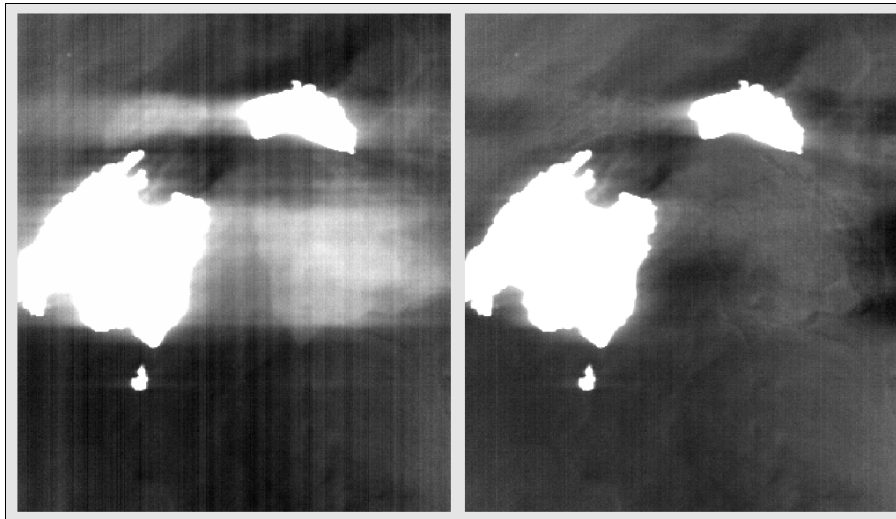


Abb. 4.6: Szene von MOS (Insel Mallorca) vor und nach der Streifen- und Reflexionskorrektur (links bzw. rechts). Die Bilder sind extrem aufgehellt um die Effekte sichtbar zu machen.

Bei den letzten Tests vor dem Transport von MOS-IRS nach Indien wurde festgestellt, daß die in MOS-A und -B eingesetzten CCD-Zeilen im unteren Pegelbereich Trapping-Effekte und Nichtlinearitäten aufweisen (die CCDs waren von einem neuen Hersteller mit modifizierter Technologie im Vergleich zu den originalen „MOS-CCDs“ hergestellt worden). Obwohl eine Optimierung der CCD-Elektronik erfolgte, konnten die Effekte in der Kürze der Zeit bis zum Start nicht vollständig beseitigt werden. Sie führten in den Daten zur deutlich sichtbaren Streifenbildung im Bereich kleinster Signale, speziell über Wasser. In Zusammenarbeit mit der Universität Pisa konnte hier ein Verfahren entwickelt werden, das die Effekte weitgehend korrigiert, ohne die Radiometrie und räumliche Auflösung der Daten zu verschlechtern, wie es übliche Filterverfahren bewirken. Abbildung 4.7 verdeutlicht die erreichte sichtbare Verbesserung der Datenqualität. Zur Abbildung ist eine Anmerkung notwendig. Der Eindruck der unkorrigierten Daten ist schlechter als sie in Wirklichkeit sind, da zum einen die Hauptkomponenten variable Signalanteile verstärken und zum anderen die Bilddarstellungen zur Verdeutlichung kontrastverstärkt sind. Die Details des Verfahrens können den Veröffentlichungen entnommen werden.

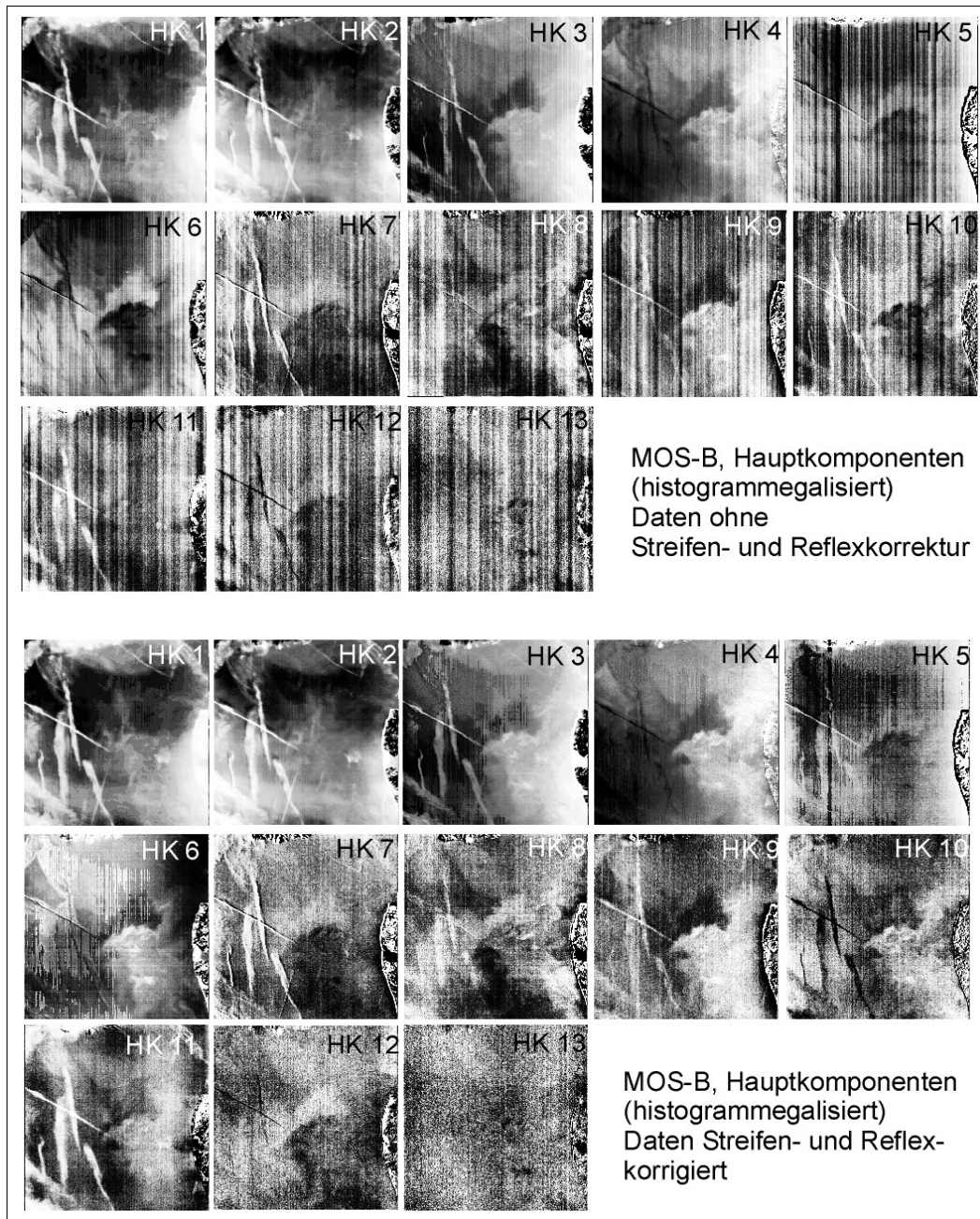


Abb. 4.7: Verbesserung der Datenqualität durch den Destriping-Algorithmus

4.4.2 Tools zur Auswertung von in-Orbit-Kalibrationsdaten

Während der Mission werden Kontrolldaten übertragen, die zur in-Orbit-Kalibration und Stabilitätsüberwachung der Geräteparameter dienen (vgl. Bericht „Fernerkundungsexperiment MOS-PRI“, FKZ 50EE9201):

- interne Kontrolle mittels Kontrolllampen; diese wird am Beginn jeder Einschaltung (Kurze Kontrolle) und im Zusammenhang mit der Sonneneichung (lange Kontrolle) durchgeführt
- Sonneneichung: hier wird in größeren Abständen eine Messung der extraterrestrischen Sonnenstrahlung beim Überflug über den Terminator vorgenommen.

Beide Messungen erzeugen Daten, die außerhalb des Routineprozessings ausgewertet werden müssen. Zur Aufbereitung dieser Kalibrierdaten für die weitere Auswertung wurden

eine Reihe von Softwarewerkzeugen erstellt (Datenselektion, Formatierung und Kalibrationsarchiv).

5. Informationsgehalt spektral hochauflösender Daten

Der Grund für den Einsatz spektral hochauflösender Instrumente in der Fernerkundung ist die genauere Erfassung der spektralen Signatur der betrachteten Objekte. Dies ermöglicht (speziell bei der Landfernerkundung) die Unterscheidung und Zuordnung einer größeren Zahl von Objektklassen. Bei der quantitativen Fernerkundung ist die Zielstellung etwas anders: es sollen die Variationen der Spektralsignatur innerhalb einer Objektklasse erfaßt werden, um über diese Variation Aussagen über den biologischen und/oder physikalischen Zustand des Objektes abzuleiten. Die größere Zahl von Spektralkanälen wird hier nicht benötigt, um eine größere Zahl von Zustandsparametern abzuleiten, sondern um eine bessere Auflösung und quantitative Genauigkeit der aus den Daten abgeleiteten Parametern zu erreichen. Dies ist insbesondere dann wichtig, wenn sich die Wirkungen mehrerer physikalischer Effekte in ein und demselben Spektralbereich überlagern.

Für den vorliegenden Fall der Fernerkundung von Ozeanen und Küstengewässern mit dem abbildenden Spektrometer MOS wurden daher spezielle Untersuchungen zum Informationsgehalt an Hand simulierter Meßdaten durchgeführt, die dann in Kombination mit den entsprechenden physikalischen Modellen (biooptische und Atmosphären-Modelle) die Grundlage für die Entwicklung der Interpretationsalgorithmen (s. Kapitel 7) für MOS bildeten. Die Fragen nach dem Informationsgehalt bedeutet hier, in wie weit sich die Variation der gesuchten physikalischen Parameter (Phytoplanktonkonzentration, Gelbstoff- und Sedimentgehalt, atmosphärische Trübung) in den von MOS gemessenen spektralen Radianzen am Oberrand der Atmosphäre (TOAR) ausprägt und für die Auswertalgorithmen genutzt werden kann.

Grundsätzlich gilt, daß nur die Variation in den TOA-Radianzen für die Inversion genutzt werden kann, die von den Wasserinhaltsstoffen herrührt und auch ohne Korrektur des (störenden) Atmosphärenanteils nachweisbar ist: „Wenn du es nicht siehst, kannst du es auch nicht invertieren.“ Anders gesagt, eine Atmosphärenkorrektur vergrößert nicht das Auflösungsvermögen bezüglich der Wasserinhaltsstoffe, sie entfernt lediglich eine variable aus den multivariaten Meßdaten und vereinfacht damit (scheinbar) das Inversionsproblem.

Auf dieser Erkenntnis aufbauend wurde ein qualitativ neuer Ansatz für einen Interpretationsalgorithmus entwickelt. Kapitel 7 gibt dazu einen Überblick, Details können dem ATBD „MOS-IRS Ocean Colour Level 2 Algorithm“ im Anhang entnommen werden.

An Hand umfangreicher Untersuchungen an simulierten Radianzspektren (s. Literatur) konnte gezeigt werden, daß mit den für MOS angestrebten radiometrischen und spektralen Werten eine sehr gute Ableitung der physikalischen Parameter möglich ist:

- Trennung zwischen Atmosphäreneinfluß und Wasserinhaltsstoffen
- Unterscheidung verschiedener Wasserinhaltsstoffe auf Grund ihrer spezifischen Spektraleigenschaften
- Gute Genauigkeit bei der Quantifizierung der Parameter (vgl. Kap. 7).

Damit stehen erstmals Satellitendaten zur Verfügung, die auch für den komplizierten Fall der Küsten- und Binnengewässer, in denen gleichzeitig verschiedene Inhaltsstoffe in verschiedenen Kombinationen auftreten, die Ableitung quantitativer Auswertalgorithmen erlauben.

6. Problemspezifische Datenkompression

Zu Beginn der Arbeiten am MOS-Projekt stand die Forderung, die Ausgangsdatenrate von MOS durch geeignete Verfahren der Datenkompression an die geringere Datenrate des geplanten Telemetriesystems anzupassen. Auf Grund der hohen Anforderungen an die Meßgenauigkeit (Radiometrie) der MOS-Daten erschien hierfür die Nutzung der üblichen Bildkompressionsverfahren (Blockkodierung, Kosinustransformation, ...) nicht möglich. An Hand von Daten der Vorgängerspektrometer der MKS-Serie (nicht abbildende Spurspektrometer) wurden daher umfangreiche Untersuchungen zur Datenkompression mittels statistischer Codes (Huffman, Fano) durchgeführt. Es konnte gezeigt werden, daß für Ozeandaten mit diesem Verfahren eine ausreichende Kompression erreicht werden kann (ca. Faktor 4). Auf Grund des später für PRIRODA entwickelten leistungsfähigeren Telemetriesystems wurden diese Verfahren jedoch nicht mehr benötigt.

Für eine operationelle Datenübertragung mit geringer Telemetrikapazität konnte später, basierend auf dem real-time-fähigen Interpretationsalgorithmus (s. Kapitel 7) und der inzwischen immens gestiegenen Leistungsfähigkeit der Bordcomputer eine direkte Berechnung der physikalischen Parameter an Bord vorgeschlagen werden. Diese würde zwar einerseits einer Datenreduktion um etwa das zwanzigfache ermöglichen, andererseits jedoch die Nutzung der Daten für andere Anwendungen (Land, Atmosphäre) versperren. Da das für eine wissenschaftliche Experimentalmission nicht wünschenswert ist und die Algorithmen zum Zeitpunkt des Starts auch noch nicht validiert waren, wurde auf die Implementierung dieser Möglichkeit verzichtet. Für zukünftige, dedizierte Missionen steht das Verfahren zur Übertragung von Chlorophyll- oder Schwebstoffkarten, z.B. über eine HRPT-Telemetrie zur Verfügung.

Die durchgeführten Untersuchungen zum Informationsgehalt und zur Dimensionalität der MOS-Daten mittels Hauptkomponentenanalyse zeigen, daß mittels Hauptkomponententransformation und anschließender Unterdrückung der „nicht signifikanten“ Komponenten eine dem Datentyp adäquate Datenreduktion erreicht werden kann. Eine anschließende statistische Kodierung erlaubt eine weitere Kompression bei der heute zur Verfügung stehenden Rechenleistung an Bord stellt die Implementierung kein prinzipielles Problem mehr dar. Die Datenqualität ist im Vergleich mit den üblichen (verlustbehafteten) Bildkompressionsverfahren deutlich besser.

7. Algorithmenentwicklung für die Ozean-Fernerkundung

Die Entwicklung von speziellen Auswertalgorithmen zur quantitativen Ableitung von Wasserinhaltsstoffen aus MOS-Daten war neben der experimentbezogenen Softwareentwicklung der Hauptschwerpunkt des Fördervorhabens. Zwei Themenkomplexe wurden hier bearbeitet:

- a) Implementierung eines einfachen Verfahrens zur Atmosphärenkorrektur
- b) Entwicklung und Testung eines multispektralen Algorithmus zur Bestimmung von Chlorophyllkonzentration, Sedimentgehalt und Gelbstoffgehalt aus den VIS/NIR-Daten von MOS-B.

Beide Algorithmen wurden implementiert, erfolgreich getestet und an Hand von Fallbeispielen validiert.

7.1 Einfache Atmosphärenkorrektur über Wasser

In Abstimmung mit dem separaten Fördervorhaben „Atmosphärenkorrektur MOS“ (FKZ 03EE4649) wurde ein einfacher Korrekturalgorithmus für MOS-Daten über Wassergebieten implementiert. Er beruht auf dem sogenannten Gordon-Ansatz, bei dem davon ausgegangen wird, daß die bei Wellenlängen oberhalb 700 nm gemessene Radianz am Satelliten nur vom Oberflächenterm und der Streuung in der Atmosphäre herrührt und nicht von Wasserinhaltsstoffen beeinflusst wird („black water condition“). Für die Charakterisierung der Spektralabhängigkeit des Aerosolterms wird ein Potenzansatz nach Angstroem benutzt. Diese Atmosphärenkorrektur dient im wesentlichen dem Vergleich mit anderen Sensoren (z.B. SeaWiFS) und als schnelles Hilfsmittel solange die komplizierteren Verfahren noch nicht validiert zur Verfügung stehen.

Für die eigenen Arbeiten und ausgewählte Kooperationspartner wird die Software zur Bereitstellung atmosphärenkorrigierter MOS-Daten genutzt. Ein Beispiel ist die routinemäßige Berechnung von Chlorophyllkarten der Ostsee durch das Deutsche Fernerkundungsdatenzentrum DFD.

7.2 Bestimmung von Wasserinhaltsstoffen mittels Hauptkomponenteninversion

Aufbauend auf den Untersuchungen zum Informationsgehalt der MOS-Daten und den verfügbaren physikalischen Modellen wurde ein neuer Ansatz für einen Interpretationsalgorithmus entwickelt, implementiert und getestet. Für die Details sei auf die Anlage „Algorithm Theoretical Basis Document – MOS-IRS Ocean Colour Level-2 Algorithm“ (ATBD) verwiesen. Im vorliegenden Bericht werden nur die Grundansätze und wesentliche Ergebnisse vorgestellt.

Die „klassischen“ Inversionsverfahren zur Ableitung von Wasserinhaltsstoffen verwenden Verhältnisse der aus dem Wasser austretenden Strahlung in zwei Spektralkanälen (Farbverhältnisalgorithmen). Sie sind aus Korrelationsuntersuchungen zwischen Fernerkundungsmessungen und in-situ-Daten abgeleitet worden. Diese Algorithmen haben eine Reihe charakteristischer Eigenschaften:

- Setzen das Vorhandensein einer großen Zahl von in-situ-Datensätzen voraus (aufwendig; Nachteil)
- Gelten für den speziellen untersuchten Wasserkörper, d.h. die entsprechend gültigen inhärenten optischen Eigenschaften und Gemische der Inhaltsstoffe (Vorteil)
- Lassen sich nicht verallgemeinern, Anpassung an andere Wassertypen wiederum nur über extensive Bodenmessungen (Nachteil)
- Empirischer Ansatz, daher einerseits robust, andererseits schlecht erweiterbar (Vorteil und Nachteil)
- Für die sogenannten case-2-Gewässer, in denen mehrere verschiedene Inhaltsstoffe gleichzeitig variieren, ist die in zwei Spektralkanälen enthaltene Information nicht ausreichend, um die einzelnen Komponenten sicher zu trennen und zu quantifizieren (Nachteil).

Aus diesen Gründen und unterstützt durch die Untersuchungen zum Informationsgehalt wurden an den zu entwickelnden Algorithmus die Forderungen gestellt:

- Ableitung auf der Basis eines biooptischen Modells für den Wasserkörper mit den 3 Hauptklassen von Inhaltsstoffen und Strahlungstransportsimulation für die Atmosphäre (semi-analytischer Ansatz)
- Möglichkeit der Optimierung für verschiedene Wassertypen, d.h. inhärente optische Eigenschaften
- Nutzung des vollen verfügbaren spektralen Informationsgehaltes, d.h. Verwendung einer größtmöglichen Zahl von Spektralkanälen.

Der Vorteil dieser Klasse von Algorithmen ist, daß sie sich durch die Anpassung der verwendeten Modelle für verschiedene Einsatzfälle optimieren läßt und erreichbare Genauigkeiten sowie der Einfluß von Störgrößen analytisch untersucht werden können (Sensibilitätsanalyse).

Ebenso bestand das Ziel, einen Algorithmus zu entwickeln, der ohne Atmosphärenkorrektur die Wasserinhaltsstoffe direkt aus den Satellitenstrahldichten am Oberrand der Atmosphäre bestimmt, da diese Daten bereits alle Information bezüglich des Wasserkörpers enthalten (Top-of-Atmosphere, TOA-Ansatz).

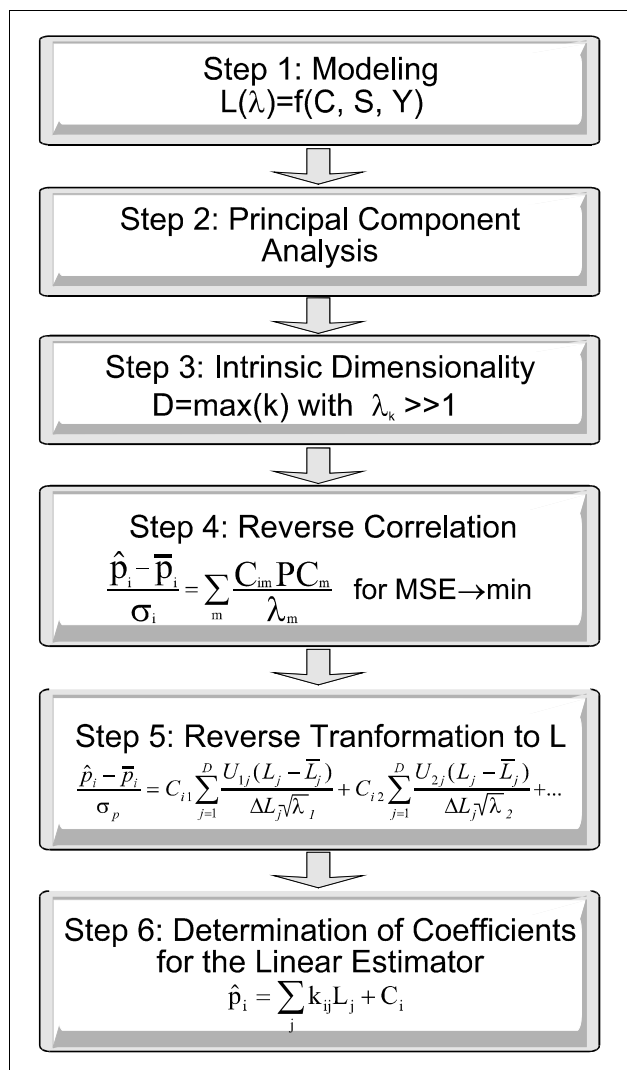


Abb. 7.1: Schema der Hauptkomponenteninversion

Das vorgestellte, qualitativ neue Ansatz konnte zu einem lauffähigen Algorithmus entwickelt und implementiert werden und wurde an umfangreichen simulierten und „echten“ MOS-Datensätzen getestet. Abbildung 7.2 zeigt das gesamte realisierte PCI-Verfahren. Die Untersuchungen an Hand simulierter Daten hat gezeigt, daß:

Der vorgestellte, qualitativ neue Ansatz konnte zu einem lauffähigen Algorithmus entwickelt und implementiert werden und wurde an umfangreichen simulierten und „echten“ MOS-Datensätzen getestet. Abbildung 7.2 zeigt das gesamte realisierte PCI-Verfahren. Die Untersuchungen an Hand simulierter Daten hat gezeigt, daß:

- Der in den Daten am Oberrand der Atmosphäre dominierende Atmosphäreinfluß durch den Algorithmus sehr gut unterdrückt wird, d.h. die Trennung zwischen Atmosphäre und Wasserfarbe gelingt

Die Schwierigkeit bei der Entwicklung eines solchen spektral hochdimensionalen Algorithmus besteht darin, daß eine multiple Regression eines korrelierten Datensatzes (spektrale Radianzwerte) mit den physikalischen Eingangsparametern der Simulation realisiert werden muß, die a priori zunächst unkorreliert sind. Die Lösung derartiger schlecht konditionierter Aufgaben ist numerisch nicht immer gut umsetzbar. Im vorliegenden Fall wurde daher ein „Umweg“ gegangen: die Spektralmessungen werden über ihr Eigenvektorsystem in die Hauptkomponenten transformiert. Diese enthalten die identische Information wie die Spektraldaten, sind jedoch untereinander unkorreliert (Orthogonaltransformation). Auf Grund ihrer mathematisch bedingten Eigenschaften kann durch Weglassen der höheren Hauptkomponenten auch eine „Rauschunterdrückung“ erfolgen, d.h. nicht physikalisch interpretierbare Anteile in den Daten bleiben bei der Analyse und Ableitung des Algorithmus unberücksichtigt. Die eigentliche Bestimmung der gesuchten physikalischen Parameter aus den Multispektraldaten erfolgt dann durch gewichtete Linearkombination der Spektraldichten. Die Wichtungsfaktoren werden aus den Hauptkomponenten abgeleitet. In Abbildung 7.1 sind die einzelnen Schritte des Verfahrens dargestellt. Es wird auf Grund der methodischen Vorgehensweise als Hauptkomponenteninversion (Principal Component Inversion, PCI) bezeichnet. Bezüglich der mathematischen Details und der verwendeten physikalischen Modelle wird nochmals auf die ATBD verwiesen.

- Die Trennung der 3 Hauptklassen von Wasserinhaltsstoffen (Chlorophyll, Sediment, Gelbstoff) an Hand der Spektralinformation möglich ist
- Die Quantifizierung der Wasserinhaltsstoffe, auch für den schwierigen Fall von case-2-Gewässern, in einem weiten Variations- und Kombinationsbereich der einzelnen Komponenten mit einem Fehler $\leq 30\%$ möglich ist
- Der Algorithmus durch die Verwendung angepaßter Look-Up-Tabellen für die spezifischen Eigenschaften verschiedener Wasserkörper optimiert werden kann (saisonale und regionale Spezifika).

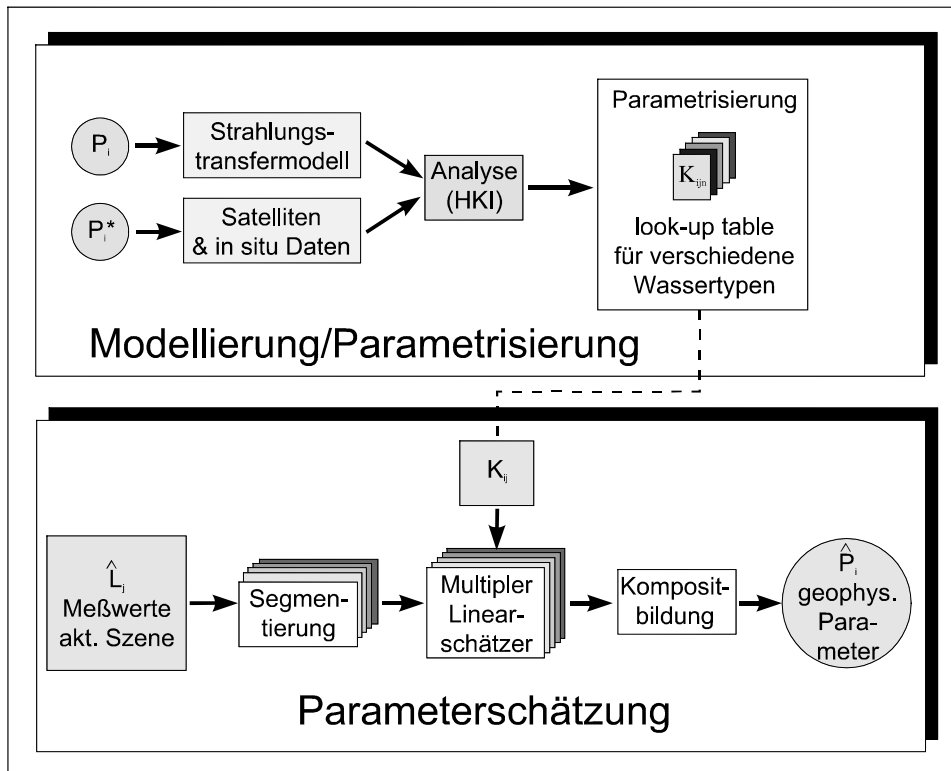


Abb. 7.2: Implementierung des PCI-Algorithmus

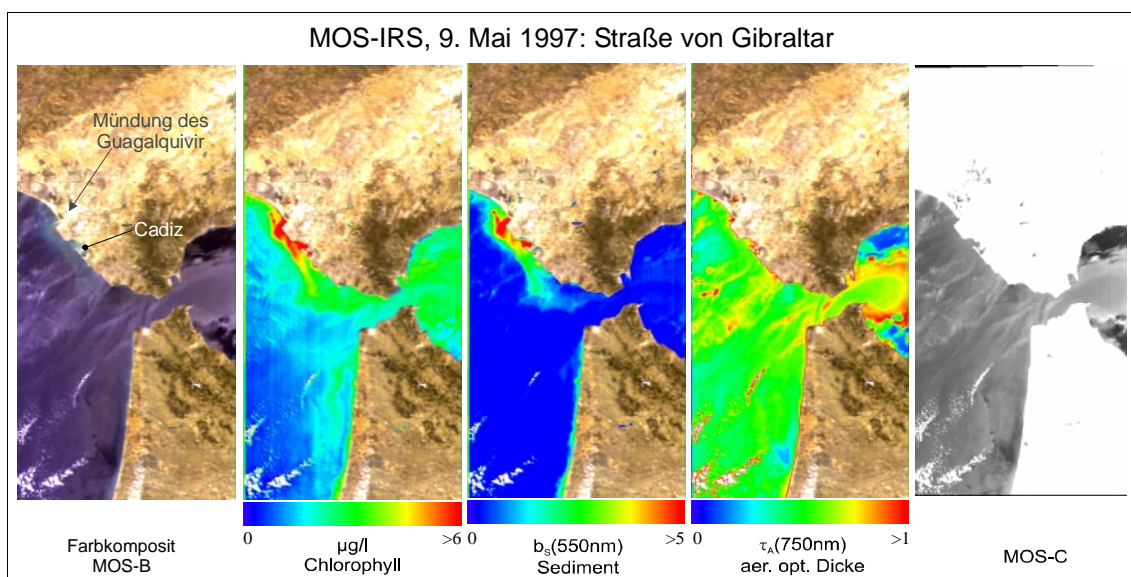


Abb. 7.3: Trennung der Komponenten aus den MOS-TOA-Radianzen mittels PCI

In Abbildung 7.3 ist ein Beispiel gezeigt, das sowohl die Realisierbarkeit des TOA-Ansatzes als auch die grundsätzliche Leistungsfähigkeit des PCI-Algorithmus an Hand von MOS-Daten demonstriert: in der dargestellten Szene ist eine starke Dynamik in der Atmosphäre vorhanden (vgl. Bild von MOS-C) als auch ausgeprägte räumliche Variationen der Wasserinhaltsstoffe. Die mittels PCI aus den TOA-Daten abgeleiteten physikalischen Parameter zeigen deutlich, daß auch unter solch schwierigen Bedingungen die Trennung zwischen den einzelnen Komponenten sehr gut gelingt, eine „über-Kreuz“ – Beeinflussung erfolgreich unterdrückt wird.

7.3 Spezifisches biooptisches Modell für die Ostsee

Für alle semianalytischen Algorithmen sind die verwendeten (optischen) Modelle ein kritischer Punkt. Nur wenn sie die physikalische Realität adäquat widerspiegeln, können erfolgversprechende und robuste Algorithmen abgeleitet werden. Im konkreten Fall der Ableitung von Wasserinhaltsstoffen aus Fernerkundungsdaten tritt dabei generell das Problem auf, daß sich die optischen Eigenschaften des Wasserkörpers, speziell im Fall der Küsten- oder case-2-Gewässer, regional und saisonal stark unterscheiden können. Daher wird angestrebt, die Algorithmen über adaptierbare Komponenten (z.B. Look-Up-Tabellen) an solche spezifischen Eigenschaften anpassen zu können.

Für den entwickelten PCI-Algorithmus wurden bisher drei Wassertypen eingearbeitet: ein case-1-Modell für den offenen Ozean (nur Chlorophyll, z.B. Kanarenbecken), ein „globales“ case-2-Modell (Chlorophyll, Sediment und Gelbstoff für Küstengewässer) und ein spezifisches Modell für die Ostsee.

Das eigentliche biooptische Ostseemodell wurde auf der Grundlage langjähriger Messungen der Absorptions- und Streueigenschaften der Inhaltsstoffe in der Ostsee vom Institut für Ostseeforschung, Warnemünde (IOW), entwickelt. Das Institut war im PRIRODA-Verbundvorhaben mit einem eigenen Projekt „Ableitung von Wasserinhaltsstoffen aus MOS-B-Daten“ (FKZ 50EE9216) beteiligt. Basierend auf den vom IOW bereitgestellten inhärenten optischen Eigenschaften wurde eine Anpassung an das für den PCI verwendete 3-Komponenten-Modell vorgenommen und daraus spezielle Koeffizientensätze für die Auswertung von Ostseedaten generiert.

8. Algorithmvalidierung und Beispiele

Die Validierung eines Algorithmus zur quantitativen Bestimmung von Wasserinhaltsstoffen aus Fernerkundungsdaten erscheint auf den ersten Blick sehr einfach: die abgeleiteten Werte in den Pixeln, für die in-situ-Konzentrationen vorliegen, werden mit den Bodenmessungen verglichen, die absoluten bzw. relativen Abweichungen liefern die Aussage zur Qualität des Fernerkundungsverfahrens. Obwohl dieser Vergleich ein wichtiges Kriterium liefert, stellt sich die Praxis etwas komplizierter dar:

- die Bestimmung der in-situ-Konzentrationen ist selbst mit einem z.T. nicht unbeträchtlichen Fehler behaftet ($\leq 30\%$)
- die Bodenmessungen ist eine Punkt-Messung. Sie wird mit einem Integral über die Pixelfläche (bei MOS 500x500 m²) abgeleiteten Wert verglichen. Im Wasser treten jedoch kleinräumige, z.T. beträchtliche Variationen der Inhaltsstoffe auf (Patchiness), die zu Abweichungen zwischen abgeleitetem Satellitenwert und Bodenmeßwert führen können.
- die aus Wasserschöpfungen bestimmten Konzentrationswerte gelten für eine bestimmte Wassertiefe. Das Satelliteninstrument mißt hingegen ein Signal, das durch die Inhaltsstoffe in einer bestimmten Schicht bestimmt wird, deren Dicke wiederum von der Konzentration der Inhaltsstoffe abhängt.

- es wird eine große Zahl von Bodenmessungen (> einige Dutzend) bei verschiedensten Konzentrations- und Mischungsverhältnissen benötigt, um die Validierungsergebnisse statistisch abzusichern bzw. den Auswertalgorithmus zu optimieren.

Insbesondere die letzte Bedingung ließ sich in dem zur Verfügung stehenden Zeitraum und bei der durch Ressourcen und missionstechnisch beschränkten Zahl von Meßkampagnen nicht realisieren. Darüber hinaus muß angemerkt werden, daß die radiometrische Validierung der MOS-Daten bis zum Ende des Vorhabens auf Grund technologischer Probleme nicht vollständige abgeschlossen werden konnte.

Aus diesen Gründen muß die vorliegende Validierung des PCI-Algorithmus zur Ableitung von Wasserinhaltsstoffen aus TOA-MOS-Radianzen als vorläufig betrachtet werden. Die in den Abbildungen 8.1 bis 8.3 gezeigten Beispiele zeigen jedoch, daß die Vorhabenszielstellung der Quantifizierung der Inhaltsstoffe mit einem Fehler von $\leq 30\%$ realisiert werden konnte. Die weitere Optimierung wird die bisher erreichten Ergebnisse noch verbessern. Die Abbildungen 8.4 und 8.5 zeigen weitere Beispiele für die Anwendung des PCI-Algorithmus.

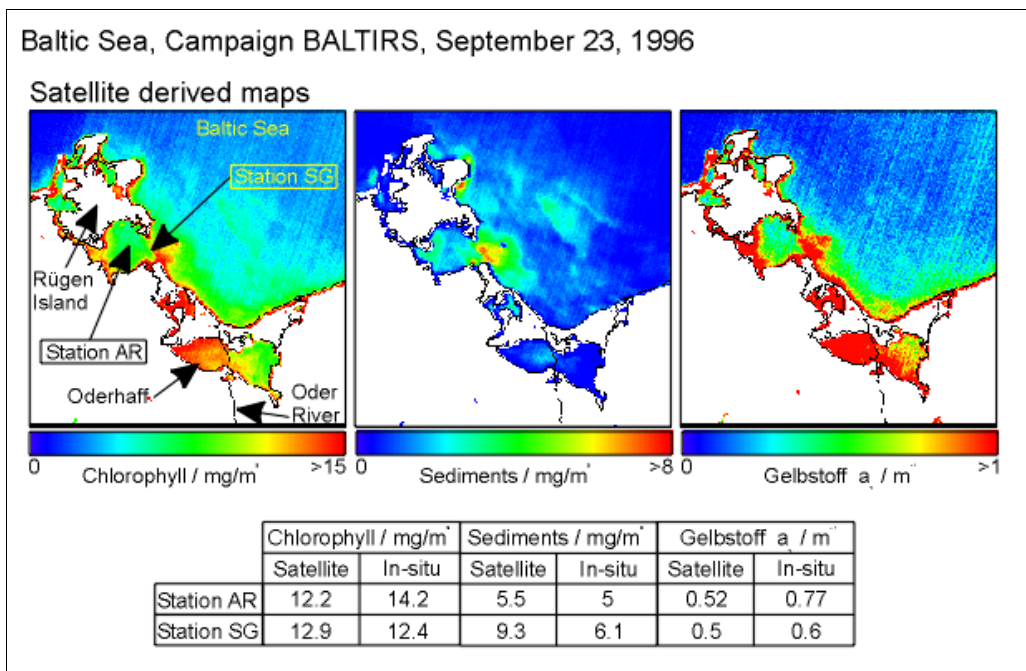


Abb. 8.1: Validierungskampagne BALTIRS-1, stark Gelbstoff-haltiges Küstenwasser

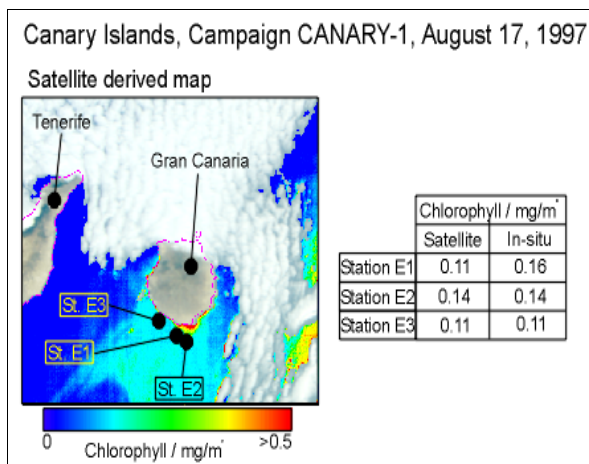


Abb. 8.2: Validierungskampagne CANARY-1, sauberes Ozeanwasser

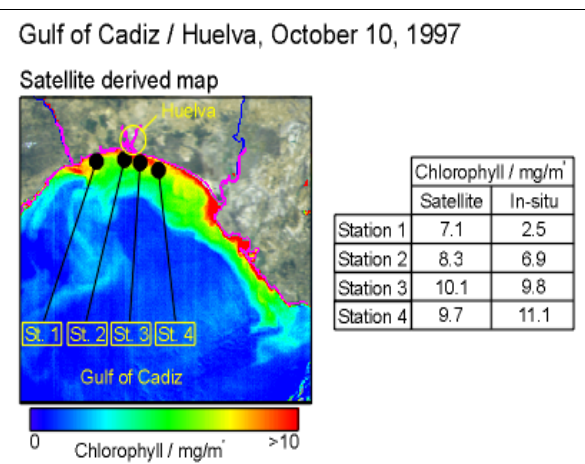


Abb. 8.3: Validierungskampagne Huelva, sedimenthaltiges Küstenwasser

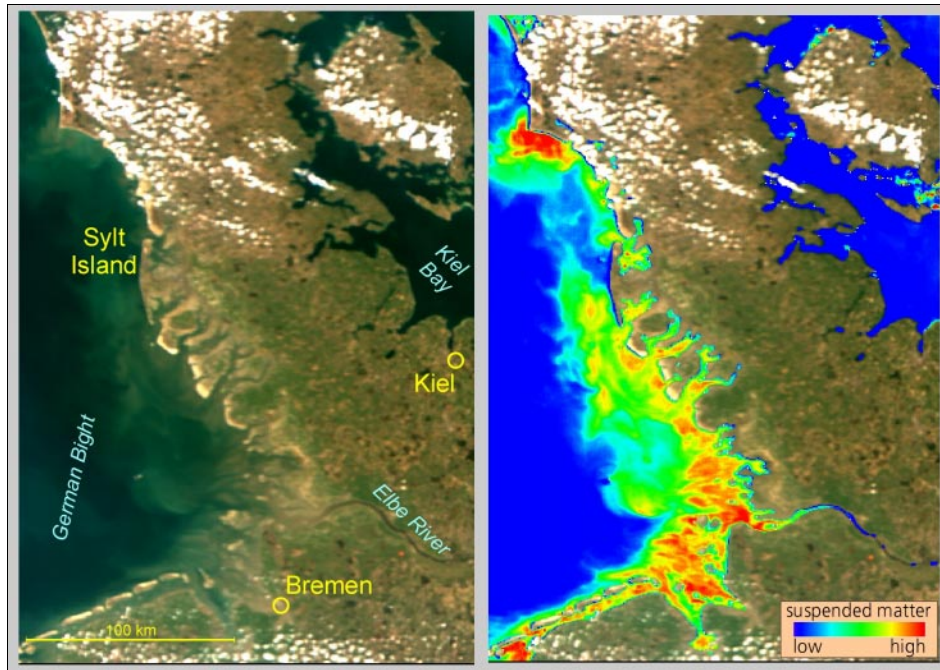


Abb. 8.4: Schwebstoffgehalt in der Deutschen Bucht, Mai 1998

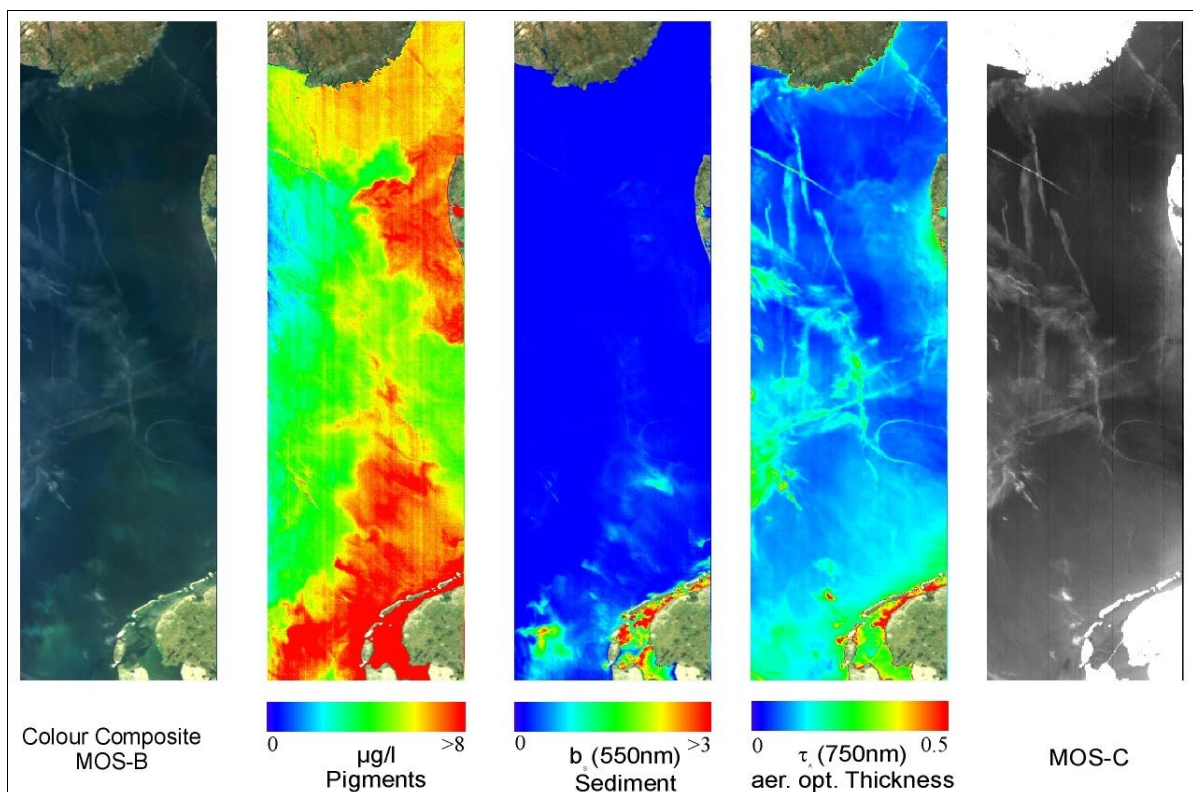


Abb. 8.5: Starke Algenblüte in der Nordsee. Ebenfalls gut erkennbar die Kondensstreifen in der abgeleiteten optischen Dicke.

9. Zusammenfassung

Es kann insgesamt eingeschätzt werden, daß die Ziele des Fördervorhabens technisch und wissenschaftlich innerhalb des Zeit- und Kostenrahmens erfüllt wurden. Es liegt in der Natur von Forschungsarbeit, daß nicht alle Möglichkeiten ausgereizt werden konnten. Daher werden die Arbeiten auch im Rahmen des DLR F&E-Programms und weiterer Projekte fortgeführt. Folgende wesentliche Ergebnisse seien hier nochmals zusammengefaßt:

- gemeinsam mit den anderen Vorhaben des MOS-Verbundes konnte erstmals für ein deutsches Langzeit-Fernerkundungsexperiment die End-to-End-Kette erfolgreich implementiert und operationell demonstriert werden
- Es wurde ein qualitativ neues, spektral hochdimensionales Auswerteverfahren entwickelt, das einerseits den vollen Informationsgehalt von Spektrometerdaten nutzen kann und andererseits für verschiedene regionale und saisonale Spezifika optimiert werden kann.
- Es konnte erstmals experimentell gezeigt werden, daß die Trennung der verschiedenen Inhaltsstoffe im schwierigen Fall der Küstengewässer an Hand von Satellitendaten möglich ist und die Quantifizierung mit guter Genauigkeit gelingt
- Es konnte erfolgreich demonstriert werden, daß die Trennung und Quantifizierung der verschiedenen Komponenten direkt aus TOA-Radianzen, d.h. ohne Atmosphärenkorrektur gelingt
- Das entwickelte Verfahren ist sehr schnell und stabil und kann daher in zukünftigen Systemen auch im Echtzeitbetrieb zur Generierung von Parameter- und Eventkarten eingesetzt werden.

Es sei im Abschluß darauf verwiesen, daß u.a. mit den Fördervorhaben des MOS-Verbundes und im Rahmen des DLR FGE-Programms allen technischen und wissenschaftlichen Problemen sowie auch politischen Widrigkeiten zum Trotz eine Führungsposition im internationalen Rahmen erobert werden konnte, die hoffentlich eine Fortsetzung finden wird. Die Ergebnisse konnten mit einem Ressourceneinsatz realisiert werden, der im Vergleich mit ähnlichen Vorhaben als eher gering eingeschätzt werden muß.

Wesentliche Erkenntnisse und Erfahrungen aus den Fördervorhaben haben sich in einem neuen Instrumenten- und Missionskonzept zur regionalen Ökosystem-Fernerkundung niedergeschlagen, das u.a. gemeinsam mit anderen europäischen Forschungseinrichtungen als „ECOMON-A Dedicated Mission for Regional Ecosystem Monitoring“ der ESA im Rahmen des Earth Explorer Opportunity Programs vorgeschlagen wurde.

9. Verzeichnis der im Rahmen des Fördervorhabens entstandenen Dokumente und Veröffentlichungen

A. Projektinterne Berichte und Dokumentationen

- A.1 „Softwaredokumentation Werks-KIA MOS“, 1992
- A.2 „Datenanalyseprogramm für MOS –System-KIA: Programmbeschreibung und Installationshinweise“, 1992
- A.3 „Datenanalyseprogramm für MOS System-KIA: Anleitung zur Durchführung der PSI-Datenauswertung“, 1992
- A.4 „Datenkonzeption MOS-PRIRODA“, 1992
- A.5 „Prolmage: Quick-Look und Verarbeitungssystem für multispektrale Bilddaten“, 1992
- A.6 „High Resolution Environment Spectrometer HiRES: Quick-Look und Datenanalyse Softwarepaket“, 1993
- A.7 „MOS-PRIRODA Data processing, Software and Data Products“, 1994
- A.8: „Statuspräsentation Ozean-Fernerkundung, November 1995“
- A.9 „International Earth Remote Sensing Mission PRIRODA: Modular Optoelectrical Scanner MOS – User Guide“, 1995
- A.10 „Experiment MOS-PRIRODA – Executive Summary“, 1996
- A.11 „MOS-IRS Data Processing, Software and Data Products“, 1995
- A.12 „Detailed Description of MOS-IRS Primary processing Package PRIMCONT“, 1996
- A.13 „Ableitung von Algorithmen zur quantitativen Bestimmung von Wasserinhaltsstoffen aus Fernerkundungsdaten – Zusammenfassung und Systematisierung“, 1994
- A.14 „One Year of Remote Sensing with MOS“ (CD-ROM), 1997
- A.15 „MOS- IRS Data Analysis Considering the Effects of Sun Glint, Aerosol and Instrument Calibration“ (mit MHI Sewastopol), 1997
- A.16 „Algorithm Theoretical Basis Document: MOS-PRIRODA Level 1B Products (Draft)“, 1996
- A.17 „Algorithm Theoretical Basis Document: MOS-IRS Level 1B Products“, 1999
- A.18 „Algorithm Theoretical Basis Document: MOS-PRIRODA Ocean Colour Level 2 Algorithm (Draft)“, 1996
- A.19 „Algorithm Theoretical Basis Document: MOS-IRS Ocean Colour Level 2 Algorithm“, 1999
- A.20 „Kurzdokumentation Softwaretools für MOS“, 1999
- A.21 Proceedings of the 1st International Workshop on MOS IRS and Ocean Colour, 28.-30. April 1997, DLR, Berlin, Germany
- A.22 „Relative and Absolute Calibration of MOS-B data: preliminary report“, February 12, 1999, (Corsini, G.; Diani, M.; Grasso, R.; Rinaldi, R., Uni Pisa)

B. Veröffentlichungen

- B.1 **Corsini G., Diani M., Grasso R., Rinaldi R., Walzel T.:** „MOS-B sensor calibration: a signal processing approach, in Vorbereitung für IGARSS 1999
- B.2 **Hetscher M., Krawczyk H., Neumann A., Walzel T., Zimmermann G.:** „Algorithm Development for the Retrieval of Coastal Water Constituents from Satellite MOS-Images“, Int. Symposium on Optical Science, Engineering and Instrumentation, 27.07.-01.08.1997, San Diego, California, USA, SPIE Vol. 3118, pp 161-167
- B.3 **Hetscher M., Krawczyk H., Neumann A., Walzel T., Zimmermann, G.:** „Capabilities for the Retrieval of Coastal Water Constituents (Case II) Using Multispectral Satellite Data“ International Symposium on Remote Sensing, September 21-24, 1998, Barcelona, Spain, SPIE Vol. 3496

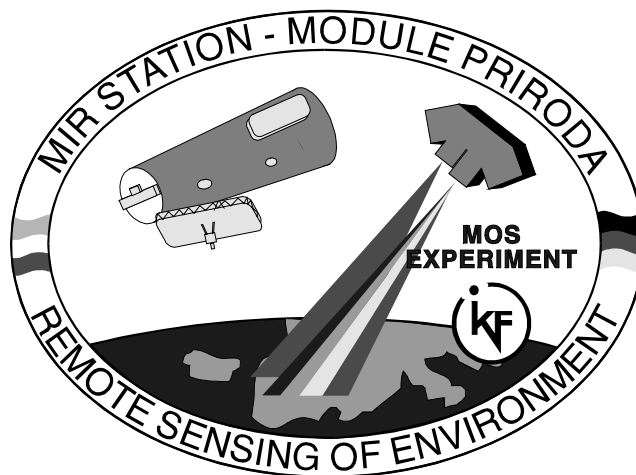
- B.4 **Hetscher M., Krawczyk H., Neumann A., Walzel T., Zimmermann, G.:** „Derivation and Discrimination of Case-II water constituents in a Multicomponent Bloom using MOS Remote Sensing Data“, Ocean Optics XIV, November 9-13, 1998, Kalilua Kona, Hawaii
- B.5 **Krawczyk H., Neumann A., Walzel T.:** „Linearer Inversionsalgorithmus zur quantitativen Bestimmung von Wasserinhaltsstoffen aus spektral hochaufgelösten Fernerkundungsmessungen“, DFD-Nutzerseminar, 12.-13.09.1995, DLR Fernerkundungsstation Neustrelitz, ESA Sammelband
- B.6 **Krawczyk H., Neumann A., Walzel T.:** „Interpretation Potential of Marine Environments Multispectral Imagery“, Third Thematic Conference on Remote Sensing for Marine and Coastal Environments, Sept. 1995, Seattle, USA, pp. II-57 - II-68
- B.7 **Krawczyk H., Neumann A.:** „Ocean Colour Remote Sensing with the Modular Optoelectronic Scanner (MOS)“, IOCCG-Workshop, 24.-27.3.1996, Toulouse, Frankreich
- B.8 **Krawczyk H., Neumann A., Walzel T.:** „Application of a new Remote Sensing multispectral interpretation algorithm for water constitutes in the Baltic sea“, Ocean Optics XIII, 22.10.-25.10.1996, Halifax/Canada
- B.9 **Krawczyk H.; Hetscher M.:** “Principal Component Inversion Algorithm for the Retrieval of Water constituents and its Applications”, 1st Workshop on MOS IRS and Ocean Colour, 28.-30. April 1997, DLR, Berlin, Germany
- B.10 **Krawczyk H., Gerasch B.:** „Multichannel Atmospheric Correction of MOS-Scenes over Water“, Proceedings of the 2nd International Workshop on MOS IRS and Ocean Colour, Institute of Space Sensor Technology (DLR), pp. 117-122, Wissenschaft und Technik Verlag, Berlin, 1998, ISBN 3-89685-559-X
- B.11 **Krawczyk H., Pflug B., Gerasch B.:** „Remote Sensing of Atmospheric Properties with the Modular Optical Scanner (MOS)“, International Symposium on Remote Sensing, September 21-24, 1998, Barcelona, Spain, SPIE Vol. 3495
- B.12 **Krawczyk H., Neumann A., Hetscher M., Zimmermann G., Walzel, T.:** „Principal Component Analysis - a Tool for Interpretation of Multispectral Remote Sensing Data“ Ocean Optics XIV, November 9-13, 1998, Kalilua Kona, Hawaii
- B.13 **Neumann A., Piesik B., v.Schönermark M., Zimmermann G.:** „Umweltorientierte Erderkundung im DLR-Zentrum Berlin-Adlershof“, DLR-Nachrichten, Heft 69, (1992), S. 7 - 11
- B.14 **Neumann A., Zimmermann G., Krawczyk H., Walzel T.:** "Test of Specific Methods for Reduction of Spectral Dimension of Ocean Remote Sensing Data", 41. Kongress der Internationalen Astronautischen Föderation, Dresden, 1990, Acta Astronautica Vol. 29 (1993), No. 1, pp. 61-66
- B.15 **Neumann A., Krawczyk H., Walzel T.:** „Optimiertes Verfahren zur Bestimmung von Wasserinhaltsstoffen aus spektral hochauflösenden Fernerkundungsdaten“, DLR-Nachrichten; Heft 77 (1995), S. 6-10
- B.16 **Neumann A., Krawczyk H.; Walzel T.:** „A Complex Approach to Quantitative Interpretation of Spectral High Resolution Imagery“, Third Thematic Conference on Remote Sensing for Marine and Coastal Environments, Sept. 1995, Seattle/Washington, USA , pp II-641 - II-652

- B.17 **Neumann A., Krawczyk H., Zimmermann G.:** „First Experience and Results from the Spaceborne Imaging Spectrometer MOS-IRS“, PORSEC-Conference, 13.8.-16.8.1996, Victoria, Kanada, veröffentlicht als Buchkapitel
- B.18 **Neumann A., Krawczyk H., Zimmermann G., Walzel T., Hetscher M.:** “Retrieval of Water Constituents from Spaceborne Imaging Spectrometer Data”, Seventh International Symposium "Physical Measurements and Signatures in Remote Sensing", 7-11 April 97, Courchevel, France, Bd.2, S. 567-573
- B.19 **Neumann A., Walzel T., Gerasch B., Tschentscher C., Mißling K.-D., Maaß, H.:** “MOS-IRS-Data Processing and Data Products”, 1st International Workshop on MOS IRS and Ocean Colour, 28.-30. April 1997, DLR, Berlin, Germany
- B.20 **Neumann A., Zimmermann G., Krawczyk H., Tschentscher C.:** “Ocean Colour Remote Sensing with MOS-IRS”, Challenger Society Meeting, 3.7.-4.7.1997, London, UK
- B.21 **Neumann A., Hetscher M., Krawczyk H., Tschentscher, C.** “Methodological Aspects of Principal Component Inversion for Case-II Applications”, Proceedings of the 2nd International Workshop on MOS IRS and Ocean Colour, Institute of Space Sensor Technology (DLR), pp. 162-170, Wissenschaft und Technik Verlag, Berlin, 1998, ISBN 3-89685-559-X
- B.22 **Neumann A. et. al.:** „ECOMON – A Dedicated Mission for Regional Ecological Research and Monitoring“, submitted in response to ESA Call for Earth Explorer Opportunity Missions, Reg-No. COP 23, November 1998
- B.23 **Zimmermann G., Neumann A.:** “MOS - A spaceborne Imaging Spectrometer for Ocean Remote Sensing”, Mitteilungen der IOCCG, Backscatter, Vol. 8, Mai 1997, S. 11-13

International Earth Remote Sensing Mission PRIRODA

Modular Optoelectrical Scanner MOS

USER GUIDE



German Aerospace Research Establishment
Institute for Space Sensor Technology
Department of Sensor Data Utilization

Rudower Chausse 5
12484 Berlin
Germany



Contents

	Foreword	4
1.	The PRIRODA Mission	6
1.1.	Space Station MIR and PRIRODA	6
1.2.	Major Goals of the PRIRODA Program	7
1.3.	PRIRODA Instrumentation	8
1.4.	PRIRODA Operation, Mission Control and Restrictions	12
1.4.1.	Orbit Geometry	12
1.4.2.	Restrictions due to Energy Budget	13
1.4.3.	Mission Control and Data Downlink	13
1.5	German Participation in the PRIRODA Program	15
2.	Organizational and Coordination Structures of PRIRODA	17
2.1.	The International Scientific Council of PRIRODA	17
2.1.1.	The Project Management Working Groups	17
2.2.	General Issues on Participation and Data Access	18
2.3.	National Organizational Structures and Responsibilities in Germany	19
2.3.1.	The German PRIRODA Council	19
2.3.2.	DLR - Institute for Space Sensor Technology	19
2.3.3.	DLR - Institute for Space Sensor Technology	19
2.3.4.	PRIRODA User Data Centre at the DLR - German Remote Sensing Data Centre	19
2.3.5.	German Space Operations Centre GSOC	19
3.	The Imaging Spectrometer MOS	20
3.1.	Spectrometer Design	21
3.1.1.	MOS-A	22
3.1.2.	MOS-B	23
3.1.3.	Calibration Concept	25
3.2.	Electronics Design	28
3.2.1.	Block Scheme	28
3.2.2.	Analogue Signal Processing Assembly	28
3.2.3.	CCD Control and Data Compression	29
3.2.4.	Main Board Processing Unit (CPU)	30
3.2.5.	Data Formatting and Telemetry Interface	31
3.2.6.	Additional Units and Interfaces	31
3.2.7.	Cooling Assembly	33
3.2.8.	Power Supply	34
4.	Spectrometer Calibration	36
4.1.	On-Ground Calibration	36
4.1.1.	Relative Calibration Procedures	36
4.1.2.	Absolute Calibration Procedures	39
4.2.	In-Flight Calibration	41
4.2.1.	Sun Calibration via Diffuser	41
4.3.	Data Quality Assurance (Internal Control)	42
4.3.1.	Timing of Internal Control	43
4.3.2.	Control Parameters	44
4.3.3.	Usage of Control Information	45
5.	MOS Data Processing, Software, Data Products and Distribution	46
5.1.	Definition of Data Levels - the CEAOS Recommendation	46
5.2.	Processing Hierarchy and Data Structures	46
5.2.1.	On-Board Processing	47
5.2.2.	Ground Pre-Processing	47
5.2.3.	Primary Processing	47
5.2.4.	Operating Timelines / Operational Modes	49

5.2.5.	Raw Data Format (RPI-Format)	50
5.2.5.	Level 1B - Format	50
5.3.	Software Tools	51
5.3.1.	Primary Processing and Quick-Look Package PRIMUS	51
5.3.2.	PC-based Quick-Look Package ProImage	55
5.4.	Higher Level Products	57
5.4.1.	Atmospheric Correction: Water Leaving Radiance/Reflectance	57
5.4.2.	"CZCS"-Pigment	59
5.4.3.	Normalized Vegetation Index NDVI	60
5.5.	Data Access via PRIRODA User Data Centre	
5.5.1-	PRIRODA News Bulletin	61
5.5.2.	Intelligent Satellite-data Information System (ISIS)	61
	Appendix to Chapter 5: Tables of data formats	65
	Appendices	73
	References	

Deutsches Zentrum für Luft- und Raumfahrt e.V.
Institut für Weltraumsensorik und Planetenerkundung

Algorithm Theoretical Basis Document (ATBD)

MOS-IRS Level-1B Products

T. Walzel, B. Gerasch, C. Tschentscher, A. Neumann



The work outlined in this document was supported in the frames of the project „Ocean Colour Remote Sensing with MOS“ by

- Deutsche Agentur für Raumfahrtangelegenheiten (DARA) under registry 50 EE 9203 and
- Bundesministerium für Bildung, Wissenschaft, Forschung und Technologie (BMBF), represented by Projektträger Biologie, Energie, Umwelt (BEO) under registry 03 EE 9203

Contents

Chapter	Page
1. INTRODUCTION	3
2. ALGORITHM OVERVIEW	3
2.1. DEFINITION OF TERMS	3
2.2. PRIMARY PROCESSING OVERVIEW	4
3. ALGORITHM DESCRIPTION	6
3.1. THEORETICAL DESCRIPTION	6
3.1.1. PHYSICS OF THE PROBLEM - SPECTROMETER CALIBRATION	6
3.1.1.1. LABORATORY (PRE-FLIGHT) CALIBRATION PROCEDURES	7
A) RELATIVE CALIBRATION PROCEDURES (DARK VALUE, OVERALL PHOTO RESPONSE NONUNIFORMITY, RELATIVE SPECTRAL SENSITIVITY FUNCTION, POLARIZATION SENSITIVITY, LINEARITY, STRAYLIGHT)	
B) ABSOLUTE CALIBRATION PROCEDURES (RADIANCE CALIBRATION [NADIR MODES], IRRADIANCE CALIBRATION [SUN-MODE])	
3.1.1.2. IN-FLIGHT CALIBRATION	10
A) SUN CALIBRATION	
B) INTERNAL CONTROL	
3.1.2. MATHEMATICAL DESCRIPTION OF THE ALGORITHM	12
3.1.2.1. RADIANCE CALCULATION	12
3.1.2.2. SUN CALIBRATION	13
3.1.2.3. COARSE CLASSIFICATION - LAND/OCEAN/CLOUD DISCRIMINATION	13
3.1.2.3. ERROR BUDGET ESTIMATES	13
3.2. PRACTICAL CONSIDERATIONS - ALGORITHM IMPLEMENTATION	14
3.2.1. CALIBRATION AND VALIDATION	14
3.2.2. QUALITY CONTROL AND DIAGNOSTICS	15
A) FORMAT CHECK, TEST FOR TRANSMISSION ERRORS AND INSTRUMENT STATUS CHECK	
B) EVALUATION OF INTERNAL CONTROL	
3.2.3. EXCEPTION HANDLING	17
3.2.4. OUTPUT PRODUCT - LEVEL-1B DATA FORMAT	17
4. ASSUMPTIONS AND LIMITATIONS	17
5. OTHER RELEVANT DOCUMENTS	18
APPENDIX I: MOS-IRS DATA PRODUCT SUMMARY SHEET	19
APPENDIX II: SCENE GEOMETRY OF MOS-IRS	21
APPENDIX III: DESCRIPTION OF DATA FORMATS FOR LEVEL-1B PRODUCTS	22

1. INTRODUCTION

This Algorithm Theoretical Basis Document (ATBD) describes the physical background and the algorithms used to generate calibrated, error-corrected and georeferenced top-of-atmosphere (TOA) radiance data from MOS-IRS raw data. This covers pre-flight laboratory calibration and in-flight calibration using measurements of the extraterrestrial sun irradiation as well as internal control measurements by internal lamps. The correction of relevant systematic errors such as vignetting, photo response non-uniformity (PRNU) and dark signal non-uniformity (DSNU) is considered. All necessary processing steps and the resulting data formats are described in detail.

2. ALGORITHM OVERVIEW

2.1. DEFINITION OF TERMS

PHOTO RESPONSE NONUNIFORMITY (PRNU): The relative deviation of pixel sensitivity in one CCD-line (spectral band). It is determined by measuring a uniform input radiance and calculating the relative response for the single pixels of each band ($R_{ij} = U_{ij}/U_{ij}^{\max}$). The PRNU is caused by properties of the CCD-detector as well as vignetting in the optical path of the instrument.

LEVEL 0 (TELEMETRY DATA): Pure digital data stream from the MOS instrument to the telemetry system, formatted in blocks of 1369 Bytes length added by 8 bytes time tag from formatter at ground station.

HOUSEKEEPING DATA: Part of the raw data containing information on MOS instrument status, such as operational mode (internal control, nadir measurement, sun calibration, command status, status of the main subassemblies)

INTERNAL CONTROL: At the beginning of each data take MOS starts with the commanded „internal control cycle“: powering the internal calibration lamps at different currents data are acquired for corresponding light levels in the focal plane. Such a control cycle consists of:

- dark values (no illumination)
- 4 different illumination levels for a short control
- 16 different illumination levels for a long control (on command only, before sun-calibration data readout).

All the readouts for these measurements are transmitted and serve for evaluation of the instrument spectral and radiometrical parameters by comparing them to pre-launch references.

RESET VALUES : These values are readouts, which describe the dark offset of a CCD line. Each pixel of the CCD line has to be corrected by the reset values.

DARK VALUE MATRIX: These values are the readouts from the CCD-lines without any illumination on the focal plane. They give the „offset“ for which every pixel has to be corrected during primary processing.

SUN CALIBRATION: The measurement of the extraterrestrial sun irradiation serves for absolute calibration of the instrument in orbit. It requires a command to rotate a diffuser to sun view position. Crossing the terminator over the north pole MOS instruments are directed to the sun. At this time sun measurement data will be stored to a RAM memory. Overpassing the ground station sun calibration data will be transmitted.

ANCILLARY DATA: Data that come independently from MOS data stream originating from the IRS-P3 pre-processing system. They mainly contain information on the trajectory of IRS-P3, time referencing, subsatellite point and orientation of the satellite.

MASTERFRAME: An internal structure of MOS data consists of 28 blocks of 1377 bytes. It contains three scan lines of MOS-B/C (3 swaths by 14 bands) and one complete scan line of MOS-A data (1 swath by 4 bands). It is defined because MOS-A, -B and -C have a different swath frequency and ground resolution. The ratio of A/B and A/C is equal to 3 (see scene geometry in the Appendix II).

SCENE: A complete (nearly) square image on the earth's surface for the three instruments in all bands. It consists of 384 pixels by 384 swaths for MOS-B, 299 pixels by 384 swaths for MOS-C and 140 pixels by 128 swaths for MOS-A, i.e. 128 masterframes.

2.2. PRIMARY PROCESSING OVERVIEW

The primary processing of MOS data is a part of the ground processing procedure of IRS data. It follows the pre-processing where single experiment data from the complex telemetry data stream are decommutated and referenced to time, orbit and orientation data from the IRS-P3 spacecraft. For MOS the pre-processing procedure outputs 2 data files: MOS level 0 and ancillary data for time and georeferencing of the data take. The raw data contain the full information from one MOS data take, i.e. dark values, internal control data and measurement data. The internal control and the housekeeping data allow the evaluation of instrument status and provide information for corrections during primary processing, if necessary.

The primary processing itself covers the following steps:

- format check: test for transmission errors based on data formatting and counters
- housekeeping check: operational modes, systematic errors, malfunctions of single subassemblies of the instrument
- error and format correction: generation of logically corrected level 0 data
- evaluation of internal calibration data: comparison of actual values to the references for checking sensitivity, linearity and alignment of the CCD-lines
- dark value correction of measurement data
- separation of different data types: measurement data MOS-A, MOS-B and MOS-C, internal control data, sun calibration measurements
- time referencing and georeferencing: scene generation, Level-1B header
- radiometric data calibration: conversion from digital numbers to radiances
- coarse classification and mask generation: land, water, clouds/ice/snow
- generation of Level-1B products for MOS-A and MOS-B/C (formatted TOA radiance files plus header), log-files, DBMS ancillary data files, internal control files and database of dark values

Figure 2.1. shows the flow-chart for the primary processing of MOS-data.

The input to primary processing are the MOS level 0 data and ancillary files generated by the pre-processing. The output product of Level-1B are formatted HDF scenes containing all bands radiometrically corrected and calibrated, 16 bit per pixel, band interleaved by line, a quicklook image, a coarse classification image plus a header containing information on:

- orbit and path number, operational modes
- UTC time referencing
- georeferencing (corner pixels, North direction)
- sun zenith and azimuth angles
- reference to raw data and calibration files
- minimum and maximum values for each band
- percentage of land, water, clouds/snow/ice.
- scaling values for conversion of counts to radiances
- temperatures of focal planes of MOS-A, -B, -C

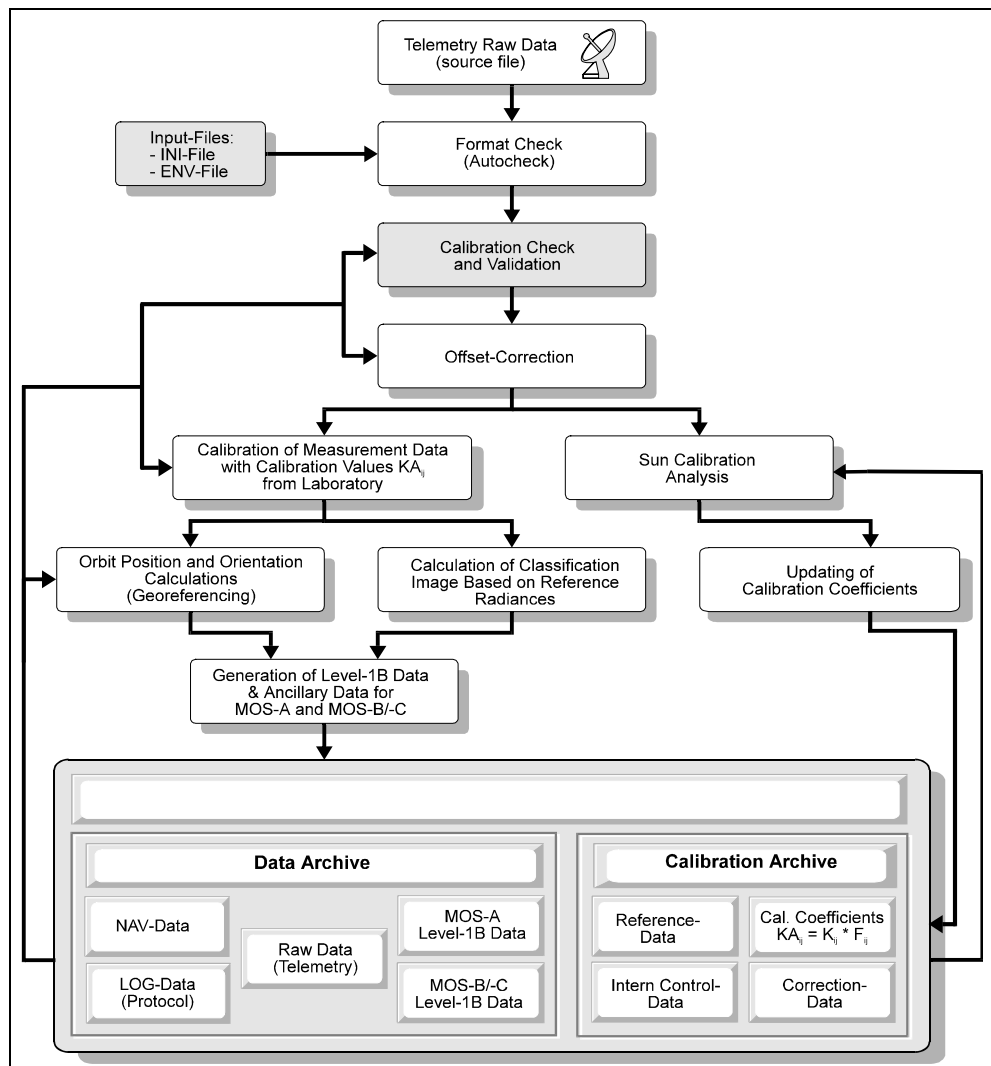


Fig. 2.1.: MOS Primary Processing

These data will be held in the Data Base Management System (DBMS) at the IRS User Data Centre in Neustrelitz and are accessible to the user community. In addition to the Level-1B products all level 0 data, the measurements from internal control, sun calibrations, protocols and database files are stored in separate non-public databases..

3. ALGORITHM DESCRIPTION

3.1. THEORETICAL DESCRIPTION

3.1.1. PHYSICS OF THE PROBLEM - SPECTROMETER CALIBRATION

The MOS instrument measures incoming spectral radiances at the top of the atmosphere. The position and halfwidth of the spectral bands are determined by the design of the imaging spectrometer. The detectors are CCD-lines, the readout signals of each pixel are amplified and converted to digital numbers for transmission over the telemetry system. The corresponding spectral radiance $L_{ij}(\lambda_c)$ of pixel i in spectral band j is calculated from the digital numbers U_{ij} using the sensitivity function $S_{ij}(\lambda_c)$ [relative functions $s_{ij}(\lambda) = S_{ij}(\lambda) / S_{ij}(\lambda_c)$ and $l_{ij}(\lambda) = L_{ij}(\lambda) / L_{ij}(\lambda_c)$, with: λ_c - central wavelength of the band] corresponding to the equation:

$$L_{ij}(\lambda_c) = U_{ij} / S_{ij}(\lambda_c) \{ \int l_{ij}(\lambda) * s_{ij}(\lambda) d\lambda / \int s_{ij}(\lambda) d\lambda \}. \quad (3.1)$$

The radiometric calibration to a standard source with known radiances $L_{nij}(\lambda)$ provides the sensitivity function:

$$S_{ij}(\lambda_c) = U_{nij} / L_{nij}(\lambda_c) \{ \int l_{nij}(\lambda) * s_{ij}(\lambda) d\lambda / \int s_{ij}(\lambda) d\lambda \}. \quad (3.2)$$

At the end, for the calculation of the spectral radiance $L_{ij}(\lambda_c)$ the ratio of integral term with the standard and the scene relative radiation function remains as a correction term in brackets {}:

$$L_{ij}(\lambda_c) = L_{nij}(\lambda_c) * [U_{ij} / U_{nij}] * \{ \int l_{nij}(\lambda) * s_{ij}(\lambda) d\lambda / \int l_{ij}(\lambda) * s_{ij}(\lambda) d\lambda \} \quad (3.3)$$

The goal of the calibration is to determine the spectral sensitivity of all detector elements is realized in two steps:

1. The pre-flight calibration for determination of all relevant parameters in the laboratory gives a basic set of characteristic values needed for pre-launch testing and at-launch calibration.
2. The in-flight calibration and control provides absolute calibration factors from measurements of the extraterrestrial sun radiation and allows to monitor the in-orbit stability by the use of internal calibration lamps.

The laboratory calibration consists of relative measurements, giving functions like the relative spectral sensitivity $s_{ij}(\lambda)$, linearity curves and polarization sensitivity, and absolute radiation measurements which require suitable radiation standards calibrated in physical units (radiative sheres, calibration lamps and diffusors).

3.1.1.1. LABORATORY (PRE-FLIGHT) CALIBRATION PROCEDURES

A) RELATIVE CALIBRATION PROCEDURES

Some of the quantities characterizing the main MOS parameters can be determined in relative units by using mechanic, optic and electronic means. However, a careful experimental determination is important, because the results are needed during data interpretation and evaluation.

RESET VALUE

The reference value U_{rij} is necessary to correct all readouts of the CCD lines. It is a mean offset of last 12 reset pixels of the CCD line for each readout. This value has to be subtracted from each measured pixel value.

DARK VALUE

The dark value U_{0ij} (reference value U_{rij} already subtracted) is required for correcting the spectrometer readouts to get the voltages U_{ij} (digital numbers) from which the measured radiances can be calculated.

OVERALL PHOTO RESPONSE NONUNIFORMITY

The Photo Response NonUniformity (PRNU) characterises the differences in the pixel sensitivity, caused by optical properties (e.g. vignetting) and the detector single element sensitivity. It will be corrected along the scan line (i.e. in each spectral band) based on the sensitivity $S_j(\lambda)$ for the maximum sensitive pixel for each CCD-line:

$$S_{ij}(\lambda_c) = S_j(\lambda_c) * R_{ij} \quad (3.4)$$

The PRNU is determined by measuring the spectral radiance of a photometric sphere, which has an uniform radiance distribution deviating less than 0.5 %. The source is mounted in the near field distance, causing, that each sensor element of the spectrometer measures the radiation from basically the same source area. Figure 3.1 shows examples of PRNU curves for MOS-B. The underlying convex curve is caused by vignetting of the ray path inside the spectrometer optics. The corrected spectral radiance of a measured scan line is thus given by

$$L_{ij}(\lambda_c) = U_{ij} / R_{jj} * S_j(\lambda_c) \{...\} \quad (3.5)$$

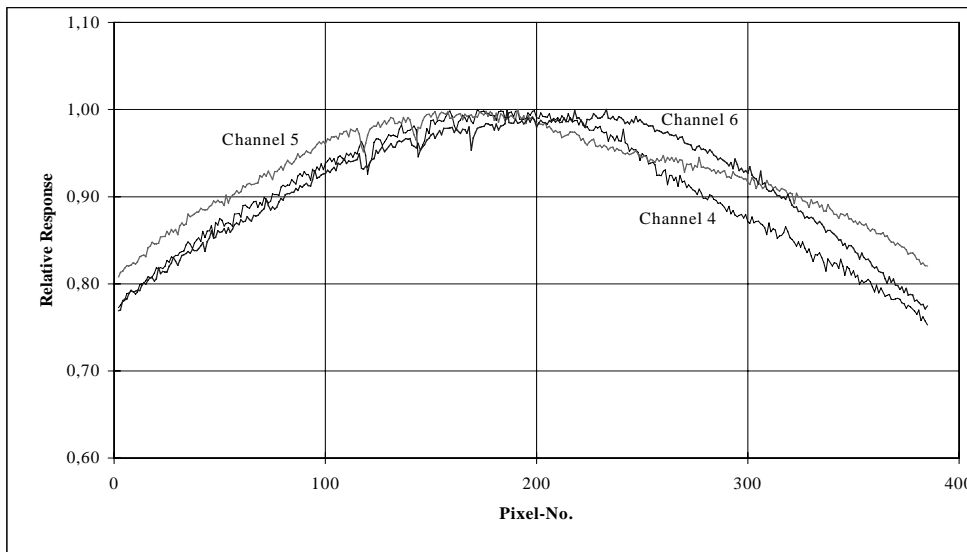


Fig. 3.1: Examples for PRNU, MOS-B

RELATIVE SPECTRAL SENSITIVITY FUNCTION

The relative spectral sensitivity functions $s_{ij}(\lambda)$ have to be measured for all pixels in each band. For the measurement a monochromator (400 - 1100 nm, gratings with 600 and 1200 groves/mm resp.) with a spectral resolution up to 0.1nm, a collimator (4/300), a calibrated reference detector and an adjustable mount for the spectrometers are used.

The results show only a small difference in the centre wavelength and in the shape of the curvature between the different pixels of one spectral band (see Fig. 3.2 for illustration). Therefore, only 3 sensitivity functions at equidistant pixels (MOS-A: 1; 210; 420; MOS-B: 1; 192; 384) for every band are documented and the remaining functions can be calculated by interpolation.

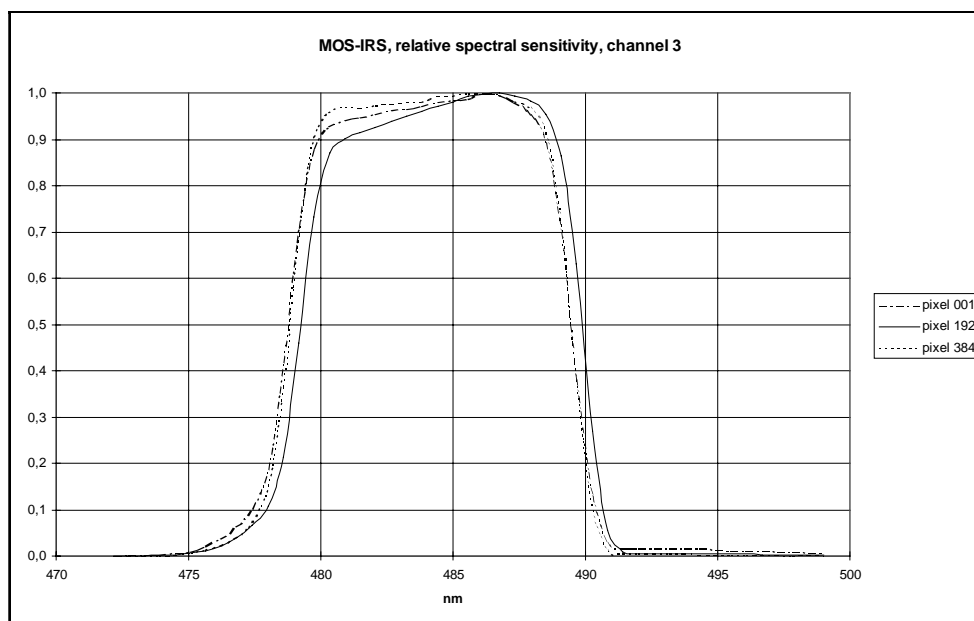


Fig. 3.2: Examples for Relative Spectral Sensitivity Function, MOS-B

POLARIZATION SENSITIVITY

Polarization sensitivity of the spectrometers is measured using different foil polarizers for all bands at the same pixels as the spectral sensitivity. The polarization sensitivity values are 3.3 to 3.9 % for MOS-A, 0.9 to 7.8 % (Channel 1-8) and 9 to 15.1 % (Channel 9-13) for MOS-B.

LINEARITY

The linearity of the conversion from incoming radiation to the digitized output values over the entire dynamic range was proved experimentally for the validity of the proposed sensitivity functions S_{ij} and other corrections to be applied for measurement data calibration and correction. The linearity of the CCD-lines was tested with intensity modulated monochromatic light in comparison with a calibrated linear detector. The measured output signals showed a deviation from linearity for very low and very high data of the dynamic range, which varies from channel to channel. Therefore special corrections will be applied after primary processing.

STRAYLIGHT

Stray light inside the spectrometer produces an additional irradiance on the CCD elements, which depends on the total incoming radiation and its spectral composition. It distorts the measured signal in a manner, which cannot be corrected fully and accurately. The measured amount of stray light in the MOS spectrometers is less than 0,4% (MOS-A, -B) and less than 1% for MOS-C.

B) ABSOLUTE CALIBRATION PROCEDURES

The absolute calibration derives the absolute sensitivity of each pixel in each spectral band. A photometric sphere of known spectral radiance ($\mu\text{W}/(\text{cm}^2 \text{ nm sr})$) is used as the uniform source and allows to determine the sensitivities of the instruments. For sun calibration mode the effective diffuse transmission of the diffuser is determined in laboratory. It will be an "effective" value because of interreflections between diffuser and entrance optics, which influences the irradiance on the diffuser.

RADIANCE CALIBRATION (NADIR MODE)

The calibration is carried out with a radiometric sphere that was calibrated via a reflective diffuser against 2 standard irradiance lamps of 1000 W (based on the PTB scale, PTB = Physikalisch-Technische Bundesanstalt, German Bureau of Standards). The sphere was used in different radiance levels for the two spectrometers MOS-A and MOS-B and the CCD line camera MOS-C. The total field of view of a MOS module is covered by the sphere's aperture; the nonuniformity of the radiation field is less than 1,0 %. The readouts U_{nij} give the sensitivity $S_{ij}(\lambda_c)$ referring to equation (3.2):

$$S_{ij}(\lambda_c) = U_{nij} / L_{nij}(\lambda_c) \{ \int I_{nij}(\lambda) * s_{ij}(\lambda) d\lambda / \int s_{ij}(\lambda) d\lambda \} \quad (3.6)$$

$L_n(\lambda)$ is the spectral radiance function of the sphere. The sensitivity values $S_{ij}(\lambda_c)$ were corrected for PRNU using R_{ij} to one sensitivity value $S_j(\lambda_c)$ for each spectral band referring to equation (3.4).

IRRADIANCE CALIBRATION (SUN-MODE)

Laboratory standard lamps illuminating the diffuser in front of the entrance optics are used to produce an irradiance $E_{sij}(\lambda)$ [relative values $e_{ij}(\lambda)$].

The resulting readouts U_{sij} give the sensitivity values $S_{sij}(\lambda_c)$ that have to be the same as the ones determined on the sphere:

$$S_{sij}(\lambda_c) = \pi * U_{sij} / \beta_{ij}(\lambda_c) * E_{sij}(\lambda_c) \{ \int e_{sij}(\lambda) * s_{ij}(\lambda) d\lambda / \int s_{ij}(\lambda) d\lambda \} \quad (3.7)$$

with: $\beta(\lambda)$ - diffuse conversion factor of the sun diffuser

From these measurements the real sensitivity value is determined for each band by using the factor R_{ij} .

Because of the fact, that the sensitivity of the spectrometer alone (without diffuser conversion) is always the same, the conversion factor can be derived from the equations (3.6), (3.7) taking into account that the values in brackets { } are equal:

$$\beta_{ij}(\lambda_c) = \pi * L_{nij}(\lambda_c) * U_{sij} / U_{nij} * E_{sij}(\lambda_c) \quad (3.8)$$

The values will be used for the sun calibration in orbit to calculate the nadir sensitivity (or calibration factor) from sun calibration readouts U_{sij} .

3.1.1.2. IN-FLIGHT CALIBRATION

During the mission it is necessary to perform a periodical calibration of the instrument. This is done using the extraterrestrial sun radiation, because it is on one hand the most stable radiation source and on the other hand the source to which the object measurements have to be normalized.

A) SUN CALIBRATION

The sun calibration measurements are averaged over the valid readouts giving the sun calibration measurements $U_{\odot ij}$:

$$U_{\odot ij} = E_{\odot ij}(\lambda_c) \cdot S_{ij}(\lambda_c) \cdot \tau_{ij}(\lambda_c) \cdot \beta_{ij}(\lambda_c) \int e_{\odot j}(\lambda) \cdot s_{ij}(\lambda) d\lambda / \pi \int s_{ij}(\lambda) d\lambda \quad (3.9)$$

Using the $E_{\odot ij}(\lambda)$ [tables from Neckel & Labs 84] the sensitivities respectively the calibration coefficients can be calculated:

$$S_{ij}(\lambda_c) = \pi U_{\odot ij} / \beta_{ij}(\lambda_c) * E_{ij}(\lambda_c) * \{ \int e_{\odot j}(\lambda) * s_{ij}(\lambda) d\lambda / \int s_{ij}(\lambda) d\lambda \}. \quad (3.10)$$

B) INTERNAL CONTROL

A long term satellite mission requires measurements for monitoring the instrument stability during its lifetime, checking the stability of parameters which influence the absolute spectral sensitivity of each spatial pixel in each wavelength band. MOS uses internal lamps (2 miniature incandescent lamps in each spectrometer) to check for relative changes and to assess the actual state of the measuring system. The integration of light sources in the spectrometer for checking the sensitivity relatively to an initial state gives the possibility to control the actual parameters at any time the instrument operates. Together with other control procedures and as their complement, the internal control allows it to:

- check device parameters with only internal means
- mutual control of the 2 lamps
- test of influences of launch stress on parameters
- provide a link between subsequent sun calibration procedures.

A supposition of successful work with such lamps is the long term stability of their irradiation as well as the stable mechanic and electronic integration in the spectrometer. The lamp stability was tested in laboratory experiments and in spectrometers of the MKS-series on satellites and space stations SALUT and MIR. Figure 3.3 shows the internal setup of the calibration lamps in the spectrometers.

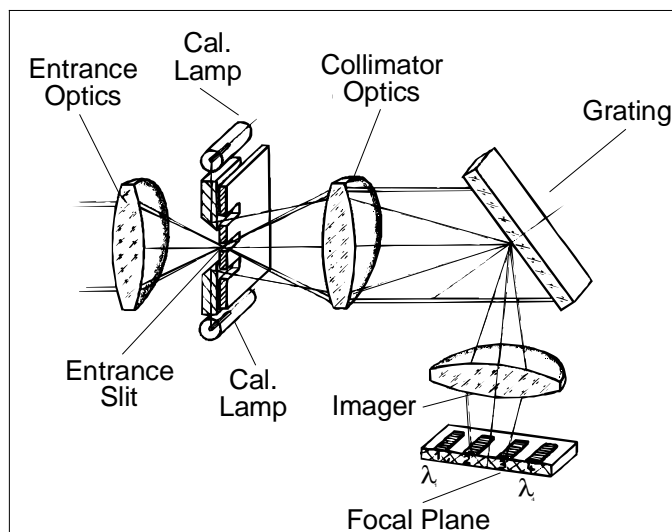


Fig. 3.3.: Setup of Internal Calibration Lamps in the Spectrometers

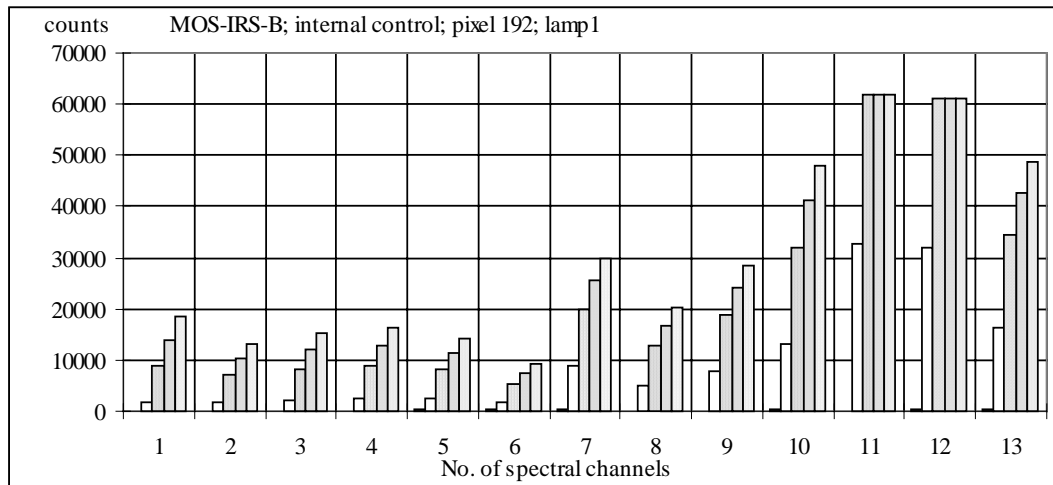


Fig. 3.4: Example for Short Internal Control (13 bands, MOS-B)

Each lamp can be operated at 4 different currents. Using both lamps together that allows 16 different illumination levels (see figure 3.4 and 3.5). The shutter is closed during this procedure for blocking the incoming radiation and for dark signal determination. The short internal control is running once on each active orbit, the long control is realized only by command in connection with sun calibrations.

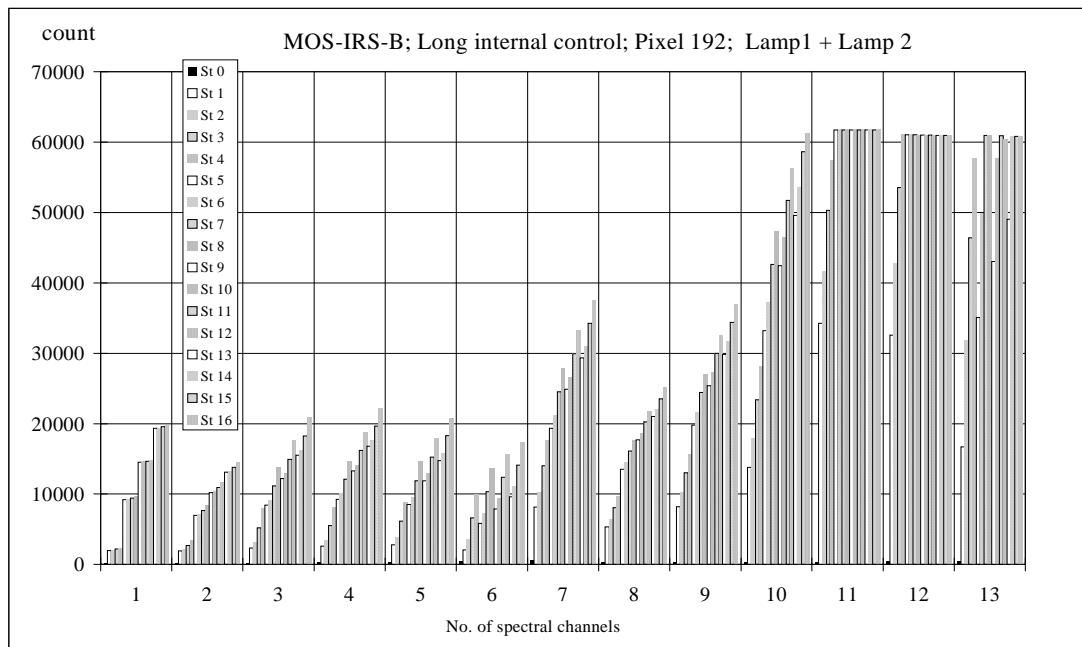


Fig. 3.5: Example for Long Internal Control (13 bands, MOS-B)

3.1.2. MATHEMATICAL DESCRIPTION OF THE ALGORITHM

3.1.2.1. RADIANCE CALCULATION

Summarizing all effects influencing the sensitivity of single pixels in a spectral band (cross-track-direction) for systematic correction and calibration one has to account for:

- vignettation due to properties of the internal optical path
- different sensitivity of different pixels in one CCD-line (band)

Because of linearity both effects can be considered using one correction function f_{ij} for each pixel in every wavelength band (i - pixel number, j - band number). The application of f_{ij} to the dark-value corrected pixel readouts therewith performs the sensitivity correction along the CCD-line. The resulting pixel values then can be transformed to radiance values ($\mu\text{W} / (\text{cm}^2 \text{ nm sr})$) by using one identical scaling factor K_j for all pixels of one spectral band. That gives the following equation for the radiance calculation:

$$L_{ij} = (U_{ij} - U_{0ij}) * f_{ij} * K_j \quad (3.11)$$

- where i - pixel number in scan line, 1..420 for MOS-A, 1..384 for MOS-B
1..299 for MOS-C
- j - band number, 1..4 for MOS-A, 1..13 for MOS-B. 1 for MOS-C
- U_{ij} - readout pixel value (in digital numbers)
- U_{0ij} - dark value (digital numbers, measured during internal control)
- f_{ij} - sensitivity correction function
- K_j - scaling factor

The calculated radiance values L_{ij} base on the pre-flight laboratory scaling factor K_i . This is valid for the early period of in-orbit operation where first a laboratory based calibration factor is used for the calculation corresponding equ. (3.13). After performing the sun calibrations from orbit it will be substituted by the sun-derived factors, which are adapted during mission, if necessary.

3.1.2.2. SUN CALIBRATION

In the case of sun calibration one has to account for the diffuser in front of the entrance optics to convert E_0 to L_0 values. Therefore an additional wavelength-dependent factor β_j for the sun diffuser has to be applied to calculate the irradiance respectively the calibration factors by inverting the equation:

$$E_{ij} = \pi * \beta_j * (U_{ij} - U_{0ij}) * f_{ij} * K S_j, \quad (3.12)$$

with the meaning of variables as in equations (3.7, 3.11) and $K S_j$ being the sun calibration factor.

3.1.2.3. COARSE CLASSIFICATION - LAND/OCEAN/CLOUD DISCRIMINATION

Based on the calibrated TOA-radiance values a coarse classification map will be generated that can be used for quick-look, scene selection and mask generation purposes. This image is a raw classification for the three main classes land, ocean/water and clouds/snow/ice.

The classification is done pixel by pixel with a simple thresholding algorithm using two spectral bands of MOS-B: 443nm and 750nm. The following formulae gives the radiance threshold values used for distinction of the classes:

- Cloud/snow/ice : $L(443 \text{ nm}) > 20 * \cos(\theta_s)$
- Land : $L(443 \text{ nm}) < 20 * \cos(\theta_s)$ and
 $L(750 \text{ nm}) > 1.5 + 5.5 * \exp(-(\theta_s * \theta_s)/0.4)$
- Water : $L(443 \text{ nm}) < 20 * \cos(\theta_s)$ and
 $L(750 \text{ nm}) < 1.5 + 5.5 * \exp(-(\theta_s * \theta_s)/0.4)$

where: L - TOA radiance in $\mu\text{W} / (\text{cm}^2 \text{ nm sr})$
 θ_s - sun zenith distance in degrees

3.1.2.3. ERROR BUDGET ESTIMATES

The error budgets for the derived TOA-radiance values depend on the uncertainty of absolute calibration in laboratory and in orbit respectively. The pre-flight calibration factors are determined based on standard sources of spectral radiance and irradiance. The uncertainty of the calibration factors is in the order of 3.4 %, mainly caused by the uncertainty of the secondary radiometric standards themselves.

From in-orbit sun calibrations an accuracy of about 1% is expected. Using the measurements of sun calibration and internal control, changes in the sensitivity can be detected and corresponding corrections are applied to the data.

A serious problem in accuracy can be caused by polarization of the incoming radiance. The real error depends on the situation in the actual scene and therefore has to be evaluated by modelling and additional measurements. Based on these estimates it can be necessary to correct for the polarization sensitivity of the instrument. However at the given status these corrections have not be implemented.

3.2. PRACTICAL CONSIDERATIONS - ALGORITHM IMPLEMENTAION

The goal of primary processing is to convert the received level 0 data using calibration, ancillary and navigation data to Level-1B-TOA radiance data. This entire processing is implemented in the software system PRODOMUS, that performs all necessary tests and calculations as well as formatting and generation of output files.

In Level-1B-files the dark value corrected pixel values multiplied by the sensitivity correction function (i.e. $(U_{ij} - U_{0ij}) * f_{ij}$) are stored as 16-bit digital numbers. The scaling factors K_j are written to the file header. So one easily can obtain the radiance values from a data file.

Additionally the file header contains necessary information on georeferencing, references to raw data files, used calibration files and more. The data format and content is described in detail under chapter 3.2.4. „Output Products“ and in Appendix III.

The PRODOMUS software can be run from the console command line or included in automatic processing by the use of corresponding shell scripts. The program runs under UNIX environment, in particular Sun- and SGI-systems. This limitation is valid due to different internal representation of data on other machines:

- Sun workstation or compatible clones with operational system Solaris 2.5 or higher
- SGI workstations with operational system IRIX

3.2.1. CALIBRATION AND VALIDATION

Post-launch calibration and validation can be achieved only by corresponding dedicated measurements, synchronous from space and on ground plus in-orbit sun calibration. Several activities have been planned to provide the needed ground-truth data for calibration:

- measurement of spectral ground (object) reflectance
- measurement of spectral atmospheric transmissivity and aerosol characteristics
- acquisition of additional parameters (wind speed and direction, temperature, humidity and pressure profiles etc.).

The optical spectral measurements are realized using instruments that are calibrated to the same radiance sources as the MOS instrument in laboratory and to the sun irradiance by special high altitude measurements. This ensures a radiometrical link between spaceborne and ground measurements.

Additionally to ground-truth calibration cross-calibration measurements over dedicated targets with other spaceborne instruments such as SeaWiFS give opportunity to evaluate the radiometric and spectral data quality.

3.2.2. QUALITY CONTROL AND DIAGNOSTICS

A) FORMAT CHECK, TEST FOR TRANSMISSION ERRORS AND INSTRUMENT STATUS CHECK

The format check procedure performs an extensive checkup of the MOS-IRS-P3 level 0 data, corrects errors as far as possible and generates a completed and corrected level 0 file according to the MOS-IRS-P3 logical data format. Data lacks will be filled up by zero values.

1. Synchronous check

Each subframe starts with a 64 bit frame sync. This synchronous sequence will be checked and all found subframes are written to a temporary file.

2. Subframe check
The subframe counter will be checked modulo 28 comparing with the input blockcounter to format a masterframe, that consists of 28 subframes.
3. Housekeeping check
One masterframe contains 5 equal housekeeping blocks. The content of these data has to be analysed to get information about scene and subscene counters and about the operational status of the instruments.
4. Scene check
All counters have to be tested for consistency. Data losses will be filled up.
5. Protocol
The check results, warnings, errors and status information will be written to a protocol file (LOG-file).

Of course fatal errors can occur, which cannot be corrected automatically (e.g. specific malfunctions of power supply or control devices of MOS, significant transmission errors). In such cases a remark will be written to the LOG-file. The data then have to be undergo special treatment by operator, which is outside routine processing.

B) EVALUATION OF INTERNAL CONTROL

The readouts for each illumination level k are averaged during ground processing and the resulting actual control values U_{cijk} are compared with reference values U^*_{cijk} , obtained initially during pre-flight laboratory measurements and replaced by in-flight measurements at the beginning of the mission. The resulting coefficients C_{ijk} can be used to evaluate the state of the instruments:

$$C_{ijk} = U_{cijk} / U^*_{cijk} \quad (3.13)$$

with: c - number of control lamp: 1 = lamp 1, 2 = lamp 2, 3 = lamp 1+2
 k - number of illumination level: 1...4 for short control mode, 1...16 for long control mode using both lamps).

Basically the measurements from short control in level 4 (highest signal level) are applied to evaluate the state of the MOS instrument. The following quantities are used:

1. C_{ij4} as a function of i with j as parameter to investigate the behaviour of single pixels in one spectral band,
2. The values C_{j4} , averaged over all pixels i resulting in one value for each spectral band. It shows deviations, which are valid for the entire spectral band.

The internal control measurements will not be used for data correction following a fixed program. Before making corrections the reasons for changes in the spectrometer parameters, indicated by control values, have to be investigated. Therefore, only after looking at a few of

control data sets and analysing possible trends in changes and reasons for it, specified changes in calibration may be applied. The following steps of analysing the control data sets can give clues for necessary corrections:

- looking at the dark current of the measurements: are there any clues on changes in the behaviour of the detectors?
- calculation of the ratios C_{ijk} from each control data set: are any changes of spectrometer parameters indicated?
if yes: for one/few pixels, entire band, in several bands, the same pixels? Is there any relation to possible changes in dark values?
- comparison of C_{ijk} values from consecutive measurements: is there a trend in the changes?
- comparison with the ratios C_{ijk} getting from the alternative control lamp: is there the same behaviour?
- looking at the housekeeping informations: are there any reasons from instrument status (cooling, power supply, ...) to explain the changes?

The dark values of the instruments are increasing in mission time. Sometimes there is no internal control within the received datatake. Therefore a dark value database was generated.

3.2.3. EXCEPTION HANDLING

Standard Exception Handling covers two steps:

- as already outlined under 3.2.2. synchronisation losses or heavy reception errors are recognised and located based on the logical MOS data structure. If these errors exceed a certain value the complete data take has to be treated out of routine procedures
- the instrument has cold redundancies for most of the electronic subassemblies. They can be activated in the case of malfunction by special preselection command. A corresponding information is written in the housekeeping blocks of MOS level 0 data. The processing runs in standard manner as long as the data are correct and valuable.

A special situation occurred for MOS-A : the shutter does not close the aperture completely and therefore incident light comes to a part of the CCD lines. Due to this only dark values obtained by closing the sun calibration unit are used for dark value correction in MOS-A. Only after launch a striping and residual internal reflections were discovered in the data. Both effects can be corrected by use of an extra tool to be applied to the Level-1B-data.

3.2.4. OUTPUT PRODUCT - LEVEL-1B DATA FORMAT

The standard Level-1B output products for MOS-IRS-P3 are formatted scenes containing all spectral bands of either MOS-A or MOS-B/C, radiometrically corrected and calibrated, 16 bits per pixel, band interleaved by line plus a header containing reference information, a coarse classification map and a quick-look image. Additionally meta-information data are generated for the data base management system at the IRS-P3 User Centres.

A scene is defined as a square image from each spectrometer and contains 128 swaths of MOS-A and 384 swaths of MOS-B/C respectively. Also during the primary processing the 420 subpixel values per channel of MOS-A are superimposed (mean value) to calculate 140 square macropixels per scanline.

The output files start with a header of 2560 bytes containing ancillary, calibration and reference information. The detailed structure is given in the Appendix III. The header is followed by a classification image giving the opportunity to generate land, water and cloud/snow/ice masks for further processing and a quick look image. They are stored as single bands in BYTE-format. The measurement pixel values are the fourth part of the file, stored band interleaved by line (BIL) in unsigned SHORT INTEGER-format (16 bit per pixel).

Time referencing and georeferencing will be done with an algorithm, taking the input from the ancillary file, which is a result of the Indian preprocessing software. The results of this algorithm are geographical longitude and latitude and the sun-elevation and sun-azimuth-angles of the four corner pixels of a scene. These coordinates, together with the UTC time reference are written to the header of each resulting image file.

The entire file is packed in an HDF-format, containing a corresponding HDF-header and a Raster-8 quick-look-image, based on MOS-B channel 9. The entire structure of Level-1B-data is given in the Appendix III.

4. ASSUMPTIONS AND LIMITATIONS

n.a.

5. Other Relevant Documents

Sümlich K.-H.: „MOS-PRIRODA Calibration Concept“, DLR, Institute for Space Sensor Technology, 1992

Neumann A., Walzel T., Tschentscher C., Gerasch B., Krawczyk H.: „MOS-IRS Data Processing, Software and Data Products“, DLR, Institute for Space Sensor Technology, 1995

Walzel T., Tschentscher C., Gerasch B.: „Detailed description of Primary Processing Package PRIMCONT“ DLR, Institute for Space Sensor Technology, 1996

Krawczyk H.: „Algorithm Theoretical Basis Document: MOS-IRS Ocean Color Level 2 Algorithm“, DLR, Institute for Space Sensor Technology, 1996

MOS-IRS-P3 DATA PRODUCT SUMMARY SHEET (I)

Product Name : MOS-A TOA radiances
Product Code : n.a.
Product Level : 1B
Description of Product : corrected, calibrated and georeferenced multispectral TOA radiance data

Product Parameters:

Coverage : 195 x 200 km
Packaging : band interleaved by line (BIL), 16 bit per pixel
Units : $\mu\text{Wcm}^{-2}\text{nm}^{-1}\text{sr}^{-1}$
Range : wavelength dependent
Sampling : 1.57 x 1.4 km pixel size
Resolution : $\leq 1\%$
Accuracy : relative stability +/- 0.5%
absolute accuracy 3.5 %
Geo-location
Requirements : n.a.
Format : HDF
Appended Data : georeferencing, time reference, coarse classification, quick-look-image
Frequency of
Generation : daily
Size of Product : ≈ 200 kByte

Additional Information:

Identification of Bands used in Algorithm: BIL, no special identification
Assumptions on Input Data: MOS-Level-0-data
Identification of Ancillary and Auxiliary Data: explicit in image header
Assumptions on Ancillary and Auxiliary Data: MOS-Level-0-data

MOS-IRS-P3 DATA PRODUCT SUMMARY SHEET (II)

Product Name : MOS-B TOA radiances
Product Code : n.a.
Product Level : 1B
Description of Product : corrected, calibrated and georeferenced multispectral TOA radiance data

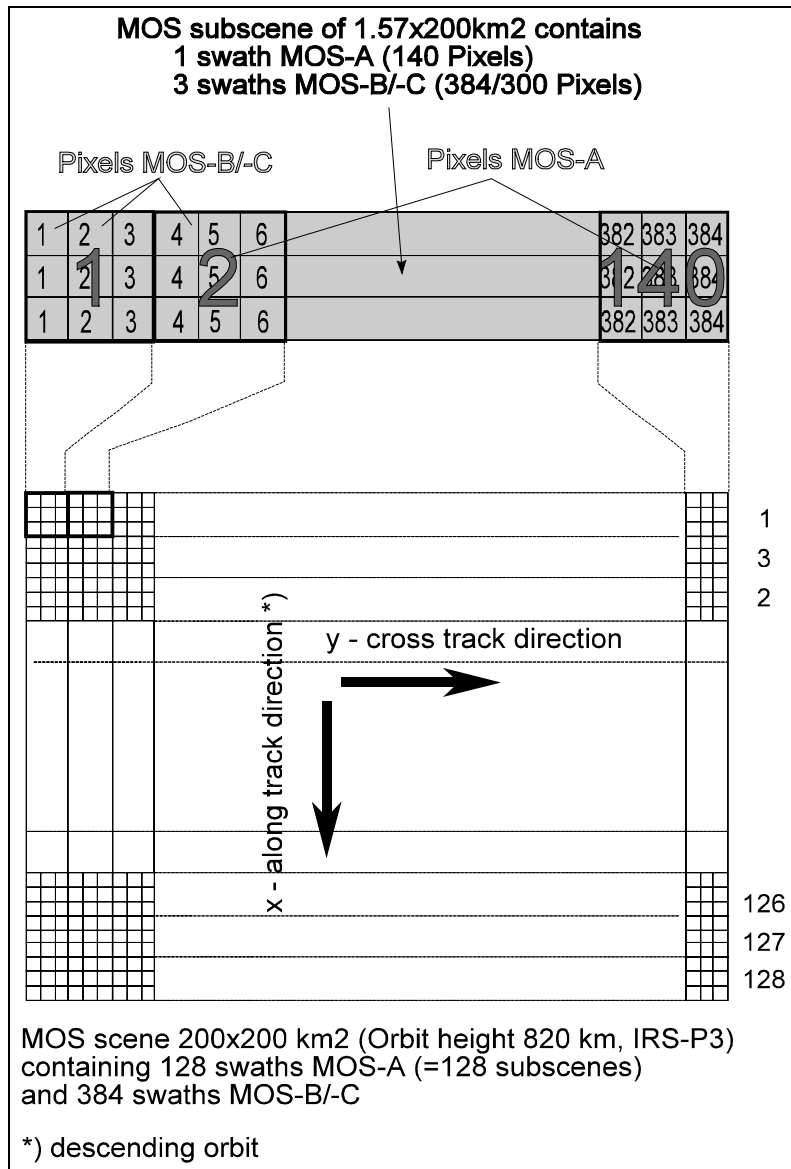
Product Parameters:

Coverage : 200 x 200 km
Packaging : band interleaved by line (BIL), 16 bit per pixel
Units : $\mu\text{Wcm}^{-2}\text{nm}^{-1}\text{sr}^{-1}$
Range : wavelength dependent
Sampling : 0.52 x 0.52 km pixel size
Resolution : $\leq 1\%$
Accuracy : relative stability +/- 0.5%
absolute accuracy 3..5 %
Geo-location
Requirements : n.a.
Format : HDF
Appended Data : georeferencing, time reference, coarse classification, quick-look-image
Frequency of
Generation : daily
Size of Product : ≈ 4.5 MByte

Additional Information:

Identification of Bands used in Algorithm: BIL, no special identification
Assumptions on Input Data: MOS-Level-0-data
Identification of Ancillary and Auxiliary Data: explicit in image header
Assumptions on Ancillary and Auxiliary Data: MOS-Level-0-data

APPENDIX II: SCENE GEOMETRY OF MOS-IRS-P3



APPENDIX III: DESCRIPTION OF DATA FORMATS FOR LEVEL-1B PRODUCTS

TABLE II-1: STRUCTURE OF LEVEL-1B DATA, MOS-A (ONE SCENE)

HDF - Header	
File - Header	
1 st swath	classification image

128 th swath	classification image
Quick-Look Image (R8 image)	
1 st swath	λ_1 MOS-A

1 st swath	λ_4 MOS-A

128 th swath	λ_1 MOS-A

128 th swath	λ_4 MOS-A

TABLE II-2: STRUCTURE OF LEVEL-1B DATA, MOS-B (ONE SCENE)

HDF - Header	
File - Header	
1 st swath	classification image

384 th swath	classification image
Quick-Look Image (R8 image)	
1 st swath	λ_1 MOS-B

1 st swath	λ_{13} MOS-B
1 st swath	λ_1 MOS-C

384 th swath	λ_1 MOS-B

384 th swath	λ_{13} MOS-B
384 th swath	λ_1 MOS-C

TABLE II-3: HEADER-STRUCTURE OF MOS-DEVICE-FILE OF 1 SCENE (ALL DATA WRITTEN IN ASCII-FORMAT)

MISSION	IRSA (for MOS-A) or IRSB (for MOS-B/C)	char(4)
ORBIT	Orbit number	num(5)
MODE	Operational mode	char(7)
TAKE	Data take number	num(5)
SCENE	Scene number	num(4)
OP_BEG_DATE	Date and Time at the beginning of the scene	date
OP_BEG_MS	Miliseconds of Time at the beginning of the scene	num(6,1)
OP_END_DATE	Date and Time at the end of the scene	date
OP_END_MS	Miliseconds of Time at the end of the scene	num(6,1)
NADIR_SUN	Measurement/ Sun Calibration	char(2)
WATER_PERC	Percentage water	num(4)
LAND_PERC	Percentage land	num(4)
CLOUD_PERC	Percentage cloud/snow/ice cover	num(4)
NORTH_ANG	Angle to north	num(4)
UL_LONG_SRECT	Geographical longitude of upper left corner of surrounding rectangle	num(8,2)
UL_LAT_SRECT	Geographical latitude of upper left corner of surrounding rectangle	num(8,2)
LR_LONG_SRECT	Geographical longitude of lower right corner of surrounding rectangle	num(8,2)
LR_LAT_SRECT	Geographical latitude of lower right corner of surrounding rectangle	num(8,2)
LONG_UL	Geographical longitude (upper left pixel)	num(8,2)
LATI_UL	Geographical latitude (upper left pixel)	num(8,2)
SUNZ_UL	Sun zenith angle (upper left pixel)	num(8,2)
SUNA_UL	Sun azimuth angle (upper left pixel)	num(8,2)
LONG_UR	Geographical longitude (upper right pixel)	num(8,2)
LATI_UR	Geographical latitude (upper right pixel)	num(8,2)
SUNZ_UR	Sun zenith angle (upper right pixel)	num(8,2)
SUNA_UR	Sun azimuth angle (upper right pixel)	num(8,2)
LONG_LL	Geographical longitude (lower left pixel)	num(8,2)
LATI_LL	Geographical latitude (lower left pixel)	num(8,2)
SUNZ_LL	Sun zenith angle (lower left pixel)	num(8,2)
SUNA_LL	Sun azimuth angle (lower left pixel)	num(8,2)
LONG_LR	Geographical longitude (lower right pixel)	num(8,2)
LATI_LR	Geographical latitude (lower right pixel)	num(8,2)
SUNZ_LR	Sun zenith angle (lower right pixel)	num(8,2)
SUNA_LR	Sun azimuth angle (lower right pixel)	num(8,2)

Keyword	Content	width
PROC_DATE	Date and time of file-processing	date
SCENE_FILE	File name of scene file, reference to DBMS	char(160)
QL_PATH	Filename of quick-look file, reference to DBMS	char 160)
RAW_FILE	File name of raw data file, reference to DBMS	char(160)
CONTR_FILE	File name of intern control file, reference to DBMS	char(160)
ORBIT_FILE	Filename of orbit file, reference to DBMS	char(160)
CONTR_SET	Set number of used internal control in control file	num(4)
CALIB_SET	Set number of used calibration set in calibration file	num(4)
CORRECT_SET	Set number of used correction set in correction file	num(4)
ORBIT_SET	Set number of used orbit data set in orbit file	num(4)
AMAX_VAL	Absolute maximum pixel value of each wavelength of MOS-A	num(4*6)
BMAX_VAL	Absolute maximum pixel value of each wavelength of MOS-B	num(13*6)
CMAX_VAL	Absolute maximum pixel value of the wavelength of MOS-C	num(2*6)
AMIN_VAL	Absolute minimum pixel value of each wavelength of MOS-A	num(4*6)
BMIN_VAL	Absolute minimum pixel value of each wavelength of MOS-B	num(13*6)
CMIN_VAL	Absolute minimum pixel value of the wavelength of MOS-C	num(2*6)
TEMPA	Temperature of focal plane MOS-A	num(5,1)
TEMPB	Temperature of focal plane MOS-B	num(5,1)
TEMPC	Temperature of focal plane MOS-C	num(5,1)
HEAD_NUM	Number of headers in file (equal 1, if scenewise)	num(3)
SWATH_NUM	Number of swaths (128 for MOS-A or 384 for MOS-B/C)	num(5)
ACAL_VAL	Scaling values $\lambda_1 \dots \lambda_4$ MOS-A	sci(4*12,5)
BCAL_VAL	Scaling values $\lambda_1 \dots \lambda_{13}$ MOS-B	sci(13*12,5)
CCAL_VAL	Scaling value λ_1 MOS-C	sci(2*12,5)
QUALITY	Quality of data ("good" or "bad")	char(20)
REASON	Reason, if value of quality is "bad"	char(30)
DISTURBED	Percentage of disturbed image lines	num(7,2)
FILLED_UP	Percentage of lines, which are filled up by "0"	num(7,2)
MOS_A_FAIL	Percentage of failed pixels MOS-A	num(7,2)
MOS_B_FAIL	Percentage of failed pixels MOS-B	num(7,2)
REMARKS	Comment, Remarks (optional)	char(249)

Comments on Table II-3:

- num (m) : an integer number with m digits
 num (m,n) : a real number with m as field width and n decimal digits
 sci (m,n) : a real number with m as field width and n digits mantisse
 date : a string DD/MM/YYbHH:MM:SS with DD -day, MM - month, YY -year, b - blank, HH - hour, MM - minute, SS – second (hour : UT)
 char(m) : a character string of m characters

Deutsches Zentrum für Luft- und Raumfahrt e.V.
Institut für Weltraumsensorik und Planetenerkundung

Algorithm Theoretical Basis Document (ATBD)

MOS-IRS Ocean Colour Level-2 Algorithm

H. Krawczyk, A. Neumann, M. Hetscher

The work outlined in this document was supported in the frames of the project „Ocean Colour Remote Sensing with MOS“ by

- Deutsche Agentur für Raumfahrtangelegenheiten (DARA) under registry 50 EE 9203 and
- Bundesministerium für Bildung, Wissenschaft, Forschung und Technologie (BMBF), represented by Projektträger Biologie, Energie, Umwelt (BEO) under registry 03 EE 9203

Contents

1.	Introduction	4
2.	Algorithm Identification	4
3.	Background and Overview	4
4.	Theoretical Description	7
4.1	Physics of the Problem	7
4.2	Description of the Physical Model	11
4.2.1	The Atmospheric Model	11
4.2.2	„Global“ Case-2 Water Model	14
4.2.3	Specific Model for the Baltic Sea	15
4.3	Mathematical Description	17
4.3.1	Step 1: Modeling	17
4.3.2	Step 2: Principal Component Analysis	18
4.3.3	Step 3: Intrinsic Dimensionality	20
4.3.4	Step 4: Reverse Correlation	20
4.3.5	Step 5: Reverse Transformation into Radiances	21
4.3.6	Step 6: Determination of Coefficients for the Linear Estimator	21
5.	Practical Realization	21
5.1	Semi-Logarithmic Approach	22
5.2	Program Realization	23
5.3	Choice of Coefficient Set	23
6.	Error Budget Estimates	26
7.	Exception Handling	27
8.	Literature	28

1. Introduction

This document describes a semi-analytical algorithm for the interpretation of multispectral satellite measurements over water resources developed for the Modular Optical Scanner (MOS-PRIRODA, MOS-IRS). It is applicable to different water types, open ocean and coastal zones. As the result there are produced geophysical parameter maps characterizing the state of the atmosphere-ocean system, Pigment concentration maps [Chlorophyll-a], inorganic suspended matter [Sediment] maps, characterized by the sediment backscattering coefficient $bs(550nm)$, dissolved organic matter maps [Gelbstoff], characterized by the yellow substance absorption coefficient $ay(440nm)$. The algorithm accounts for the influence of atmospheric effects on the satellite radiances and produces as an additional interpretation result a map of aerosol optical thickness $\tau_A(750nm)$. The algorithm uses bio-optical ocean-models, to account for specific inherent optical properties, different parameter variation ranges and also possible correlations between them for different geographical regions, for the interaction of the sun light with the water constituents below the air-sea-interface, coupled with a (simplified) atmospheric propagation model of the light. This is to simulate the apparent at the satellite radiance at the wavelengths of MOS-channels. The geophysical parameters are estimated using a linear inversion technique via Principal Component Analysis. The algorithm works directly with Level-1B MOS TOA radiance data [Neumann et. al. 1996]. An explicit atmospheric correction like in other algorithms is not required. For the algorithm development the knowledge of the inherent optical properties of the water body (depending on site and season) is necessary, as well as some knowledge on the aerosol type (described by the Angstroem coefficient, which must be assumed or estimated independently from the here applied algorithm). In the model there are used a number of fixed parameters which must be chosen accordingly to the actual environmental situation during the measurement.

2. Algorithm Identification

PRINCIPAL COMPONENT INVERSION ALGORITHM FOR MULTISPECTRAL SATELLITE DATA OVER WATER BODIES (PCI)

Input: Level-1B data from the Modular Optical Scanner (MOS-B), corrected and absolutely calibrated Top of Atmosphere Radiance

Output: Maps of estimated

- | | |
|---|----------|
| • Pigment [Chlorophyll-a] concentration | C |
| • Sediment backscatter coefficient at 550nm $bs(550nm)$ | S |
| • Gelbstoff absorption coefficient at 440nm $ay(440nm)$ | Y |
| • Atmospheric optical thickness at 750nm | τ_A |

3. Background and Overview

The ecosystem ocean plays an important role in ecological and climatic processes of the earth's environment. The algae in the oceans are one of the largest chlorophyll producers (probably the largest together with the Brazilian rain forests). Due to their photosynthesis they are important for the production of oxygen and as a sink of carbon dioxide. There are theories that the world ocean is the largest absorber of CO_2 and therefore plays an outstanding role for the development of the greenhouse effect. Passive remote sensing of the ocean is a powerful tool for the investigation and understanding of earth's environment. It makes it possible to assess large areas with high time frequency what is practically impossible by ground truth measurements.

If remote sensing of the earth's environment wants to contribute to the actual challenges of ecosystem-related research it has to move towards quantitative estimation of geophysical parameters of different objects and at different scales. For ocean remote sensing this means distinction between different water constituents and quantification of their total content. According to [Morel and Prieur 1977] one can optically distinguish between two water types: case-1 waters are characterized by the fact that only one variable component is influencing the color: chlorophyll and pigments and constituents highly covarying with them. This type of water one finds in open oceans and in special regions, where other constituents (e.g. Seston) are highly correlated with the chlorophyll concentrations. The situation is different in smaller basins (e.g. Baltic Sea, Adriatic Sea) and coastal waters which are strongly influenced by land-sea interaction, river discharges and human activities. Several constituents of different origin and optical behavior are influencing the water color and vary more or less independently (case-2 waters). The problem is to find a methodical approach to investigate these regions regarding to their detailed water characteristics. To make a step towards the solution of this problem the research focuses on three general classes of constituents:

- an organic suspended component, pigments – characterized by their chlorophyll concentration C
- an inorganic suspended component, like sand from river discharges or resuspended matter, the sediments S
- and an organic dissolved component, the yellow substance (Gelbstoff) Y .

These constituents independently influence the spectral characteristics of the remitted light from the water by different absorption and/or scattering behavior. For the chlorophyll and pigments are typically characteristic absorption bands in the green part of the spectrum, sediments are mainly characterized by scattering behavior over the entire visible part of spectrum and Gelbstoff is characterized by strong absorption in the blue part of spectrum following an exponential spectral law.

Since CZCS there is a broad experience in ocean color remote sensing, especially in the determination of Phytoplankton concentration in the open ocean, with only varying chlorophyll concentration. Hence ratios of reflectances in two spectral bands (usually blue and green) can be used successfully to derive chlorophyll concentrations from remotely sensed data [Gordon H. et. al. 1982].

Due to the more complicated biooptical situation in case 2 waters more sophisticated algorithms are needed to discriminate and quantify the single components. A prerequisite for the development of such algorithms on the instrumental side are spectrally high resolved measurements which provide a sufficient number of spectral samples in the entire VIS/NIR range of the spectrum. Imaging spectrometers are an adequate instrument technology to realize this kind of measurements. The first spaceborne, experimental imaging spectrometer is the Modular Optoelectronic Scanner MOS built by DLR and launched on board the Indian remote sensing satellite IRS-P3 in March 1996.

The problem always includes two sides: development of advanced measurement technology (i.e. higher spectral resolution and radiometric accuracy) and the improvement of interpretation algorithms on the other hand. On the technological side during the last years airborne imaging spectrometers and hyperspectral scanners were used to investigate the potential of this new technology for quantitative remote sensing. For a short time higher resolution spaceborne instruments are available, especially for ocean remote sensing. These are for example the SeaWiFS on SeaStar, OCTS on ADEOS and the imaging spectrometer MOS, which was launched on the PRIRODA-module to the Russian space station MIR and on the Indian remote sensing satellite IRS-P3 [Zimmermann 1993, Neumann 1995]. On the

other hand one has to say that the interpretation methodology (measurement inversion) has not yet really developed adequate capabilities compared to the instrument's improvement. There are still a lot of empirical approaches to data interpretation. But the problem of algorithm development becomes more complicated for imaging spectrometers or hyperspectral data sets. Recently new approaches were proposed in the preparation of SeaWiFS and MERIS [Carder 1994; Doerffer 1993, Esaias 1994] trying to find a more systematic semi-analytical understanding of remote sensing data using radiative transfer modeling and fast computational schemes to solve the inverse problem.

In developing case-2 interpretation algorithms the main problem is to formulate the relationship between the spectrum of water leaving radiances and the corresponding concentrations of water constituents using as much spectral bands as available. This is nearly impossible to do on an empirical basis. Radiative transfer modeling is therefore the tool that can be used to solve the problem. This also has the advantage that an analytical approach can be developed. The main problem is that the direct inversion of the problem mathematically is very complicated. Therefore indirect solutions and approximations have to be used. One possible way is the inverse modeling technique developed by Doerffer and Fischer. But this inversion technique is very consumptive with respect to computing power and convergence problems may occur. Due to that a simplification and a more straight forward computing strategy is needed, what lead to the neural network approach (Doerffer et. al. 1997).

However, in a lot of algorithms still subsets of two or three channels are used to estimate geophysical parameters based on more or less empirical a priori knowledge. A reason for this is that it is complicated to handle imaging spectrometer or hyperspectral data sets of tens or even hundreds of bands (i.e. entire spectral signatures) at once to derive object parameters. Therefore a systematic algorithm for the analysis of spectral high dimensional data is needed that allows the derivation and optimization of parameter retrieval under consideration of measurement accuracy concerning different remote sensing objects, viewing geometry as well as different spectral resolution and radiometric accuracy.

The main question of deriving such an approach is: how can one systematically determine the weighted contribution (information content) of each wavelength band to the estimate of the desired geophysical parameter to be computed from the measurement data. The answer to this problem cannot be given on an empirical basis. It also cannot be solved using geophysical a priori knowledge and modeling only. Although both are substantial parts of the algorithm development -, more mathematical and information theory based understanding has to be applied additionally to find a practicable solution of the problem. This is already essential because of the huge mass of data that appear for spectral high resolution imagery. This document presents an approach where methods from information theory and signal statistics are used to form the basis of an algorithm, which includes radiative transfer modeling of the ocean-atmosphere system as well as noise and accuracy estimates for the derived results. The estimation and weighting of information content is done by Principal Component Analysis (PCA). It will be shown how to build a model-based *linear inversion algorithm* to estimate water constituents (pigment, yellow substance, sediments) under consideration of atmospheric influence and, optionally, to derive atmospheric turbidity map.

The experimental background for the algorithm presented in this paper is the development of ocean-related interpretation algorithms for the imaging spectrometer MOS that was built at DLR Institute for Space Sensor Technology and launched in March 1996. The spectrometer was especially designed for remote sensing of the ocean-atmosphere system, providing 17 spectral bands: 4 channels at the O₂A absorption band around 760nm, $\Delta\lambda = 1.4$ nm and 13 channels in the VIS/NIR from 408nm to 1010nm, $\Delta\lambda = 10$ nm. The developed ocean color

algorithm shall be capable for operational or even real-time implementation in future processing systems. For the main MOS parameters see the table 1 below.

Table 1 Modular Optical Scanner MOS-IRS main characteristics

Parameter	MOS-A	MOS-B
Spectral Range [nm]	755 - 768	408 – 1011
No. of Channels	4	13
Wavelengths [nm]	757.3; 760.5; 763.2; 765.5 O ₂ A-band	408; 444; 485; 521; 570; 615; 650; 685; 750; 868; 1011 814; 942 (H ₂ O-vapor)
spectral halfwidth [nm]	1.4	10
FOV along track x [deg]	0.343	0.094
across track [deg]	13.6	14
Swath Width [km]	195	200
No. of Pixels	140	384
Pixel Size x*y [km ²]	1.57x1.4	0.52x0.52
Measuring Range L _{min} .. L _{max} [μWcm ⁻² nm ⁻¹ sr ⁻¹]	0.1 .. 40	0.2 .. 65
ΔL/L [%]	0.3	1.0
Orbit Height	sun synchronous 98° inclination 817 km	

4. Theoretical Description

The following chapter gives a description of the *LINEAR INVERSION ALGORITHM BASED ON PRINCIPAL COMPONENT ANALYSIS*.

4.1 Physics of the Problem

The classical approach of determining chlorophyll from remote sensing ocean color data was developed for CZSZ [Gordon 1978] for case-1 water. The near infrared channel at 670nm is used to estimate the atmospheric influence on the signal (the path radiance). This was done under the assumption that the water constituents (chlorophyll only) do not influence the radiance at this wavelength. This is the so called “black water condition”. One has only to consider the (specular) reflectivity of the ocean surface. Basing on a maritime aerosol model the path radiances in the visible channels (443nm 520nm 570nm) are extrapolated linear proportionally to that at 670nm. The atmospheric influence in the visible is removed and the resulting water leaving radiances are used to built two ratios 443/550 and 520/570. From in situ measurement a high correlation was found between these ratios and the Chlorophyll concentration. The 443/520 ratio is used for low concentrations below 1.5 μg/l and the 520/550 ratio for higher concentrations above 1.5 μg/l through a power law.

Scattering and absorption processes in the atmosphere and water are the physical background determining the spectral signature of the remitted light at satellite level, caused by the air molecules and aerosol particles, water constituents and the water itself. For case-2 waters two or more components are influencing the spectrum. Usually three classes of water constituents are considered: Phytoplankton containing the Chlorophyll (scattering and absorption), Gelbstoff or dissolved organic matter DOM (absorption) and suspended inorganic material or sediments (scattering). Figure 1 illustrates quantitatively the influence of these components on the reflectance spectrum. Due to the nearly total absorption of light

by the pure water below 400 nm and above 700 nm only this limited range allows to assess water constituents. One clearly sees that no part of the spectrum can be related to the influence of one component only (see also table 2).

Table 2: Effects of water constituents in different parts of optical spectrum

	Chlorophyll	Gelbstoff	Sediment	optical thickness
blue	absorption	strong absorption	scattering	scattering
green	scattering	weak absorption	scattering	scattering
red	scattering, absorption fluorescence	absorption	scattering	scattering
infrared	weak scattering	no	scattering	scattering

In practice different mixtures and covariations of the constituents may occur for wide ranges of variability of each component making the inversion even more complicated. Especially in coastal regions and river estuaries high concentrations of suspended matter may mask the influence of other constituents. This leads to limits for the discriminability and retrievability of different water constituents.

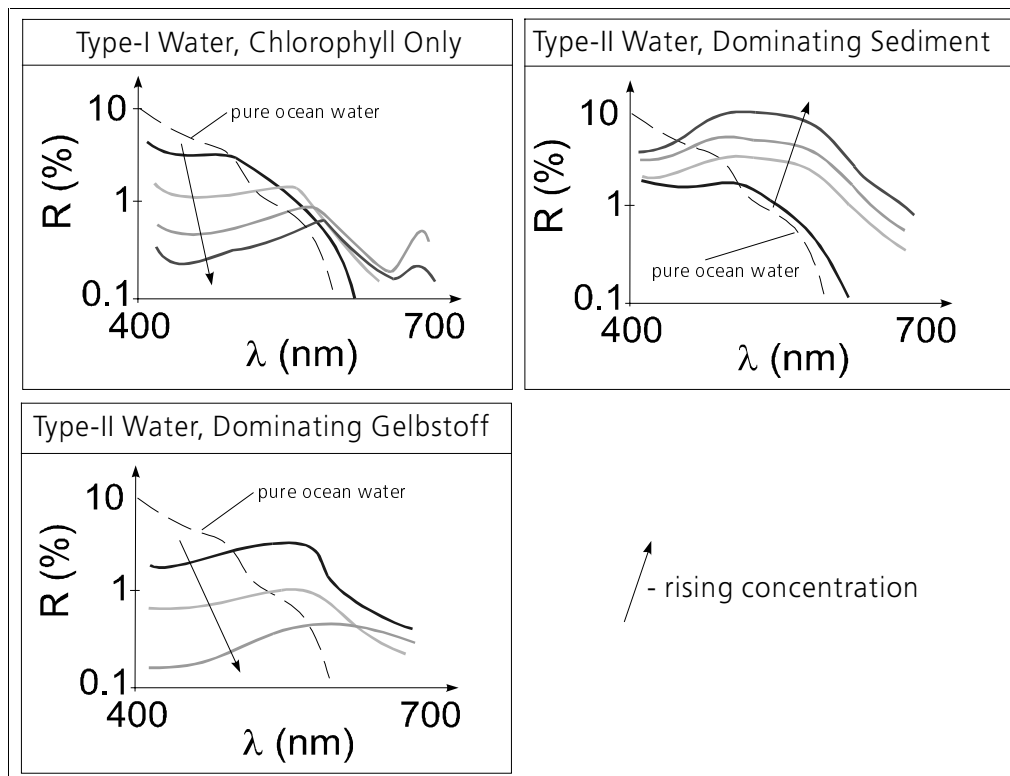


Fig. 1: Influence of different water constituents on the reflectance spectrum

In a more general sense this described situation for case-2 waters obviously causes limitations for the applicability of the “classical” color ratio algorithms since they are not able to separate the single components and may be heavily influenced by the cross-correlation between them. Thus multiband or even hyperspectral retrieval algorithms are needed. Although, of course, the signals in different spectral band will not be uncorrelated, each band

contributes a part of the information that allows the distinction and quantification of the parameters. To build such kind of algorithm is the attempt to assess not only radiance/reflectance values in the single bands but also the shape of the spectral signature as an additional information.

The algorithm described in this ATBD establishes a (quasi) linear relationship between the spectral signature represented by the radiance values in all usable channels and the desired physical parameters, i.e. the water constituents and aerosol optical thickness.

$$\hat{p}_i = \sum_j k_{ij} L_j + A_i \quad (1)$$

where \hat{p}_i - estimate of the geophysical parameter, e.g. Chlorophyll, Gelbstoff
Sediment and Optical Thickness
 k_{ij} - weighting coefficient in band j for parameter i
 L_j - measured radiance in band j
 A_i - offset value for parameter i
 j - spectral band number, from 1 to N , where N - number of spectral bands
of MOS used for interpretation

The coefficients for the estimator in equ. (1) hardly can be derived by an empirical approach. Therefore a model - based on specific optical properties (absorption and scattering) of the different constituents is used to describe the forward relationship between constituents and spectrum.

The general idea of the algorithm is as follows. With the help of a known model, describing the dependence of satellite radiances on geophysical parameters (usually a radiative transfer code) a huge number of spectra corresponding to different parameter combinations over a defined range (possibly with defined correlations) is simulated. Then a statistical analysis is made to find a multiple regression formula, establishing the inverse relationship. The main problem here is the high correlation between the radiances. One has 4 independent parameters and (for MOS) 13 channels, so the problem is overestimated. For the regression the covariance matrix of the radiances must be inverted. But this is a singular matrix and cannot be inverted in a usual manner. A number of methods exist to regularize the problem. One is the Singular Value Decomposition (SVD), which is widely used for the solution of Fredholm Integral Equations of 1st kind. The method chosen for the described algorithm here has some common with this method. It calculates the Principal Components (PC) and Eigenvalues (the same as singular values) from the multivariate spectral radiances and extracts for further analysis the informative part not yet masked by measurement noise. This is possible because the principal components are the "most informative" (artificial) parameters which exist in a linear sense. The geophysical parameters are then correlated to these PC to find an expression of these parameters through the PC. This was also tried earlier, but the problem is that the PC are strongly dependent on the statistics of the investigated data set and therefore on the statistic of the used geophysical parameters. Therefore a formula relating concentrations to principal components cannot hold a common character and is not applicable to any scene. The solution to the problem is, that the Principal Component Analysis (PCA) is a transformation from radiances to an artificial parameter called Principal Components (PC) which is **reversible**. The reverse transformation is given by the calculated Eigenvectors. Thus the relation between PC and geophysical parameters can be related back to satellite radiances using the reverse transformation. And these radiances carry universal character, the formula can be applied to any measured spectrum. Nevertheless the formula was derived for a given situation described by the parameter combinations and variability ranges and is therefore only optimal for the whole parameter set in a mean square sense. It is necessary to derive a number of weighting coefficient sets for different situations, e.g. case 1 water, Gelbstoff dominated

water. The same procedure has to be applied for different optical properties, i.e. specific water bodies.

Additionally this approach of course cannot give always exact interpretation results, since the linear estimate is a strict limitation compared to real nonlinear dependence of the radiances on the geophysical parameters. But relevant arguments have to be considered:

- The nonlinearity is not so strong that the linear assumption will principally fail. As one can see more detailed in the model description part, the nonlinearity mostly comes from the absorption processes (caused by Chlorophyll and Gelbstoff). The scattering processes in the atmosphere due to the aerosols show a very good linear behavior and lead to a linearisation of the multivariate system. So we got the paradox situation (on first view) that an additional parameter, the aerosol optical thickness, improves the potential of the linear inversion approach. But one should not forget that the atmosphere causes a damping of the water leaving signal (due to atmospheric transmission loss) and produces its own variable offset (the pathradiance). One pays for the improvement in applicability of the algorithm by a certain loss of parameter retrieval accuracy. So the described approach is a compromise between accuracy and simplicity. However it has to be noted, that the “classical” approach using atmospheric correction and applying the retrieval procedure to the reconstructed water leaving signals is only excluding this problem from consideration by assuming “correct” water leaving radiances. The overall error budget, i.e. errors from atmospheric correction plus errors of the biooptical algorithm probably will have similar values as the TOA linear approach.
- The second advantage is the stability. Once the weighting coefficients for interpretation are calculated, the inversion procedure is very simple and fast. The direct inversion modeling techniques often have problems with the convergence and stability of their results. They fit **one** given spectrum (not an ensemble) through a given atmosphere ocean model. Every inherent error caused by measurement noise or model non-adequateness causes problems in the inversion convergence. The Gaussian functional to be minimized often has the form of a very flat bowl. For the minimization procedure it is difficult to decide which of the parameters has to compensate for the errors and there is the danger that the results are randomly disturbed from pixel to pixel. In opposite by the Principal Component Inversion Algorithm (PCI) a large number of spectra is used to find one inversion formula. That is the reason for the better stability. Random measurement errors also cause random distortions in the parameters, but it is easier to follow the behavior of the results through the linear estimation formula. Model errors will cause systematic misinterpretations in the concentrations (offsets), but they will not destroy the relative patterns which correspond to the reality.

Finally the Inverse Modeling should have the higher accuracy because of its better consideration of the dependence spectral radiances and concentrations. But in practice this potential has to be paid for: high computer power, development of smoothing filters, consideration of neighboring pixel correlations. The whole calculation procedure must be repeated for every scene from beginning, is very consumptive with respect to computer power and time.

The time consumption for the PCI is fully moved into the forefield of interpretation and must be performed for every type of water only once.

4.2. Description of the Physical Model

The analysis process needs a data set as input where top-of-the atmosphere (TOA) radiances in all available spectral channels are combined with the corresponding values of geophysical parameters that shall be retrieved from the spectral measurements. Such data sets can be provided either from a large number of space and field data or from radiative transfer modeling. For the investigations presented in this document models were used, since a sufficient large set of spectral high resolution space data and corresponding field measurements were not available. In the actual case of ocean remote sensing the modeling gives "measured" TOA radiances depending on concentrations of different water constituents and atmospheric turbidity. The models were basically taken from literature [Gordon, 1978 ; Sathyendranath, 1989] and modified to meet the parameters and capabilities of the MOS instrument [Krawczyk, 1995]. Although the used models, of coarse, heavily influence the derived estimates, they are not principal to the general algorithm development.

In the following chapter the models used for the simulation of the Top of Atmosphere Radiances are described. Mainly they consist of two parts, the atmospheric path radiance and the water leaving radiance/reflectance. Two water models are used to implement the PCI Algorithm:

- a "global" case-2 model using general optical properties
- a specific model for the Baltic Sea based on the experimental analysis of the inherent optical properties and developed by Siegel et al.

4.2.1 The Atmospheric Model

The spectral response functions of the MOS channels are known from laboratory measurements and were used to calculate the extraterrestrial sun irradiances [Neckel and Labs 1984] as well as the Raleigh optical thickness. The atmospheric model here used is based on the atmospheric corrections models for CZCS, developed and successfully used by H. Gordon [Gordon 1978] and B. Sturm [Sturm 1981]. The basic equation for the radiance at the top of atmosphere (TOA) is:

$$L_{\text{sat}} = L_{\text{path}} + L_{\text{sky}} + L_{\text{sun}} + L_{\text{w}} \quad (2)$$

The TOA radiance is split into 4 parts:

- L_{path} - the **path radiance** is the scattered in the atmosphere sun light, never reaching the ocean surface
- L_{sky} - the surface reflected **sky light** is the scattered in the atmosphere light, Fresnel reflected at the water surface and passed through the atmosphere to the sensor
- L_{sun} - the direct transmitted **sun light**, Fresnel reflected at the surface and diffusely (i.e. scattered) transmitted to the sensor
- L_{w} the **water leaving** radiance is the light portion penetrating the sea surface, scattered in the water, back transmitted through the sea air interface and transmitted through the atmosphere into the sensor

Regarding the water constituents - L_{w} is the only informative part. The other parts are determined by atmospheric properties, especially molecular and aerosol scattering. The ozone absorption is accounted for as a thin absorbing layer at the top of atmosphere from a middle altitude summer model. The water vapor absorption will affect the 815nm and 945nm bands. These bands are especially designed for extracting water vapor content. In the here used model they are not considered exactly and therefore these channels are not used in the

described interpretation algorithm. The path radiance is calculated by a linear single scattering approximation:

$$L_{\text{path}} = E_{01} * (p_R \tau_R + p_A \tau_A) \quad (3)$$

with E_{01} extraterrestrial sun irradiance reduced by the absorption from ozone and water vapor.

p_R phase function of Rayleigh scattering
 p_A phase function of aerosol scattering, here was used a Two Term Henney Greenstein function for a maritime atmosphere with asymmetry parameters 0.8 and -0.5 and a weighting factor of 0.985.

The skylight and the sunlight are calculated by the formulas:

$$L_{\text{sky}} = \frac{\mu_0 E_{01}}{\pi} \rho_{LW}^* (T_{\text{tot}}^{\downarrow}(\mu_0) - T_{\text{dir}}^{\downarrow}(\mu_0)) T_{\text{tot}}^{\uparrow}(\mu) \quad (4)$$

$$L_{\text{sun}} = \frac{\mu_0 E_{01}}{\pi} \rho_{LW}^{\text{dir}} T_{\text{tot}}^{\downarrow}(\mu_0) (T_{\text{tot}}^{\uparrow}(\mu_0) - T_{\text{dir}}^{\uparrow}(\mu_0)) \quad (5)$$

with μ_0 cos of the sun zenith angle

μ cos of the observation zenith angle

ρ_{LW}^{dir} Fresnel coefficient of direct reflection from air to water

ρ_{LW}^* Fresnel coefficient for diffuse reflection of the diffuse part of radiance

$T_{\text{tot}}^{\uparrow\downarrow}$ total transmission function for up- or downward total radiance flux

$T_{\text{dir}}^{\uparrow\downarrow}$ direct transmission function for the direct part of the radiance flux

(direct sun beam)

The water leaving radiance is calculated by the formula:

$$L_W = \frac{\mu_0 E_{01}}{\pi} * T_{\text{tot}}^{\downarrow}(\mu_0) * t^2 / n^2 * R_V * T_{\text{tot}}^{\uparrow}(\mu) \quad (6)$$

with R_V being the volume reflectance coefficient for radiance beneath the sea surface t describes the transmission of air-sea interface and n the refractive index of seawater ($n=1.341$). t^2 / n^2 can be approximated by 0.54 [Austin 1974] The more detailed description of this follows in chapter 4.2.2.

Another question in the model is the wavelength dependence of the aerosol-optical thickness. The Raleigh scattering due to molecules can be exactly calculated using MIE-theory and then summed with the spectral response functions. Here is used the following approximation:

$$\tau_R(\lambda) = 0.0088 * \lambda^{(-4.15+0.2\lambda)} \quad \lambda \text{ in } \mu\text{m} \quad (7)$$

For the aerosol optical thickness was assumed an Angstrom law:

$$\tau_A(\lambda) = \tau_A(750\text{nm}) * \left[\frac{\lambda[\text{nm}]}{750} \right]^{-\alpha_A} \quad (8)$$

with α_A being the Angstrom coefficient for the atmosphere.

To prove the assumptions for the atmospheric part of the model test comparisons with the atmospheric radiance calculation program LOWTRAN-7 were made. [see also Krawczyk et.al. 95]. At first the wavelength dependence of the aerosol depth for maritime atmospheres with different visibilities was investigated. The results (figure 2) show a good agreement with the assumption of Angstrom law. Then the TOA radiances were calculated with the LOWTRAN-7 program and compared with the results of the simplified model. Because

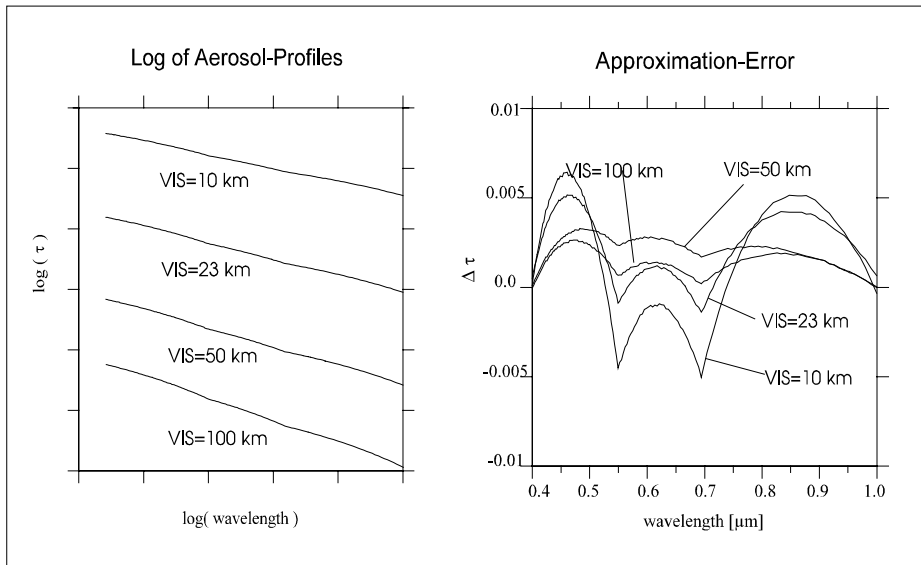


Figure 2 : Lowtran test of Angstrom law

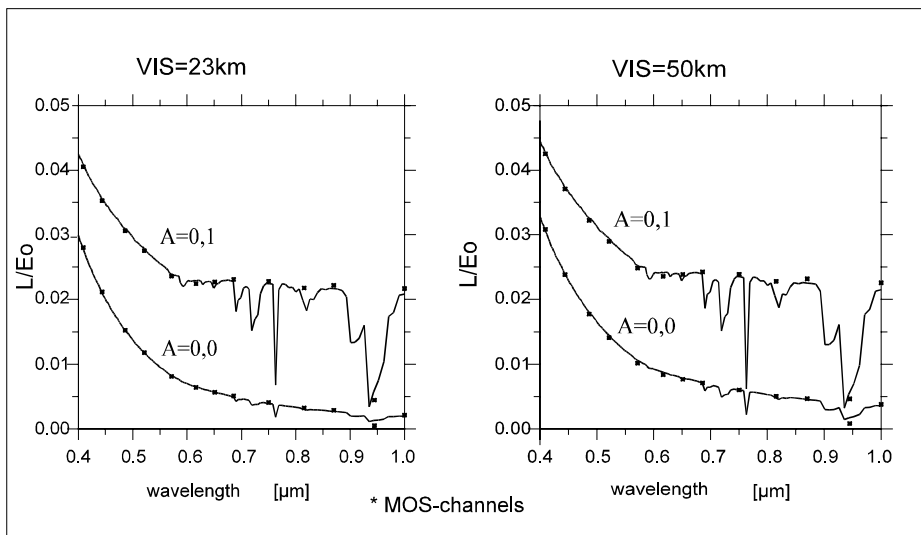


Figure 3 : Lowtran test of MOS-Radiances

LOWTRAN does not allow the incorporation of Fresnel reflectance of water surfaces the model was modified for Lambertian reflectors. Test calculations, made for a maritime atmosphere, visibilities of 23 km and 50 km, also show a good agreement with the used model (figure 3). During these test calculations was found, that LOWTRAN considers

multiple scattering effects of the Rayleigh path radiances, especially in the blue region of spectrum, what can be good approximated by a substitution of τ_R in formula (2) through $\tau_R - 0.33 * \tau_R^2$. In future releases of the atmospheric model multiple Raleigh scattering will be considered more exactly by solving in the forefield the radiative transfer equation for a Rayleigh atmosphere using a matrix operator program and parametrizing the solutions. (First results are already available, and will be built in into the next release.)

4.2.2. “Global” Case-2 Water Model

The water body (ocean) is described by a 3-component model, characterized by an organic suspended matter part C (Chlorophyll), an inorganic suspended matter part S (Sediment concentration) and dissolved organic matter part Y (Gelbstoff, Yellow Substance). The ideas and main characteristics for the 3-component ocean model were taken from [Sathyendranath et al. 1981] and adapted to the characteristics of the MOS instrument. The parameters characterizing the in-water properties are the pigment concentration $C[\mu\text{g/l}]$, the sediment concentration S , described by the scattering coefficient $b_s[1/\text{m}]$ at 550 nm and the yellow substance concentration Y , described by the absorption coefficient $a_y[1/\text{m}]$ at 440 nm. The light passing through the air sea interface here interacts with molecules and particles and therefore is being absorbed or scattered. The ratio of the incident energy flux to the upcoming flux is called the volume reflectance coefficient R_V , and can be estimated as

$$R_V = 0.33 \frac{b_B}{a} \quad (9)$$

where b_B is the total backscattering coefficient and a is the total absorption coefficient in the water. b_B is defined as

$$\begin{aligned} b_B &= 2\pi \int_{\pi/2}^{\pi} b * p(\theta) \sin(\theta) d\theta \\ &= \tilde{b}_B * b \end{aligned} \quad (10)$$

„the scattering coefficient into the upper hemisphere “, with b the total scattering coefficient and $p(\theta)$ the scattering phase function with the scattering angle θ . \tilde{b}_B is the backscattering to total scattering ratio (relative backscatter coefficient). The b_B and a in R_V are assumed to be linear depended from the water constituents:

$$a(\lambda) = a_w(\lambda) + C' * a_C^*(\lambda) + Y * a_Y^*(\lambda) + S' * a_S^*(\lambda) \quad (11)$$

$$b_B(\lambda) = \tilde{b}_{BW} * b_w(\lambda) + \tilde{b}_{BC} b_C(\lambda) + \tilde{b}_{BS} * b_S(\lambda) \quad (12)$$

with $a_w(\lambda)$ and $b_w(\lambda)$ being the absorption and scattering coefficients for pure sea water. The $a_C^*(\lambda)$, $a_S^*(\lambda)$, $a_Y^*(\lambda)$ are the specific absorption coefficients of Chlorophyll, Sediment and Gelbstoff respectively. In the “global” case-2 model there are used the coefficient sets from (Prieur, Sathyendranath 1981). The Gelbstoff absorption follows an exponential law

$$a_Y^*(\lambda) = \exp(0.014 * (440\text{nm} - \lambda)) \quad (13)$$

C' and S' are linearly related to C and S:

$$C'=0.008 + 0.070*C \quad \text{for } C < 1 \mu\text{g/l} \quad (14)$$

$$C'=0.058 + 0.018*C \quad \text{for } C > 1 \mu\text{g/l} \quad (15)$$

$$S'= -0.0029 + 0.042*S \quad (16)$$

The scattering coefficient for pure seawater was assumed to follow a power law (Morel 1974) $b_w(\lambda)=0.00288*(\lambda/500)^{-4.3}$ and was convoluted with the spectral response functions of the MOS bands. The \tilde{b}_{BW} , \tilde{b}_{BC} , and \tilde{b}_{BS} are the backscattering ratios for seawater Chlorophyll and Sediment. They are assumed to be wavelength independent and constant for a given scene. The values are fixed in the simulation programs with $\tilde{b}_{BW}=50\%$, $\tilde{b}_{BC}=0.5\%$, $\tilde{b}_{BS}=2\%$. The wavelength dependence of the Sediment scattering follows an Angstroem law $b_s(\lambda)=S*(\lambda/550)^{-\alpha_s}$. The Sediment Angstroem coefficient α_s is a parameter strongly related to size distribution of particles. Because of the comparable small coverage of one scene, a uniform origin of the particles is assumed and therefore α_s is chosen to be constant for a scene, but can be varied for different calculations. The scattering by Chlorophyll varies in complementary matter to absorption [Morel, Bricaud 1981]. In the model was taken

$$b_c(\lambda) = b_c(550)*a_c^*(550)/a_c^*(\lambda) \quad (17)$$

with $b_c(550) = 0.12*C^{0.63} \quad (18)$

4.2.3 Specific Model for the Baltic Sea

The specific Baltic Sea Model was developed in close relation to the global case-2 water model described in the previous chapter. The model itself was proposed by Siegel of the Baltic Sea Research Institute, Rostock Warnemuende [Siegel 1998], and is basing on long term measurements of the inherent optical properties of the water body together with the corresponding concentrations of the water constituents. The model for the Baltic Sea is primarily described by 3 components. These are the Chlorophyll and Gelbstoff concentrations C and Y, and the particulate matter concentration, the so called Seston C_s . This part contains both inorganic matter – Sediment S - and organic matter.

The model was developed, relating the measured optical values of upwelling subsurface radiance $L_u(\lambda)$ and downwelling above surface irradiance $E_D^+(\lambda)$ to the volume reflectance coefficient $R_v(\lambda)$. Defining the so called total inner reflection coefficient $R(\lambda)$:

$$R(\lambda) = \frac{\pi L_u^-(\lambda)}{E_D^+(\lambda)} \quad (19)$$

follows

$$R(\lambda) = \frac{t R_v(\lambda)}{1 - r_u R_v(\lambda)} \quad (20)$$

with t the transmittance for the downward flux through the air sea interface and r_u the reflectance of the upward irradiance. For the development of the model were used the proposed by Austin (1974) values of $t=0.98$ and $r_u=0.48$. The volume reflectance coefficient

$$R_V(\lambda) = 0.33 \frac{b_B(\lambda)}{a(\lambda)} \quad (21)$$

with the total backscatter and absorption coefficients $b_B(\lambda)$ and $a(\lambda)$ was related to the water constituents Chlorophyll C, Gelbstoff Y, and Sediment S. From in-situ measurements in the open Baltic Sea and in the Pomeranian Bight could be determined the specific scatter and absorption coefficients for the constituents.

$$a(\lambda) = a_W(\lambda) + Y \cdot a_Y^*(\lambda) + S \cdot a_S^*(\lambda) + C \cdot a_C^*(\lambda) \quad (22)$$

$$b_B(\lambda) = b_{BW}(\lambda) + S \cdot b_{BS}^*(\lambda) + C \cdot b_{BC}^*(\lambda) \quad (23)$$

with $a_W(\lambda)$ being the pure water absorption coefficient, $b_{BW}(\lambda)$ the pure water backscatter coefficient (Morel, 1974)

$$b_{BW}(\lambda) = 0.5 \cdot 0.0055 (500/\lambda)^{4.3} \quad (25)$$

For the specific Gelbstoff absorption a good agreement with the exponential law was found

$$a_Y^*(\lambda) = \exp(0.014(440 - \lambda)) \quad (26)$$

The specific Sediment scattering coefficient $b_S^*(\lambda)$ could be well approximated by an

Angstroem law $b_S^*(\lambda) = \left(\frac{500}{\lambda}\right)^{0.5}$ with an Angstroem coefficient of 0.5 .

Through correlation measurements it was possible to relate the Sediment concentration to the backscatter coefficient at 550nm.

$$b_{BS}(550nm) = 0.0055 \cdot S \cdot b_S^*(550nm) \quad (27)$$

From this one gets a conversion formula from Sediment S to the scattering coefficient $b_S(550)$:

$$b_{BS}(550) = \tilde{b}_{BS} \cdot b_S(550) \quad (28)$$

$$b_S(550) = \frac{0.0055}{\tilde{b}_{BS}} \cdot S \cdot \left(\frac{500}{550}\right)^{0.5} \quad (28a)$$

$$S = k \cdot b_S(550) \quad (28b)$$

with

$$k = \frac{0.0055}{\tilde{b}_{BS}} \cdot \left(\frac{500}{550}\right)^\alpha \quad (28c)$$

Assuming $\alpha=0.5$ and a relative backscatter coefficient $\tilde{b}_{BS} = 2\%$, which values were found typically for the Baltic Sea this leads to $S = 3.6 \cdot b_S(550)$.

Figure 4 shows a comparison for the specific absorption and scattering coefficients of C and S for the “global” case 2 from Sathyendranath, Prieur, Morel and the Baltic Sea specifics from Siegel.

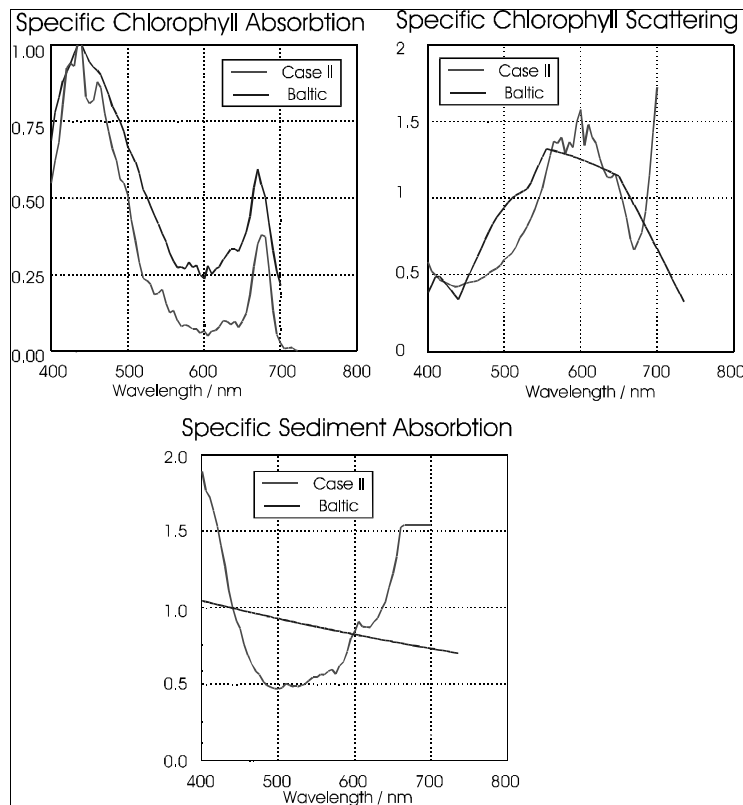


Fig. 4.: Comparison of „global case 2“ and Baltic Sea models

4.3 Mathematical Description

The following gives a detailed mathematical description of the entire interpretation procedure. Mainly it is divided into two parts, first the definition of the weighting coefficients for the interpretation formula and second the application to MOS data to derive the geophysical parameter maps. The following scheme in figure 5 shows the principal flow chart for the calculation of the needed coefficients. It consists of six separate steps which are described in the next subchapters.

4.3.1. Step 1: Modeling

The actual interpretation algorithm is the trial to find the inverse map of geophysical parameters into the satellite radiances. Every change of a concentration causes a defined change in the remote sensing satellite signal, through its optical effect on the incident light field. This map could be given through in situ measurements, or through models describing analytically the dependence of the light field on the concentrations. But the difference between these two opportunities is not essential because most (or even all) of theoretical models are basing fundamentally on measurements respectively experiments. So both methods are more or less equivalent and can be used to get a large enough data set as input where top-of-the atmosphere (TOA) radiances in all available spectral channels are combined with the corresponding values of geophysical parameters that shall be retrieved from the spectral measurements. For the investigations presented in this document models were used, since there were no spectral high resolution space data and corresponding field measurements available. In the actual case of ocean remote sensing the above described models simulate "measured" TOA radiances depending on concentrations of different water

constituents and atmospheric turbidity. Although the used models heavily influence the derived estimates, they are not principal to the general algorithm development. Concrete, more sophisticated models have to be chosen for applied studies. But this does not change the principal approach of the algorithm. For the calculation one has to consider variability range for each input parameter and the correlation between them. This is done by selecting corresponding spatial patterns (images) of chlorophyll-a, yellow substance, sediments and atmospheric turbidity that are overlaid as inputs for the modeling process. Here are realized two options:

- Choose minimum and maximum for each parameter and a desired step width, and combine all possible parameter combinations together (i.e. a 4-times folded loop). The corresponding geophysical parameter patterns are fully uncorrelated and uniformly randomly distributed. This is the case if no a-priori knowledge about the parameters is given, except the expected parameter range.
- Read the parameters pixelwise from given input files. These files are to be constructed before and can consider for given correlations between parameters and known statistic distribution. Here there were realized the case of normal (Gaussian) distributed and randomly correlated parameter patterns and the case of randomly correlated uniformly distributed parameters.

For each simulated pixel the corresponding radiance values in the 13 spectral channels of MOS and the values of input parameters are written to a special formatted data file that is then fed into the analysis and inversion process.

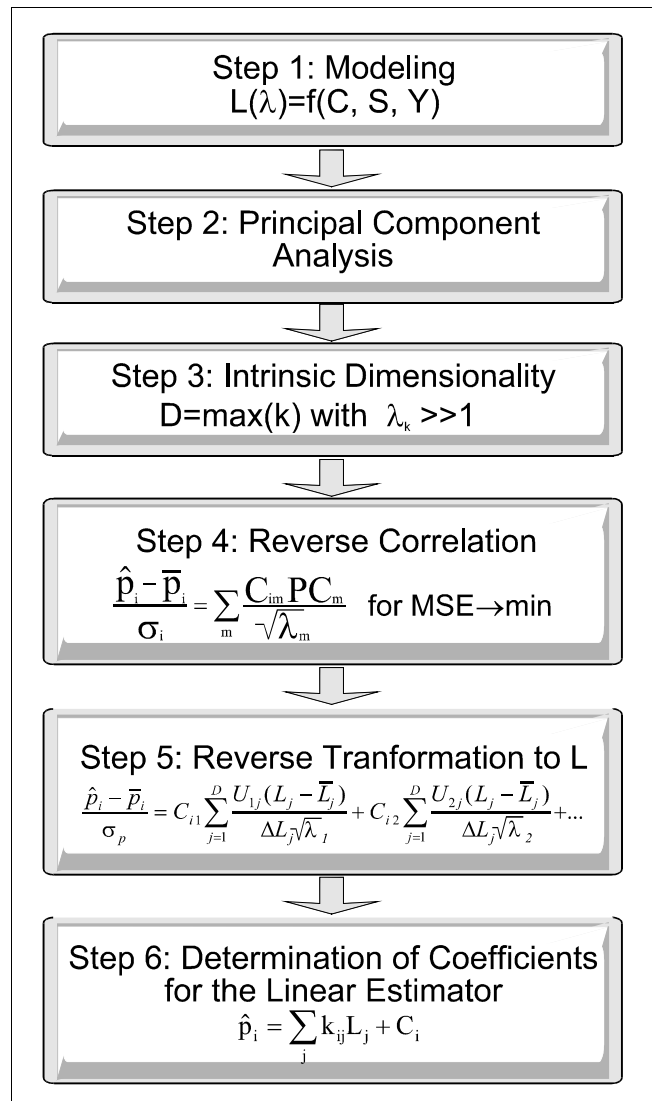


Fig. 5: Flow chart of definition of interpretation coefficients

4.3.2 Step 2: Principal Component Analysis (PCA)

PCA provides a powerful tool for the analysis of information content of high-dimensional multivariate data sets such as spectral high resolution imagery [Ingebritsen, 1985]. However, it is problematical to find a physical understanding of principal components for remote sensing applications. So in the following the PCA is used only to estimate the information content of experimental or modeled data sets, to rearrange (transform) the data in a manner, suitable for analysis and, not at least, to separate the useful information from noise

contained in the data. Principal components are computed from the input data sets using the eigenvectors of the spectral covariance matrix. The transformation builds an orthogonal representation of the original data:

$$PC_k = \sum_{m=1}^N \frac{U_{km}(L_m - \bar{L}_m)}{\Delta L_m} \quad (29)$$

where

- PC_k - k-th principal component, k from 1 to N
- N - number of spectral bands used in the original data set
- U_k - k-th eigenvector of the covariance matrix
- L_m - radiance in the m-th spectral band
- \bar{L}_m - mean radiance value in the m-th spectral band
- ΔL_m - noise-equivalent radiance, measurement error.

As it is seen from formula (19) the input radiances are meanfree and error normalized. This is not the only possibility for the information analysis. The choice depends on the point of view under which the geophysical parameters shall be retrieved. At first it is known that for the best regression between two data sets their meanfree values must be correlated (linear regression formula). From this follows that for the interpretation it is also optimal to work with meanfree radiances. The mathematical proof of this fact is a bit more expensive but fully analogous to the derivation of common linear regression formulas. By definition the Principal Components (PC) are the linearly derived **independent, uncorrelated** parameters with **highest possible mean square norm**. Because there is a free choice in the transformation coefficients U_{km} (they can be scaled by a random factor) they are normalized to unitary vector norm (sum of squares equals to one). Therefore the transformation matrix becomes a unitary matrix with the so called eigenvectors (EV) as rows. The PC and EV have the property that with them the original dataset can be progressively reconstructed in a maximum likelihood sense (i.e. the first reconstruction step will be done with only the first principal component and achieving an optimal reconstruction as possible - then adding the second PC etc.). The optimization criterion of reconstruction depends on the kind of original data used, the kind of normalization. If one wants to reconstruct the data in the sense of usual Euklidian norm, i.e. to reconstruct as good as possible the whole variation of the data set, this leads to the processing of the common covariance matrix of the multispectral data. If one wants to reconstruct the data in the sense of highest possible correlation between original and reconstructed data one has to use variance- normalized spectral channels. This leads to the further processing of the correlation matrix (the covariance-matrix of normalized to variance=1 input values). Another opportunity is the consideration of measurement noise. If the noise is known in any channel then the main goal can be to reconstruct the data with as much as possible information content and less noise. This can be done in the sense of optimal Signal to Noise Ratio (SNR) reconstruction, i. e. we want to achieve the highest possible SNRs of the reconstructed data. For this one has to use errornormalized data. Every channel is divided by its noise-equivalent radiance. This immediately has the effect that spectral channels with higher noise corruption (less resolution) - contribute less to reconstruction and interpretation. In the developed program package for the inversion algorithm all these cases are considered for and can be used, but in practical applications the last case (SNR – optimization) is applied.

By definition of the transformation the principal components are uncorrelated among each other and contain successive maximal information in the statistical sense, i.e. the higher the order of the component the smaller its total variance, the more noise or "uninterpretable" information is contained. This corresponds to the relation of eigenvalues: $\lambda_i > \lambda_j$ for $i < j$.

4.3.3 Step 3: Intrinsic Dimensionality

First the spectral covariance matrix for the entire set of (simulated) radiance data is computed and then diagonalized. The diagonalization is necessary to perform the principal component analysis. The calculation of covariances is done using error-normalized radiance values: $\text{Cov}\{L_j/\Delta L_j\}$ where ΔL_j denotes the noise-equivalent radiance for the j-th spectral band. This normalization automatically accounts for the radiometric resolution of the instrument considered in the background of algorithm development. Then are computed the eigenvalues λ_k and the eigenvectors \underline{U}_k of the spectral covariance matrix. Because of the error-normalization of radiances for calculating the covariance matrix the eigenvalues directly give an estimate on the signal-to-noise ratio of the corresponding principal component:

$$\lambda_k = \text{SNR}^2(\text{PC}_k) \quad (30)$$

where λ_k - k-th eigenvalue of the spectral covariance matrix, k from 1 to N
 SNR - signal-to-noise ratio
 PC_k - k-th principal component.

The SNR of each principal component is a measure of its significance in the statistical sense considering the measurement error. Taking the eigenvalues λ_k one can also determine the intrinsic dimensionality D of the measurement data which is equal to the number of principal components containing significant information and corresponds to the number of independent parameters that can be (theoretically) retrieved from the spectral measurement data set:

$$D = \max(k) \text{ with } \sqrt{\lambda_k} \gg 1. \quad (31)$$

Two groups of principal components are separated:

- a) ones representing significant measurement information ($k \leq D$) and
- b) ones containing non-interpretable variations such as noise, quantization error etc.

For the further analysis and determination of the coefficients in equ. (1) only the significant principal components are used, i.e. only the first group.

4.3.4 Step 4: Reverse Correlation

The question is now how the representation of the spectral information in the form of principal components can be used to derive the desired coefficients. The first one has to consider is, that the principal components contain *the same information* as the original spectral radiance data, except the small noise-like portion of information that is suppressed by reducing the number of used components to the "significant" ones. That again means that it must be possible to reconstruct not only the radiance values from the principal components (what in fact can be done very easily by the reverse transformation) but also the input parameters of the modeling as far as this is possible at all [Krawczyk, 1995]. Because of the linear estimate for the determination of the geophysical parameters defined in equ. (1) a linear estimate is also chosen with the principal components:

$$\hat{P}_i \sim \sum_{m=1}^D C_{im} \text{PC}_m \quad (32)$$

where C_{im} - correlation coefficient between the i-th parameter and the m-th- principal component.

Having in the data sets the principal components and the corresponding geophysical parameters, which can be taken from the simulated TOA radiance data, one can formulate a regression formula that allows it to determine the needed correlation coefficients C_{im} :

$$\frac{\hat{p}_i - \bar{p}_i}{\sigma_i} = \sum_m \frac{C_{im} PC_m}{\sqrt{\lambda_m}} \quad \text{for MSE} \rightarrow \min \quad (33)$$

where \hat{p}_i - estimate of the parameter
 \bar{p}_i - mean value of the parameter
 σ_i - variance of the parameter
MSE - mean square error

This regression now has to be performed for each simulated pixel and each principal component, i.e. for the entire data set. Based on the results in step 3 only the significant principal components are used for the regression analysis. This suppresses noise from the data, especially avoids noise amplification and reduces significantly the amount of computations. It does *not* reduce the accuracy of the algorithm, since all of the usable portion of information contained in the data is applied.

4.3.5 Step 5: Reverse Transformation into Radiances

Although one can now determine coefficients to estimate geophysical parameters from the principle components, this is not what is needed at the end. Computing principal components from spectral high dimensional data sets is still comparably time consuming. So there is one more step to go: since the principal components used for the analysis process are computed from the TOA radiances one can apply the reverse transformation of equ. (29) to equ. (33) and yields a representation of the regression formula based on the TOA radiance values:

$$\frac{\hat{p}_i - \bar{p}_i}{\sigma_i} = C_{i1} \sum_{j=1}^D \frac{U_{1j}(L_j - \bar{L}_j)}{\Delta L_j \sqrt{\lambda_1}} + C_{i2} \sum_{j=1}^D \frac{U_{2j}(L_j - \bar{L}_j)}{\Delta L_j \sqrt{\lambda_2}} + \dots \quad (34)$$

4.3.6 Step 6: Determination of Coefficients for the Linear Estimator

From equation (34) one now can compute the coefficients k_{ij} and A_i used in the linear estimate for each parameter and each wavelength band. These coefficients are stored separately for each investigated case.

5. Practical Realization

The interpretation procedure breaks up into 2 parts, the definition of the coefficient set and the application to a real MOS-scene. The first part consists of the explained steps 1 to 6.. The entire package is realized on a Sun platform in Fortran programs. It is constructed following a consequently modular concept, to allow easy modification of single parts in future releases and localization of possible program errors. The single steps necessary for the calculation of a coefficient table are arranged in a C-shell script. This form was chosen for universality, and to allow portation of the programs to other platforms. The programs will also run on a Personal Computer with Lahey-Fortran with only slight modifications in the Input/Output statements. The script starts with the definition of environment variables with the set statement to adapt the program to users specifics. These are mainly the locations of

necessary directories for program and data/results locations. It follows a number of statements for the definition of specifics for the coefficient set, the minimum and maximum of the desired parameters or possible parameter-file name specifications. For the calculation of the coefficient set a number of inherent parameters, necessary for the description of atmosphere and water properties are fixed. These are mainly the Ozone optical thickness and the watervapor content which are used for the calculation of the TOA - radiances. Two other parameters which are fixed for one coefficient set are the Angstroem coefficients for the wavelength dependence of aerosol and sediment scattering. It is known from in-situ measurements, that maritime atmospheres tend to Angstroem coefficients of about zero and urbane atmospheres to values of about one. For sediments this value can vary between 0 for large particles and 2 for very small particles.. Both Angstroem coefficients are fixed during the interpretation of one MOS-scene by selecting the interpretation coefficient set. In the case of no a-priori knowledge values of 0.5 for atmosphere and 1.0 for sediments are good recommendations. Another fixed value for the production of a coefficient set is the sun elevation, which influences the radiance simulation. To consider this - coefficient sets for sun angles between 0° and 80° in steps of 1° are calculated and stored. In most cases the change of sun zenith distance in one MOS-scene (an area of 200km x 200km on earth surface) is not significant - mostly in an order of magnitude of 1°. So for the interpretation of one scene the interpretation is made with a fixed sun angle related to the scene center. This is justified also because of the approximation character of the used model. It makes no sense to make efforts in this place which do not correspond to the model accuracy. A few words to the number of used spectral channels. The program allows any choice of channel subsets. MOS-B provides of 13 channels. For the derivation of water constituents the two water vapor channels (820nm and 945nm) are omitted, since the applied models do not account for variable atmospheric water vapor. The mean water vapor content used in the algorithm is accounting for a (very) slight influence in a few other channels. Because the 7th MOS-B channel (650nm) is corrupted due to electronics malfunction, it is not used for interpretation. Finally for the derivation of the 4 geophysical parameters 10 spectral channels are used. They are considered for with equal relative measurement errors, what is justified by preflight laboratory measurements and is underlined also by the in-flight calibration analysis (internal lamps, sun calibration). The coefficient set containing the values for all different sun angles is stored in a binary data format and then used for the actual interpretation process.

5.1 The semi-logarithmic approach

During the experimental evaluation of the developed algorithm two problems became evident: for wider simulation ranges the nonlinearity became more and more significant, second, for small concentrations the interpretation results because of its approximate character could tend to negative values, what is physically not real. These values could have been flagged out. But this is not preferable because the retrieved relative parameter patterns are reasonable and should not be lost. On the other side the negative values are mainly an indicator for very small parameter values. The classical color ratio algorithms do not have this difficulty, because they are estimating the parameter through a power law $p = (L_1 / L_2)^q$. Translated into the linear approach this means to work with the logarithms of the physical values $\log p = q \log L_1 - q \log L_2$.

From this arose the idea to use for small values the logarithms instead of the original values p . At the same time the logarithm could better account for the inherent nonlinearities in the model especially for the absorbers. Through extensive numerical investigations it was found that the direct use of the logarithm does not solve the problem satisfactory. It avoids the negative concentrations, but the overall retrieval quality is decreasing. The logarithm is already “too” “nonlinear”. The reason for this is the linearisation of the entire multivariate

system through the atmospheric influence. So a compromise had to be found between the linear and logarithmic assumption ending up in a combination of both in the form

$$q = p + \alpha \log p \quad (35)$$

i.e. at first there are found the transformed parameters q , which are then retransformed into the original geophysical parameters p . This semi-logarithmic approach avoids negative values as interpretation results and also accounts better for nonlinearities. The backtransformation is made with a special routine, because of the transcendence of the $p + \alpha \log p$ function equ. (35), realized through an adapted Newton – inversion method for finding zeros of a transcendent function. For the parameter α there was found an optimal value of 0.1 for the water constituents C, S and Y. For the atmospheric optical thickness the semi-logarithmic approach is not necessary.

5.2 Program Realization

The interpretation part of the algorithm (i.e. computation of the maps of geophysical parameters) is realized in the C – program “mosloginvers”. Input data are Level 1B MOS scenes in HDF – format. [ATBD Level - 1B products MOS-IRS] and the precalculated coefficient sets in binary format. The user must specify the name of the coefficient set to be used. The appropriate sun angles for the scenes are chosen from the header information of the MOS level 1B data. In a first step there are calculated the semi-logarithmic parameters which are retransformed into the original geophysical parameters. The output product, the 4 parameters Chlorophyll concentration, Sediment scattering, Gelbstoff absorption and Aerosol optical thickness, are stored in a multiband file. The user can choose between raw data format, Khoros – Cantata output format (this is an image processing system, freeware, available on all platforms) or an HDF format analogous to the input level 1B format. Any number of scenes can be processed in one run. The land-cloud masks are transformed from input data into the output product with special flags.

5.3 Choice of Coefficient Set

The implementation of the PCI Algorithm uses three different types of modeling

- Open ocean case 1 water
- “Global” case 2 Coastal water
- Baltic sea case 2 water.

For each type of water a separate set of coefficients was calculated and stored in the Look up Tables (LUT). The variability ranges of the geophysical parameters were chosen according to typical characteristics in real situations. Table 3 gives an overview of the variability ranges.

The user has to select the coefficient set that is used for the interpretation of an actual scene.

In the first release of the final program “mosloginvers” only coefficient sets for the entire variability ranges are implemented. The extreme concentrations of all different water constituents in the global case 2 water can lead to dominating effects of one single constituent and therefore to masking of the other parameter in the spectral signal. This masking results in limited capabilities especially near the borders of the parameter ranges. This requires a segmentation of the simulation ranges and the retrieval procedure.

Table 3: Simulated ranges of water constituents for the PCI algorithm

Coefficient Set	Parameter	Range of variability
Global case 1	Chlorophyll a Sediments - $b_s(550nm)$ Yellow Substance - $a_Y(440nm)$ Aerosoloptical Thickness - $\tau_A(750nm)$	0-3 mgm^{-3} n.a. n.a. 0-0.25
Global case 2	Chlorophyll a Sediments - $b_s(550nm)$ Yellow Substance - $a_Y(440nm)$ Aerosoloptical Thickness - $\tau_A(750nm)$	0-30 mgm^{-3} 0-15 m^{-1} 0-0.5 m^{-1} 0-0.25
Baltic Sea	Chlorophyll a Sediments - $b_s(550nm)$ Yellow Substance - $a_Y(440nm)$ Aerosoloptical Thickness - $\tau_A(750nm)$	0-15 mgm^{-3} 0-15 m^{-1} 0-0.5 m^{-1} 0-0.25

Because of the dominance of the atmospheric parameter and its well known behavior a segmentation concerning the variation of the aerosol optical thickness is not necessary. Thus the variability ranges have to be divided in 4 subranges for each water parameter separately. Simulations show that the sediment concentrations are most insensitive with respect to the influence of other parameters and give the best accuracy of the retrieval of all water constituents. In the result the global case 2 parameter range are splitted into 4 subsets with different variability ranges of the sediment concentration:

$$(0 \leq b_s < 1) m^{-1} \quad (1 \leq b_s < 3) m^{-1} \quad (3 \leq b_s < 7) m^{-1} \quad \text{and} \quad (7 \leq b_s < 15) m^{-1}$$

The other parameters are varied in the global range. In the result the derived water constituent concentrations for each subset were discriminated in scope and out of scope dependent of the corresponding sediment concentrations i.e. only if the derived sediment concentrations lies within the range of input simulation the resulting concentrations are expected to be valid.

The procedure to compute the derived geophysical parameter maps then is as follows:

- the water constituents are computed using all coefficients representing the segmented subranges for the entire scene yielding 4 maps for each parameter and 1 final map for the aerosol optical thickness
- applying the known validity ranges for each subrange, all parts outside the borders are flagged out
- the resulting subrange-maps are superimposed to get a parameter map for the complete variability range
- a smoothing procedure is applied to suppress border effects.

Figure 6 shows the flowchart of PCI Algorithm implementation

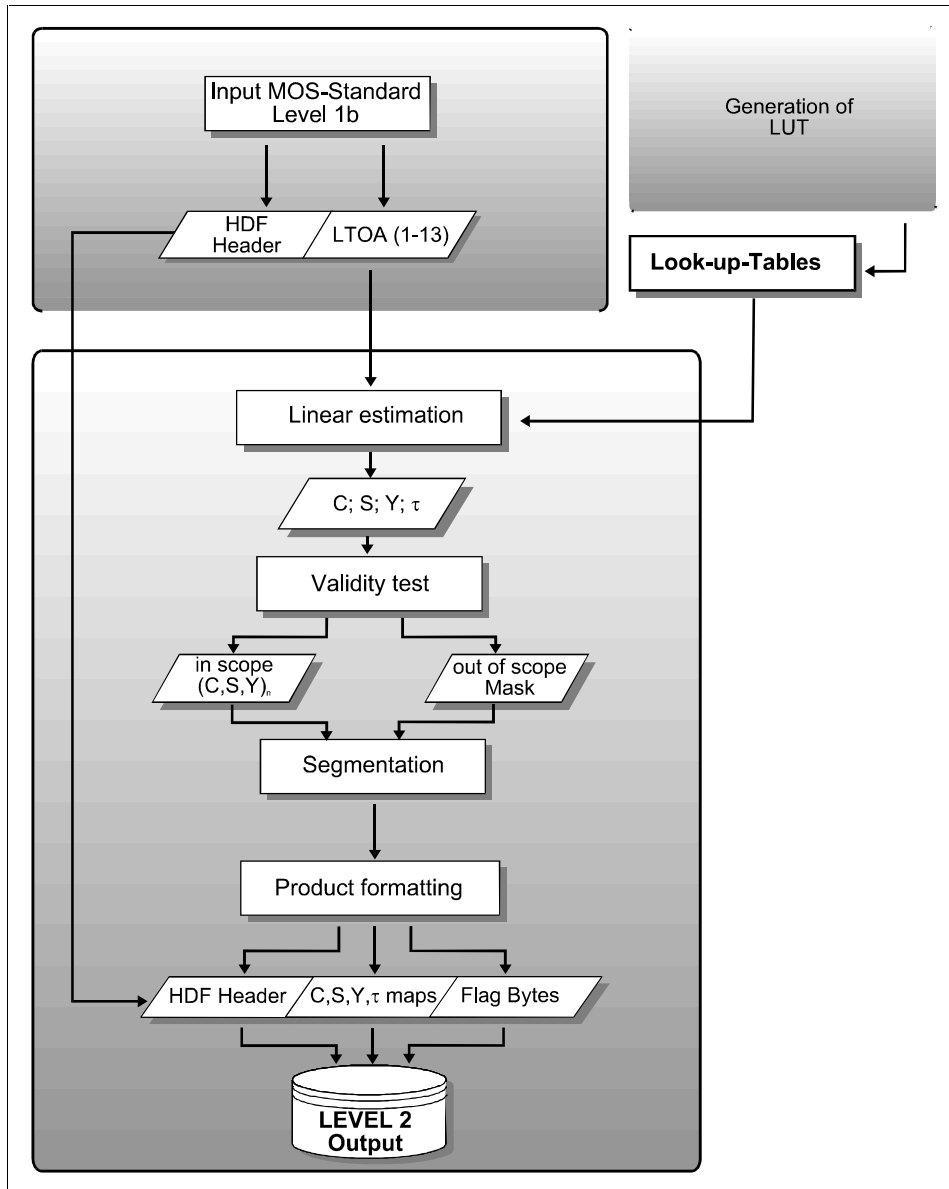


Fig. 6: Flowchart of the PCI algorithm

6. Error budget estimates

The error budget was estimated by applying the PCI-Algorithm to data sets of modeled TOA radiances. The range of simulation covers the entire variability ranges of the geophysical parameters. Figure 7 shows the histogram of the relative error for the retrieval of chlorophyll for the case 1 water model .

Simulation and retrieval are in very good agreement, the RMS is about 10 %.

For the global case 2 water the number of independent variables as well as the variability ranges increase and that results in a larger retrieval error. The figures show the relative error histograms for the different water constituents and the simultaneous derived aerosol optical thickness. The solid curve shows in the case of the three water constituents the results using the segmentation procedure, the dotted one the results without segmentation.

Despite the more complex situation for case 2 waters the RMS for all constituents is about 30 %. Improvements can be seen after the segmentation. The retrieval accuracy for the atmospheric parameter is for the entire variability range very good. The results for the ensemble of the geophysical parameters give a lower accuracy compared to other biooptical algorithms, but one has to keep in mind that these algorithms require an atmospheric correction and therefore the error budgets do not represent the complete error chain of parameter retrieval from satellite data. The used TOA approach for interpretation includes this source of errors. Nevertheless the error estimation show the potential of this new methodology and the accuracy is more than acceptable. Saying this, one has to keep in mind that also in-situ measurements of constituents concentrations have an error in the same order of magnitude.

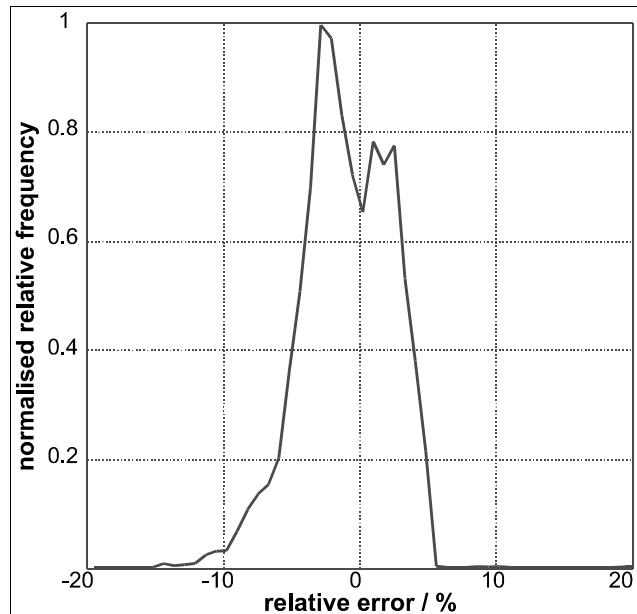


Fig. 7: relative retrieval error for Chlorophyll a in global case-1 water

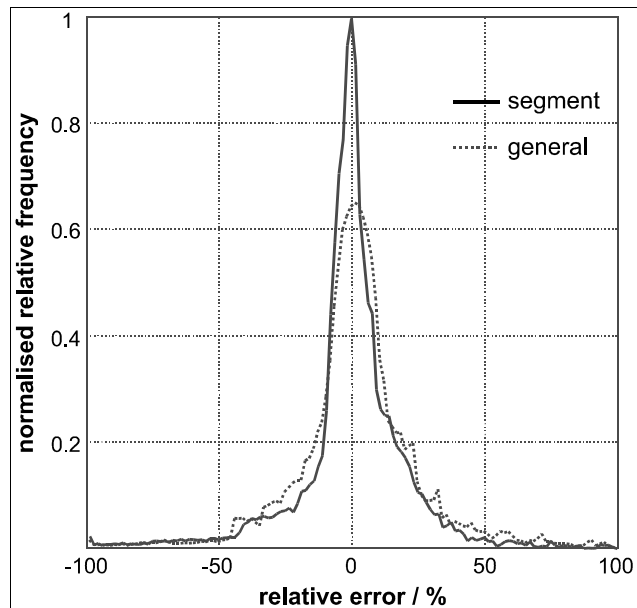


Fig. 8: relative retrieval error for Chlorophyll for case-2 water

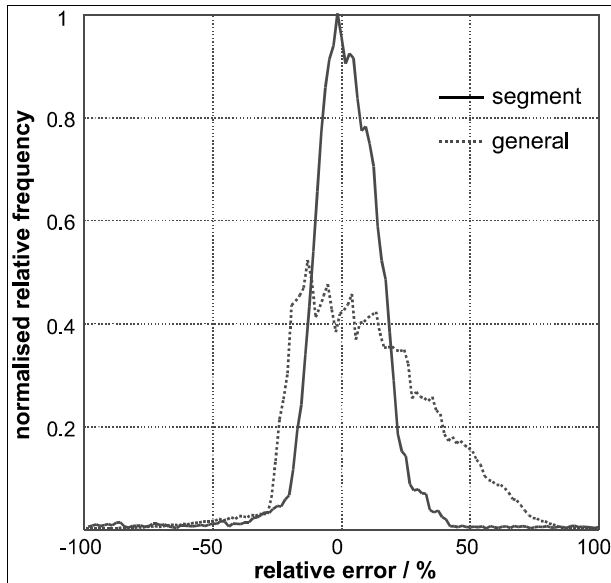


Fig. 9: Relative retrieval error for Sediments

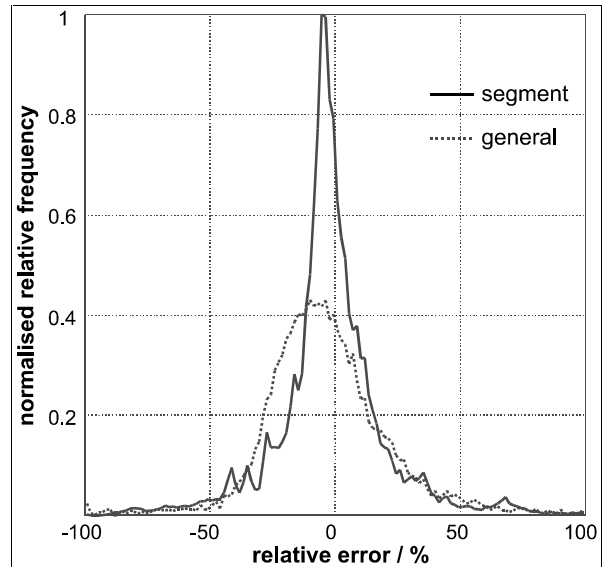


Fig. 10: Relative retrieval error for Yellow Substance

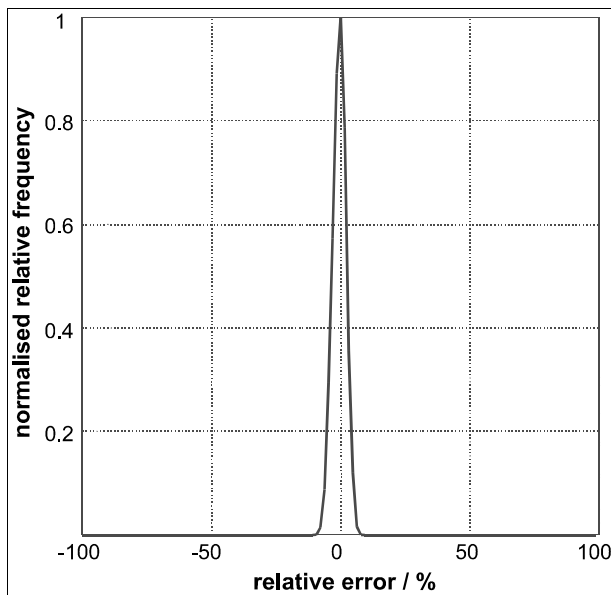


Fig. 11: Relative retrieval error for Aerosol Optical Thickness

7 Exception Handling

Will be further specified during operational implementation.

8. Literature

Austin R.W. et. al.: Ocean Color Analysis, 74 –10, (1974)

Carder Kendall L.: „Algorithm Theoretical Basis Document: case 2 Chlorophyll a Algorithm“, St. Petersburg Florida ,1994

Doerffer, R.: "Fast computational scheme for inverse modeling of multispectral radiances: application for remote sensing of the ocean", Applied Optics, Vol. 32, pp. 3280-3285, June 1993

Doerffer R. et. al.: Pigment Index, Sediment and Gelbstoff Retrieval from Direction Water Leaving Reflectance Using Inverse Modeling Technique“, MERIS-ESL Doc. No. PO-TM-MEL-GS-0005, GKSS 1997

Esaias W. (Ed.): „SeaWIFS at-Launch Standard Product Recommendations“ Notes of the SeaWIFS Science Team, 1994

Fischer J.: „On the Information Content of Multispectral Radiance Measurements over an Ocean“, Int. J. Of Remote Sensing 6 (1985) 5, pp. 773

Gordon, H.: "Removal of Atmospheric Effects from Satellite Imagery of the Oceans" in Appl. Optics, 17 (1978) 10, pp.1631ff.

Gordon H., et. al.: Journal of Marine Research 40 (1982) pp. 491

Gower J.F.R., Lin S., Borsted G. A.: „The Information Content of different optical spectral ranges for remote chlorophyll estimation in coastal waters“, Int J. of Remote Sensing 5 (1984) 2, pp. 349-364

Ingebritsen S. E., Lyon R. J. P.: „Principal Component Analysis of Multitemporal Image Pairs“, Int. J. of Remote Sensing 6, pp. 687, 1985

Krawczyk H., Neumann A., Walzel Th.: "Investigation of interpretation possibilities of spectral high dimensional measurements by means of principal component analysis - A concept for physical interpretation of those measurements", SPIE Proceedings, Vol. 1938, pp. 401-411, 1993

Krawczyk H. Neumann A., Walzel Th.: "Interpretation potential of marine environments multispectral imagery", paper presented at ERIM's Third Thematic Conference on Remote Sensing for Marine and Coastal Environments, Seattle, Washington, 18-20 September 1995

Morel A.: „Optical properties of pure seawater“, in Optical Aspects of Oceanography (London Academic Press) pp. 1-24, (1974)

Morel A., Bricaud A.: „Some theoretical results concerning optics of phytoplankton with special reference to remote sensing“ in Oceanography from Space, ed. by J. F. R. Gower (New York Plenum Press), pp.313-327, 1981

Morel A., Prieur L.: „Analysis of Variations in Ocean Colour“, Limnology and Oceanography 22, pp. 709-722, 1977

Neckel, H. Labs: Solar Physics 90, pp. 205ff., 1984

Neumann A., Walzel Th., Tschentscher C., Gerasch B., Krawczyk H.: „MOS-PRIRODA Data Processing, Software, and Data Products“, DLR, Institute for Space Sensor Technology, 1995

Neumann A., Walzel, Gerasch B., Tschentscher C.: „Algorithm Theoretical Basis Document: MOS-PRIRODA Level-1B Products“, Berlin 1999

Prieur L., Sathyendranath S.: „An optical classification of coastal and oceanic waters based on specific spectral absorption of phytoplankton pigments, dissolved organic matter and other particulate material.“ *Limnology and Oceanography* 26, pp. 671-689, (1981)

Sathyendranath S., Morel A., Prieur M.: " A three component model of ocean color and its application to remote sensing of phytoplankton pigments in coastal waters", *Int. J. of Remote Sensing*, Vol 10, pp. 1373-1394, (1989)

Siegel H. : Internal Report of Baltic Sea Research Institute, Rostock-Warnemuende, personal communication 1998

Sturm B.: "The atmospheric correction of remotely sensed data and the quantitative determination of suspended matter in marine water surface layer" in "Remote Sensing in Meteorology, Oceanology and Hydrology", ed. Cracknell A. P., Ellis Horwood Ltd. (1981)

Sturm B.: "Ocean color remote sensing and quantitative retrieval of surface chlorophyll in coastal waters using NIMBUS CZCS data" in "Oceanography from Space", Plenum Press N. Y., (1981)

Zimmermann G. et al.: "MOS/PRIRODA: an Imaging VIS/NIR Spectrometer for Ocean Remote Sensing", *SPIE Proceedings*, Vol 1937, pp. 201ff , 1993

***Kurzdokumentation
der Softwaretools
für MOS-Datenhandling***

Program	extrhdf
Description	<p>Extraction of parts of a MOS-IRS level-1B HDF file. The extraction is done without any manipulation of the contents of the data. Resulting file is in RAW format. The corresponding information from MOS level-1B header is stored in ASCII format. User can select what data parts he want to extract.</p> <p>Possible selections are:</p> <ul style="list-style-type: none"> MOS level-1B header MOS classification image MOS quick look image MOS image data <p>All selected data parts are stored in one resulting file in the order of selection.</p>
Syntax	extrhdf [<input> [<output>]]
Input	MOS-IRS level-1B file
Output	File in RAW data format or file in JPEG format, if the quick look image is selected only
Supported Platforms	Sun-Solaris 2.5.x and higher Linux
Last Version	
Update	05.05.1998

Program	extrQL
Description	<p>This program extracts the grey scaled quick-look-image from MOS-IRS level-1B files (HDF format) and stores it into a JPEG image. If in the command line a number <file_num> is given as third parameter, then the program reads <file_num> files, extracts each quicklook and concatenates them into one JPEG file.</p> <p>There are no queries within the program, so that the user has to give the number of files to process explicitly in the command line.</p>
Syntax	extrQL [<ifile> [<ofile> [<file_num>]]]
Input	MOS-IRS level 1B file(s)
Output	Quick look image in JPEG format.
Supported Platforms	Sun-Solaris 2.5.x and higher Linux
Last Version	
Update	15.09.98

Program	extrCLAS
Description	<p>This program extracts the classification image from MOS-IRS level-1B files (HDF format) and stores it into a JPEG image.</p> <p>If in the command line a number <file_num> is given as third parameter, then the program reads <file_num> files, extracts each quicklook and concatenates them into one JPEG file.</p> <p>The resulting image contain only the values:</p> <ul style="list-style-type: none"> 0 - water(ocean) 1 - land 2 - clouds/ice/snow and 3 - not classifid <p>There are no queries within the program, so that the user has to give the number of files to process explicetely in the command line.</p>
Syntax	extrCLAS [<ifile> [<ofile> [<file_num>]]]
Input	MOS-IRS level 1B file(s)
Output	classification image in JPEG format
Supported Platforms	Sun-Solaris 2.5.x and higher Linux
Last Version	
Update	15.09.98

Program	ful2scen
Description	<p>In addition to standard level-1B scene format primary processing program <i>PRODOMUS</i> can also generate full-take level-1B format. Full-take level-1B data contain a file header in ASCII format, followed by the multispectral measurement data, written in band interleaved by line order. At the beginning of each single swath and each single channel is written the time tag. The full-take data format is described in detail in „MOS-IRS Data Processing, Software and Data Products“.</p> <p>This program converts the full-take data format to standard level-1B scene format. The program works under the following conditions:</p> <p style="padding-left: 2em;">A MOS-A full-take file can be converted only if the corresponding (same path number and same day of year number) MOS-B full-take file is available in the same directory.</p> <p style="padding-left: 2em;">MOS-B scenes can be produced without the MOS-A file.</p> <p style="padding-left: 2em;">The resulting scenes have the same format as the level-1B files would be generated by primary processing program <i>PRODOMUS</i> (HDF-format).</p> <p style="padding-left: 2em;">If the format of the input files failed, the program stops with an error message.</p> <p style="padding-left: 2em;">For calling the program an initialisation file <i>mos_f2s.ini</i> is required, that contain path and file names for input and output files.</p> <p style="padding-left: 2em;">(Note:There is no other way to hand over the file names!)</p>
Syntax	ful2scen_v1.0 [<infile>]
Input	MOS-IRS-A full-take level-1B file and (or) MOS-IRS-B full-take level-1B file
Output	MOS-IRS-A level-1B scene files (HDF format) of the complete data take and (or) MOS-IRS-B level-1B scene files (HDF format) of the complete data take
Supported Platforms	Sun-Solaris 2.5.x and higher Linux
Last Version	Version 1.0
Update	16.03.99

Program	l1georef
Description	<p>This program makes it possible to calculate georeferencing parameters for MOS-IRS level-1B files received with the mobile station or to update the georeferencing parameters generated with <i>PRODOMUS</i> program. It can be used only within the TeraScan Earth Remote Sensing System from SeaSpace Corporation San Diego USA.</p> <p>The program reads any number of the MOS-IRS level-1B HDF files of the same sensor and data take. The orbital binding is done with the help of TeraScan sensor oriented earth transformation and the acquisition time, taken from the header.</p> <p>The resulting file is a MOS-IRS level-1B HDF file with an updated header. The contents of the data were not changed.</p> <p>It is possible to calculate a new classification image with updated sun angles.</p> <p>If it is necessary to obtain a very exact georeferencing there is the opportunity to enter a navigated TDF (TeraScan Data Format) file as a second input file. It is generated from the same MOS-IRS level-1B files, that have to be geocorrected, with <i>l1totdf</i> program and TeraScan navigation tools. The program checks the acquisition date and time of both files to be sure that the files belong together.</p>
Syntax	l1georef [<input1> [<input2>]]
Input	<p>MOS-IRS level-1B file(s) example for input file name: LEV00ppp_IP3Bss.ddd LEV00ppp_IP3Ass.ddd</p> <p>where: ppp - path number, ss - scene number and ddd - day of year</p> <p>MOS-IRS level-1B file(s) in TDF format</p>
Output	<p>MOS-IRS level-1B file(s) with updated header information example for output file name: LEV00ppp_IP3Bss.ddd.neu</p>
Supported Platforms	Sun-Solaris 2.5.x and higher
Last Version	
Update	09.09.98

Program	l1totdf
Description	<p>The program l1totdf is a converting tool for use MOS-IRS level-1B data within the TeraScan Earth Remote Sensing System from SeaSpace Corporation San Diego USA. Files in TDF (TeraScan Data Format) can be mapped in other projections and can be used for mosaicing of images.</p> <p>The program reads any number of MOS-IRS level-1B files of the same sensor and data take and generates a file in TDF format. The TeraScan environment is required for a correct orbital binding of data. The TDF file is stored in one multiband file of data type FLOAT. Data will be scaled with calibration values from level-1B header. The resulting TDF has a sensor based earth transformation. All data necessary for earth transformation (essentially the acquisition time) are taken from level-1B header.</p> <p>In case of MOS-IRS-B/C input file the user can select how to store data of MOS-C sensor:</p> <ul style="list-style-type: none"> as 14th channel of MOS-B file (with or without coordinate transformation from MOS-C to MOS-B), as separate file (then asking for a file name) and not saved
Syntax	l1totdf [<ifile> <ofile>]
Input	<p>MOS-IRS level-1B file(s)</p> <p>example for input file name: LEV00ppp_IP3Bss.ddd LEV00ppp_IP3Ass.ddd</p> <p>where: ppp path number ss scene number ddd day of year</p>
Output	bandsequential ordered multiband file in TDF format
Supported Platforms	Sun-Solaris 2.5.x and higher
Last Version	
Update	09.04.98

Program	mosl1corr
Description	<p>This program corrects the internal reflections and striping in the MOS-B level-1B HDF files. The destriping of the images is done by a pixelwise offset correction with equalisation curves for each wavelength. The reflection correction is done with an empirical determined formulae. Both corrections are described in detail in chapter 4.4.1. .</p> <p>The order of the corrections is :</p> <ul style="list-style-type: none"> destriping (optional) reflection correction (in any case) <p>Two other input files are required for correction of level-1B input files:</p> <ul style="list-style-type: none"> <i>mos_equalise</i>, contains the equalisation curves for each channel <i>mos_internal_db</i>, an internal data base file <p>The output file has the same structure as the level-1B file. Additional in the remarks of the ASCII-header of the level-1B file is noted, which corrections have been applied. By this double corrections are avoided. Here an example of the updated header part:</p> <pre>... MOS_B_FAIL= 0.0%; REMARKS= additional corrections: SR (stripes removal), SLC (stray light corrected); ...</pre> <p>If the user wants to correct more than one scene of a data take, he has to give the first scene name and the number of scenes he wants to correct. The correction is made in ascending order of scene numbers, separately for each file and there are the same number of output files as input files.</p>
Syntax	mosl1corr_v1.1 [<input>]
Input	<p>MOS-IRS-B level-1B file(s)</p> <p>example for input file name: LEV00ppp_IP3Bss.ddd</p> <ul style="list-style-type: none"> where: ppp path number ss scene number ddd day of year
Output	<p>Stripes and reflection corrected MOS-IRS-B level-1B file(s)</p> <p>example for output file name: LEV00ppp_IP3Bss.ddd.cor</p>
Supported Platforms	<p>Sun-Solaris 2.5.x and higher</p> <p>SGI IRIX 6.4</p> <p>Linux</p>
Last Version	Version 1.1
Update	01.03.99

Program	mosloginvers
Description	<p>Program calculates chlorophyll concentration, sediment scattering, gelbstoff absorbtion and the aerosol optical depth from MOS-IRS-B level-1B data using principal component inversion (PCI). The algorithm is described in deail in chapter 7.2. (see also Appendix 5: „ATBD MOS-IRS Level-2 Algorithm“).</p> <p>A second input file is required containing the coefficients for calculation of the water constituents.</p> <p>If the user wants to calculate the water constituents of more than one scene of a data take, he has to give the first scene name and the number of scenes. The calculation is made in ascending order of scene numbers, separately for each scene by taking the sun geometry from MOS header and searching the corresponding coefficients in coefficient file.</p> <p>The result of calculation is stored in one multiband output file of data type FLOAT. The user can select data format of the output file: RAW or XVIFF. The bands are ordered in the following way:</p> <ul style="list-style-type: none"> chlorophyll concentration sediment scattering gelbstoff absorbtion aerosol optical depth <p>The program generates a second output file of data type BYTE containig a water-land mask of the resulting image and stored in the same data format as the first output file.</p>
Syntax	mosloginvers_v1.0 [<infile> [<outfile>]]
Input	<p>MOS-IRS-B level-1B file(s)</p> <p>exapmle for input file name: LEV00ppp_IP3Bss.ddd</p> <p>where: ppp path number</p> <p>ss scene number</p> <p>ddd day of year</p>
Output	<p>File in Raw or XVIFF data format containing the water constituents</p> <p>example for (default) output file name :</p> <p>LEV2_ppp_IP3Bss.ddd.csytau</p> <p>File in Raw or XVIFF data format containing the water-land mask</p> <p>example for (default) output file name :</p> <p>LEV2_ppp_IP3Bss.ddd.maske</p>
Supported Platforms	Sun-Solaris 2.5.x and higher Linux
Last Version	Version 1.1
Update	05.03.99

Program

extrband9

Description

This program should be called after the MOS-IRS primary processing program *PRODOMUS* to generate a fulltake quick-look image.

- The program extracts MOS-B channel 9 measuring data from all available MOS-IRS Level-1B files and stores them after processing as fulltake greyscaled image of data type BYTE in a KHOROS VIFF file.
- *EXTRBAND9* uses the standard input files *mos_irs.env* and *mos_irs.ini* for initialization in the same way as *PRODOMUS*. Therefore all keywords with the parameters belonging to it have to be set (cp. "Detailed Description of Primary Processing Package PRIMCONT").
- The program looks for all scene files or the fulltake file respectively corresponding to the path number and the day of year in the directory given by the Level-1 path keyword and analyzes the file format before the processing begins.
- The extracted data will be filtered, enhanced, converted to BYTE type and stored as file with a 1024 byte KHOROS header placed first.

There is also a program version available to produce JPEG images (*EXTRBAND9JPG*).

Syntax

extrband9 [*<envfile>* [*<inifile>*]]

Input

<envfile> Name of the environment file
<inifile> Name of the initialization file

- If the name of the INI-file is missing in the command line, then the name of the standard file *mos_irs.env* is used.
- If both of input file names were missing in the command line, the names of the standard input files *mos_irs.env* and *mos_irs.ini* are used.
- All Level-1B files of MOS-B in ascending order of scene numbers

Output

The output is a channel B9 greyscaled quicklook image in XVIFF file format. The standard file name is CH9XV00*ppp*_IP3.*ddd* with *ppp* as path number and *ddd* as day of year.

Supported platforms

Sun Solaris 2.5.x or higher
SGI IRIX 6.4

Last version

2.11

Update

26.01.98

Program

mosextract

Description

This program extracts measuring data from MOS-IRS Level-1B files and produces following results:

- Classification image
- Digital Numbers, i.e. unscaled radiance values
- TOA radiance values L_{sat} in $\mu\text{W}/(\text{cm}^{-2} \cdot \text{nm} \cdot \text{sr})$
- TOA reflectance values R_{sat} (only for files with geographical information)

The data is stored as full take in a single/multiband file of data type FLOAT (without time tag) or BYTE (classification image). There are two storing modes for the output file supported, the XVIFF file format with a file header of 1024 bytes which contains all information about channel, pixel and line numbers and so on, and the raw file format (bandsequential).

MOSEXTRACT is able to concatenate the data of several Level-1 files belonging to the same overflight and to create subimages with data from any selected channels.

In case of extraction of MOS-C data (band 14) from MOS-B Level-1 files an affine coordinate transformation of MOS-C to MOS-B image format can be performed if requested.

There is also the reflection correction option for the MOS-B channels 1 to 13 available. This function is not executed for destriped and reflection corrected MOS-B Level-1 files, i.e. the input Level-1 files are results of the *MOSL1CORR* program (see also *MOSL1CORR* software description).

The program prints the geographical coordinates of the corners of the extracted part and some other image information to an output text file with the name *<ofile>.txt*.

If the Level-1 files used as input couldn't be completely processed with the matching orbit elements from the ancillary file because it was missing or wrong, then geographical information isn't available.

Syntax

mosextract_v3.1 [*<infile>* [*<ofile>*]]

Input

<infile> Name of the (first) input Level-1B file

Output

<ofile> Name of the output data file

Supported platforms

Sun-Solaris 2.5.x or higher
SunOS (Release 4.1.3_U1)
SGI IRIX 6.4
Linux

Last version

Version 3.1

Update

18.01.99

Program

atmcor

Description

The program *ATMCOR* applies an atmospheric correction to MOS-B Level-1B files based on a derived correction model of Gordon/Sturm by H. Krawczyk. Based on the "black-water" condition in the near infrared wavelengths the algorithm uses the channels 9 (749.7 nm) and 11 (868.3 nm) to estimate the aerosol optical depth in these two channels and calculates the Angstrom coefficient. Using the Angstrom-law the aerosol optical thickness of all other channels is extrapolated and the water leaving reflectances are calculated. The result is written to a Level-2 file in HDF format. The output file name is automatic generated in accordance with the input Level-1B standard file name (see below). The Level-2 output file structure is organized as shown in the table.

File element	Element type	Description
Level-2 file name	File identifier	Data File Annotation Set
Level-2 header	File description	Data File Annotation Set
Coarse classification image taken from input L1B file	8-Bit image with colour palette	Raster-8 image
Water leaving reflectances of the MOS-B channels 1-6	ATC_Data bandsequential	Scientific Data Set
Estimated atmospheric parameters (3 bands): <ul style="list-style-type: none"> • Scattering angle Ψ • aerosol optical depth $\tau_A(750\text{nm})$ • Angstrom coefficient α 	ATC_Parameters bandsequential	Scientific Data Set

Syntax

```
atmcor_v1.52 -i LEV00ppp_IP3B<scene>.ddd
```

Input

MOS-IRS Level-1B file LEV00ppp_IP3B<scene>.ddd with *ppp* as path number, <scene> as scene number and *ddd* as day of year.

Output

MOS-IRS Level-2 result file in HDF format LEV2_ppp_<scene>.ddd with *ppp* as path number, <scene> as scene number and *ddd* as day of year.

Supported platforms

Sun-Solaris 2.5.x or higher
Linux

Last version

Version V1.52

Update

12.02.99